10
I29A
#141

CIVIL ENGINEERING STUDIES
STRUCTURAL RESEARCH SERIES NO. 141

copy 3

PRIVATE COMMUNICATION
NOT FOR PUBLICATION

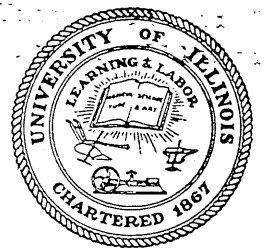

BEHAVIOR OF PRESTRESSED CONCRETE BEAMS UNDER LONG-TIME LOADING

Note Reference Room
Civil Engineering Department
3106 C. E. Building
University of Illinois
Urbana, Illinois 61801

A Thesis
by
P. E. MURPHY

Issued as a Part
of the
SIXTH PROGRESS REPORT
of the
INVESTIGATION OF PRESTRESSED CONCRETE
FOR HIGHWAY BRIDGES

SEPTEMBER, 1957
UNIVERSITY OF ILLINOIS
URBANA, ILLINOIS

BEHAVIOR OF PRESTRESSED CONCRETE BEAMS UNDER LONG-TIME LOADING

A Thesis by

P. E. Murphy

Issued as a Part of the Sixth Progress Report of the

INVESTIGATION OF PRESTRESSED CONCRETE
FOR HIGHWAY BRIDGES

Conducted by

THE ENGINEERING EXPERIMENT STATION

UNIVERSITY OF ILLINOIS

In Cooperation With

THE DIVISION OF HIGHWAYS
STATE OF ILLINOIS

and

U. S. DEPARTMENT OF COMMERCE
BUREAU OF PUBLIC ROADS

Urbana, Illinois

September 1957

TABLE OF CONTENTS

TABLE OF CONTENTS (Continued)

LIST OF TABLES

LIST OF FIGURES

LIST OF FIGURES (Continued)

LIST OF FIGURES (Continued)

I. INTRODUCTION

1. Introduction

Although tests had already been performed on four prestressed post-tensioned beams to determine the effects of time-dependent variables (1) (2), the results obtained indicated sufficient differences between the various beams and between the computed and actual deflections to warrant an entirely new set of tests. This was decided with full knowledge of the variable nature of time effects which precludes any exact prediction of their magnitude. Nevertheless, it was felt that results could be obtained which would be more uniform and agree reasonably well with analyses.

In the first set of beams, the manner of fabrication and the curing and storage conditions both seemed to introduce variables which could not be measured, but which nonetheless affected the results. For these reasons, pretensioning was substituted for post-tensioning to eliminate grouting, and beams were stored in a controlled temperature and humidity room. The use of pretensioning is not a departure from current practice as witnessed by the preponderant use of pretensioning today except in very large members. It is true that controlled humidity and temperature do not represent field conditions, but the purpose of the tests could better be served if the analyses were made on the basis of what is known or can be measured.

2. Object

The objects of this report are: (1) presentation of the data obtained from long-time strain and deflection readings on four prestressed concrete beams, two unloaded, and two loaded, and strain readings on companion cylinders, and (2) comparison of the measured

beam deflections with those computed on the basis of certain simplifying assumptions regarding the creep and relaxation characteristics of steel and concrete in the beam.

3. Outline of Tests

Four beams were subjected to long-time test. Each specimen was a pretensioned beam 4 by 6-in. in cross-section, and spanned 6 ft. Drawings of these beams and their loading arrangement are shown in Figs. 1 and 2. For control purposes, each beam had four 4 by 16-in. companion cylinders. Two of these were loaded to 2000 psi nominal stress in compression as shown in Fig. 3; and the other two were left unloaded. Twelve 6 by 12-in. control cylinders were cast with each beam. Ten of these were tested over a period of 28 days to follow the variation in concrete strength.

All beams contained the same amount of prestressing wire, and with the exception of ML-1, were to have 2000 psi compressive stress at the bottom fiber immediately upon release, and zero stress in the top fiber. The latter was obtained by placing the center of gravity of the steel at the lower kern point of the concrete cross-section. The bottom compressive stress in ML-1 was reduced somewhat to compensate for the lower tension stress induced by loading after the transformed section becomes effective. The properties of the specimens are given in Table 1.

After release of prestress, each beam was immediately transferred from the crane bay of Talbot Laboratory to a controlled temperature and humidity room and placed in a specially designed frame (Fig. 4). Here beams ML-1 and ML-2 were loaded at their third-points by springs to a nominal top fiber compressive stress of 2000 psi and 1000 psi respectively. The nominal stress distributions for loaded and unloaded beams are graphically presented in Fig. 5.

4. Acknowledgments

The studies reported herein were made as a part of an investigation of prestressed concrete for highway bridges conducted in the Talbot Laboratory of the University of Illinois in cooperation with the Division of Highways, State of Illinois, and the U. S. Department of Commerce, Bureau of Public Roads.

The program of the investigation has been guided by an advisory committee on which the following persons have served during the period covered by the work described in this report: E. F. Kelley, E. L. Erickson and Harold Allen, representing the Bureau of Public Roads; W. E. Chastain, Sr., W. J. Mackay, and C. E. Thunman, Jr., representing the Illinois Division of Highways; and N. M. Newmark, C. P. Siess, I. M. Viest, and N. Khachaturian, representing the University of Illinois.

The project has been under the general direction of C. P. Siess and under the immediate supervision of M. A. Sozen, Research Associate in Civil Engineering.

Appreciation is expressed to Mr. Sozen for his help and advice in planning the tests and preparing this report, and to the laboratory personnel for their cooperation and aid in carrying out the test program. In addition, C. E. Kesler, of the Department of Theoretical and Applied Mechanics kindly permitted the use of certain facilities under his direction during the tests.

This report was written as a thesis under the direction of Dr. Seiss, whose assistance and encouragement are gratefully acknowledged.

5. Notation

Beam Constants

b = width of beam

h = overall depth of beam

A_s = total area of wire reinforcement

Notation relating to prestressing only

F_i = initial prestress force

ΔF = loss in prestress force

F_{se} = effective prestress force after losses

Stresses

Concrete

f'_c = 7-day cylinder strength

f'_{ci} = cylinder strength at the age of loading or release of prestress

f_c = applied compressive stress

f_F^b = stress at bottom fiber due to prestressing

f_{cb} = stresses at bottom fiber of prestressed beam after loading

f_{ct} = stresses at top fiber of prestressed beam after loading

Steel

f_{si} = initial prestress

f_{sr} = relaxation loss in steel

E_s = modulus of elasticity of steel

Strains

Concrete

ϵ_c = compressive strain

ϵ_{ce} = concrete strain at level of steel due to effective prestress force F_{se}

ϵ_c^{2000} = strain after 2000 hours

E_c = modulus of elasticity of concrete

II. MATERIALS, SPECIMENS AND FABRICATION

6. Materials

(a) Cement

Marquette Type III Portland Cement, purchased locally, was used in all beams.

(b) Aggregates

Wabash River sand and gravel were used for all beams. The maximum size of the gravel used was 3/8 in. The major constituents of the gravel were limestone and dolomite with minor quantities of quartz, granite, gniess, etc. The sand consisted mainly of quartz. The sand had an average fineness modulus of 3.30. Typical aggregate sieve analyses are reported in Table 2. Tests for surface moisture content were made one day prior to the mixing of concrete. The range in surface moisture content for the sand was 0.2 to 1.9 percent, and 0.5 to 3.2 percent for the gravel. One percent by weight of the surface dry aggregate was allowed for absorption of both sand and gravel.

(c) Concrete Mixes

Mixes were designed by the trial batch method. A 7-day concrete strength of approximately 4500 psi and a slump of three inches were desired. Table 3 contains the proportions of the mixes, slumps and 7-day compressive strengths for the concrete used in each beam. The strengths are based on standard 6 by 12-in control cylinders.

(d) Reinforcing Wire

Steel designated as Type X was used as prestressing reinforcement for the beams. This was manufactured by the American Steel and Wire Division of the United States Steel Corporation and is designated by the manufacturer as "Hard Drawn Super-Tens Stress Relieved Wire". The following steps were involved in its manufacture: hot rolling, lead patenting,

cold-drawing and stress relieving. The wire was delivered in coils about 6 ft in diameter and weighing approximately 300 lb each. The following heat analysis has been furnished by the manufacturer: 0.81% C, 0.76% Mn, 0.01% P, 0.027% S and 0.23% Si.

To improve the bond characteristics, all wires were first wiped with a cloth dipped in a hydrochloric acid solution, and then placed in the moist room for about two weeks to rust. This operation produces a slightly pitted surface. All wires were cleaned just before use with a wire brush to remove loose rust.

The diameter of the wire was measured to be 0.196 in. Two wire specimens were tested in a 120,000-lb capacity Baldwin hydraulic testing machine for the determination of stress-strain characteristics. Strains were measured with an 8-in. extensometer and recorded with an automatic recording device. The extensometer had a range of about 4 percent strain. The manufacturer's values of $E = 29,400,000$ psi and minimum $f_{su} = 250,000$ psi compared well with the average measured values of $E = 30,000,000$ psi and $f_{su} = 264,000$ psi. The stress-strain curve for the wire is shown on Fig. 6. Relaxation losses at the stress level to be used (about 56.5 percent of ultimate) were not expected to exceed 3.5 percent, on the basis of previous relaxation tests (1). For a determination of loss in these tests, two specimens of Type X wire were placed in the steel wire relaxation frames at levels of approximately 51 and 55 percent. The method of measuring the loss by vibrating the wires has been described in a previous report (3), and will not be repeated here. Relaxation curves for the two specimens are shown on Fig. 7.

7. Description of Specimens

All beams tested were pretensioned beams nominally 4 by 6 in. in cross-section and 7 1/2 ft long (Figs. 1 and 2). Each beam contained six 0.196-in. high strength steel

wires for tension reinforcement. Nine inches overhang were allowed at each end for the development of the prestressing force. Bond specimens in tests reported by Janney (4) required 10 to 13 inches for transfer length using rusted 0.197-in. wire stressed to 120,000 psi; thus, the nine inches allowed here may have been somewhat short. The center of gravity of steel reinforcement in all beams was 2 in. above the bottom of the beam.

Beams were designated MU-1, MU-2, ML-1, and ML-2. The letter U indicates unloaded, and L indicates loaded. The unloaded beams MU-1 and MU-2 were placed in the storage frame in the control room immediately after release of prestress, and periodic deflection and strain measurements were taken (Fig. 4). Beam ML-1 was placed in the frame and loaded at its third-points but with a total load of 4000 lb. Beam ML-2 was also loaded at its third-points but with a total load of 2000 lb (Fig. 4). Dimensions of the storage frame are shown on Fig. 8.

Four 4 by 16-in. cylinders were cast from the batch used in each beam to determine the effects of shrinkage and creep. One cylinder was loaded through springs for long-time creep readings (Fig. 3). A total load of 25,130 lb was required to produce a uniform compressive stress of 2000 psi in the concrete. A second cylinder was loaded to the same load in a 200,000-lb Olsen testing machine for about a week (Fig. 8). The other two cylinders were left unloaded in order to observe shrinkage strains. All concrete strains were measured mechanically with a 10-in. Whittemore gage.

III. FABRICATION OF SPECIMENS

8. Prestressing Frame

Since the beams were to be pretensioned, it was necessary to provide some sort of prestressing frame or bed in which to tension the wire before casting the concrete. The small size of beams and the desire to measure the instantaneous loss led to the adoption of a portable frame which would fit around the concrete form (Fig. 10). This frame consisted of two 3-in. standard pipes fitted to heavy end-plates by means of rings of the same inside diameter as the pipes welded to the end plates. The end plates were 5 by 2 by 19 in. They were drilled with two rows of five .201-in. holes;— a smooth fit for the prestressing wires. The holes were 3/4 in. on centers horizontally and vertically. This separation allowed sufficient room for full bond between wires while providing a minimum one-inch cover on the sides and bottom of the beam.

9. Tensioning of Wires

(a) End Details of Wires

Threaded connections were chosen for the following reasons: simplicity in anchoring the wires, compact arrangement of the wires with a relatively small spacing between them, and practically no loss of prestress when the stress in the wire is transferred from the jack to the bearing plate. The level of prestress planned (50 -55 of ultimate) was not sufficient to overstress the wire at the threads.

Specially heat-treated, 24-threads-to-the-inch chasers in an automatic threading machine were used to cut the threads on the end three inches of the wires. The threads on the wires were cut to provide a medium fit with the threads in the nuts.

This resulted in a thread which was slightly larger than a No. 10 which has a basic major diameter of 0.190 in. The nominal and measured diameter of the wire used was 0.196 in.

The nuts were specially made in the laboratory machine shop. They were sub-drilled with a No. 16 tap drill and tapped with a standard No. 12, 24-threads-to-the-inch tap. This provided a full No. 12 thread in the nuts. Nuts with a No. 10 thread required that too much material be cut from the wires to be practical. The thread cut on the wires to fit the No. 12 thread in the nuts was sufficient to develop at least 160,000 psi in the wires for several days and was considered to be the most suitable. The nuts were 5/8 in. long.

(b) Measurement of Tensioning Force

The tensioning force in each wire was determined by measuring the compressive strain in aluminum dynamometers placed on the wire between the nut and the bearing plate at the end of the beam opposite that at which the tension was applied. They consisted of 2-in. lengths of 1/2-in. aluminum rod, with 0.2-in. diameter holes drilled through their centers. Strains were measured by means of two Type A-7, SR-4 electric strain gages attached to opposite sides of the dynamometer and wired in series. Thus, readings were obtained which were an average of the two gages. With this arrangement small eccentricities of load did not affect the strain readings. The gages were carefully protected against handling and moisture by a heavy wrapping of electrical pressure tape over a generous coating of petrosene wax. The dynamometers were calibrated using the 6000-lb range of the 120,000-lb Baldwin hydraulic testing machine. The calibrations of the dynamometers were nearly the same; the strain increment necessary to measure a tensioning stress of 150,000 psi in the 0.196-in. wires was approximately 2700 millionths. The large increment

of strain allowed a fairly precise measurement of stress in the wires, since the strain indicator used had a sensitivity of 2 to 3 millionths.

(c) Tensioning Procedure

The frame was assembled on two concrete block supports. The wires were slipped through the end-plate of the form and the end-plates of the prestressing frame (Fig. 11). At the end opposite the prestressing end dynamometers were slipped on the wires, then the nuts were screwed down against them. About 3/8 in. of thread was exposed. At the prestressing end nuts were placed on each wire, the jacking frame was positioned for either the upper or lower row of wires. Then, the pull-rod was run through the slot in the jacking frame and screwed onto the wire to be tensioned. The other end of the pull-rod was run through a 30-ton Simplex center-hole hydraulic ram operated by a Blackhawk pump, and was secured by a large nut at the end. Immediately before tensioning, dynamometer readings were taken on all wires. Wires were tensioned individually. Slotted shims about 5/8 in. in length were used to take up the elongation of the wire. When the desired stress was reached, the nut was turned down tight against the shims and the force on the jack was released at the pump. Because of slight deformations in the frame with progressive tensioning, it was necessary to go back and adjust the stress in the wires. All wires were stressed to within $\pm$ 1.5 microinches of the required value.

After tensioning the six wires in the frame, the frame was transported to the form where the wires were placed inside the form and the end plates were positioned. The beam was ready for casting the next morning.

10. Casting and Curing of Specimens

The concrete forms were made of heavy 2-in. nominal size boards. A preliminary check revealed a slight vertical warp in the side boards. To remedy this, clamps were used

throughout the length of the beam.

All concrete was mixed about 3 minutes in a non-tilting drum-type mixer of 6 cu ft capacity, and was placed in the forms and cylinder molds with the aid of a high frequency internal vibrator. The mixing water was added after the dry materials had been mixed for a short time.

Several hours after casting, the top surface of the beam was troweled smooth and all cylinders capped with neat cement paste. Beams and cylinders were allowed to cure in their forms in the air of the laboratory. The beams were left in the forms until they had reached sufficient strength to be released. Bottom fiber stress desired immediately after release was 2000 psi. The wires were released when the fiber stress was from 50% - 55 % of the concrete strength. Variation in concrete strength was obtained from compressive tests of 10 concrete cylinders over a period of 28 days (Fig. 12). For beams MU-1, MU-2, and ML-1, five days were required to reach the desired strength. For beam ML-2, seven days were required. A chronology of tensioning, casting, prestressing, etc., through final positioning of the beam in the storage frame appears in Table 4.

IV. MEASUREMENTS AND INSTRUMENTATION

11. Strain Measurements

(a) Electric Strain Gages

Electric strain gages were used in the following location for each specimen:

Beams: On the dynamometer only (discussed previously in Section 9-b).

Cylinders: Two type A-7, SR-4 electric strain gages were mounted on each of the three rods used in the cylinder loading frame and connected in series to give average strains. These were used for strain measurements in the load-strain calibration of the rods performed on the 120,000-lb Bladwin dydraulic testing machine. The gages were used only during loading to measure the load on the cylinder, and were not depended upon for readings after the load was applied.

All electric strains were read with a Baldwin SR-4 portable strain indicator. Type A-7, SR-4 gages for temperature compensation were mounted on an unstressed steel block.

(b) Mechanical Strain Gages

Strain distribution through the depth of the beam as well as creep and shrinkage cylinder strains were measured by means of a 10-in. Whittemore strain gage. Measurements on all gage lines were read twice or until readings agreed within 0.00001 in./in. There are four gage lines on each side of the beam with one measurement on each side of the center line for the unloaded beams. For the loaded beams the four gage lines remained, but the two readings per line were overlapped 5 inches to insure flexural strains free of shear distortions. Layout of gage lines is shown on Figs. 1 and 2. Because of insufficient

clearance between the pipes of the prestressing frame and the beam, readings on two gage lines were in doubt before release. For this reason, two rows of gage lines with one reading on each side of the gageline were added to the top and bottom of the beam. These were read only before and immediately after release to obtain accurate instantaneous strains. This layout is also to be seen in Figs. 1 and 2. The three 10-in. gage lines for the cylinders were arranged symmetrically around the circumference of the cylinders (Fig. 3).

For these tests, it was decided to locate the gage plugs in the concrete flush with the surface rather than gluing them on the outside as in previous tests and thus avoid the danger of breaking them off. Several methods were attempted but finally the following was chosen as giving the best results: Holes 15/32 in. in diameter were drilled in the wood forms at the desired location of the gage plugs. Just before casting, steel rods 3 in. long and 7/16 in. in diameter were placed in the holes and extended 1/2 in. past the inside surface of the form. These remained in place about 7 hours after pouring, long enough to allow the initial set to take place, and then were pulled out.

One day before release of prestress, steel gage plugs 5/17 in. in diameter and 5/16 in. deep, drilled at the center with a No. 54 drill to a depth of 1/8 in. and reamed, were positioned in the preformed holes in the manner described in Section 14. The same gage plugs were used on the cylinders in holes drilled in the concrete. Gage plugs 3/8 in. in diameter and 1/4 in. deep drilled in the same manner as above were glued on the top and bottom gage lines of the beam with Duco cement. This was also done for the 4 by 16-in. cylinder loaded in the 200,000-lb Olsen machine. Glue was considered satisfactory in these cases because of the short duration of their use.

12. Deflection Measurements

Instantaneous and long-time deflections were measured at the mid-span of each beam with a 0.001 Ames dial indicator. Two additional dials were installed on ML-2, 7-1/2 in. on either side of the center line. For a description of the mounting of these gages see Section 15(a).

13. Modulus of Elasticity of Concrete

"Instantaneous" rather than "electric" has been used to describe strains and deflections in the beams at release of prestress and at loading. This was done because a certain portion of these deflections and strains represent creep. To determine approximately what portion of the measured change was creep and what portion elastic, two methods of determining the modulus of elasticity were used: Compressometer readings on 6 by 12-in. cylinders during a compression test, and loading and unloading a 4 by 16-in. cylinder to 2000 psi in the 200,000-lb Olsen testing machine. This was done on the day of release of prestress. In both cases an initial tangent modulus was desired. The results were more consistent for the "unloading" procedure, and these are the values shown in column (3), Table 5. Comparison with values of modulus of elasticity obtained from measured instantaneous strains at the bottom fiber of the beam at release are shown in column (6), Table 5. These are discussed in Section 20(b).

An average curve of initial tangent modulus versus time was desired for the analysis. This was obtained by making several "unloading" tests over a period of time and interpolating between them by means of a curve reflecting the increase in modulus of elasticity with increase in concrete strength similar to Jensen's expression for the modulus of elasticity (5). Concrete strengths were measured from 6 by 12-in. cylinders. The

resulting average moduli of elasticity versus time curve for beams MU-1, MU-2, and ML-1 are shown on Fig. 13. A separate curve is shown on Fig. 13 for beam ML-2. Values from this curve are about 15 % less than the average curve for the other beams. Zero time on this curve refers to the time of release of prestress.

V. TEST PROCEDURE AND LOADING FRAMES

14. Test Procedure

The actual beams were preceded by two trial beams in order to work out an efficient procedure for prestressing, casting, releasing and storing. After this pilot operation, the production of the four test beams was completed in six weeks.

On the day before release of the wires, the beam and prestressing frame were placed on two large concrete support blocks. Here the beam was prepared for release (Fig. 14). A thick mixture of Hydrocal (high-strength gypsum cement) was forced into the preformed gage plug recesses by means of a tube and plunger. The plaster was allowed to harden slightly, and then the gage plugs were guided into position through a transparent plastic template which lined the plugs up vertically and horizontally on center lines previously laid out on the beam. A standard 10-in. spacer bar was used as a final check. All this had to be done quite rapidly, as the plaster set up in 10 to 15 minutes. This procedure was followed for all beams. As mentioned before, the top and bottom gage plugs were glued into place, since only a few readings were required of them. After the gage plugs were located, the beam was placed on bearing plates. The bearing support at one end consisted of two steel plates 4 by 4 by 3/4 in. with a machined surface and a 3/4-in. round roller. One plate rested on the concrete support block, and the other bore against the bottom of the beam. The roller was placed between them. The bearing plates at the opposite end were exactly the same size, but had a transverse notch in each in which a 1-in. round roller was fitted to provide hinge support. The center line of the roller was located three feet from the beam center line. All bearing plates were plastered to their bearing surfaces with Hydrocal.

As soon as the beam was prepared, holes for gage plugs were drilled in the 4 by 16-in. cylinders with the exception of that to be placed in the 200,000-lb Olsen testing machine. The holes were drilled with a stationary type shop drill having vertical travel only and equipped with a 3/8-in. diameter carborundum-tipped bit. Some difficulty was experienced here when drilling into gravel. Again Hydrocal was used as the cementing agent for the gage plugs.

On the morning of release, a 4 by 16-in. cylinder was placed in the 200,000-lb Olsen testing machine and loaded to 25,120 lb, or 2000 psi stress (Fig. 9). Periodic strain readings were taken and a close check kept on the weighing beam to keep it balanced, especially during the first few days after loading when the creep deflections were larger. The purpose of this cylinder was to obtain creep information when the cylinder was the same age as the beam at release, to check initial creep strains of cylinders loaded in the frame, and to obtain the modulus of elasticity (Section 13).

A single 0.001-in. Ames dial was set up at midspan of the beam to measure instantaneous deflection. Initial strain readings were taken on all gage lines. The nuts were loosened slowly, about a quarter-turn each time, until the total load in the wires had been transferred to the beam. This precaution was necessary because the stress level was high for threaded connections. It took about 20 minutes to release all the wires. As soon as this was completed, center line deflection was read, and then strain readings were taken. These readings represented instantaneous deflection and strains. Next, readings on several side gage lines were taken as a check on the top and bottom readings. Finally, the pre-stressing frame was removed along with the end plates. Strains and deflections were again read, but the changes were insignificant.

The beam was then ready to be transported to the controlled temperature and humidity room and placed in the storage frame. By means of automatic moisture, heating, and cooling devices, this room is kept constantly at 50 percent relative humidity and 75 deg F temperature. All beams were placed in the room immediately after release, and all control cylinders within 24 hours of release with the exception of the cylinder loaded for a week in the 200,000-lb Olsen testing machine.

15. Loading Frame

(a) Beams

The loading frame consisted of longitudinal angles welded between vertical end channels (Fig. 8). The two unloaded beams were placed in the bottom two berths. Bearing plates and rollers exactly the same as on the concrete support blocks were again used here. The bottom plates were welded to the frame. A .001-in. Ames dial was fastened to the frame by a horizontal steel dowel bolted to the angles. The dial plunger was centered on the beam and reacted against a small aluminum plate.

Two beams, ML-1 and ML-2, were loaded on the frame by means of four 2-in. diameter springs. To obtain a concentric load on the springs, small circular steel caps were fitted to the springs top and bottom, and provided with a 1/2-in. diameter hole at the center. The springs were calibrated in the 120,000-lb Baldwin hydraulic testing machine with the caps on. Readings were taken with a direct reading compressometer equipped with a 0.001-in. Ames dial indicator. There are sufficient variation that a general spring constant could not be employed, and for best results load-deflection readings were taken from calibration curves for each spring. The springs in place rested directly on a half-round 2-3/8-in. diameter bar 10 inches long which provided a point reaction against a 1/4-in.

bearing plate plastered to the beam. A total of 4000 lb for ML-1 and 2000 lb for ML-2 was applied by tightening down nuts on 1/2in. diameter rods bolted to the frame angles. Some of these rods had been fitted with A-7, SR-4 strain gages, but the sensitivity of the rods was so small compared to that of the springs that the electrical readings were used only during loading to obtain a uniform distribution of load. The springs alone were relied on to give final load readings.

It was anticipated in the design of the frame that there would be an upward deflection of the angles caused by loading. To acquire a set of readings which represented only the downward deflection of the beams relative to the ends, a 2 by 3/8-in. steel strap supported exactly at the support points of the beam was included in each berth for a loaded beam (Fig. 8). The strap was supported by smooth polished steel dowels to prevent twist at the support. Ames dials attached to this strap at the center of the beam measured only deflection of the center relative to the support points of the beam. Just before loading, deflection gages of other beams on the frame were also read. The loading caused a 0.0016-in. increase in the dial reading of the beam immediately below, but had no effect on the second beam. This gage was returned to its original reading.

The beam springs have a high spring constant and are therefore susceptible to losses when the beam deflects. This was considered in the calculations (Figs. 15 and 16). There was practically no eccentricity in the loaded springs and reading on both sides of the spring were the same obtained during calibration for that particular load.

(b) Cylinders

Cylinders in loading frames were always loaded the morning of the day following prestress release—approximately 20 hours later.

The loading frame (Fig. 3) consists of the following: three 5 1/2-in. diameter railroad car springs, and three one-inch round rods threaded at each end which hold the springs in line with the rest of the frame. The force of the compressed springs react on the top of the cylinder through a top bearing plate, and on a bottom bearing plate beneath the cylinder through the three rods. In loading, the hydraulic jack was placed on top of the upper spring plate between the three rods and another plate having holes for the rods was slipped down onto the ram of the jack. The nuts were then turned down flush with the topmost plate and the three springs were compressed simultaneously by operating the hydraulic ram which reacted against the topmost plate and upon the upper plate of the springs. The lower nuts were then screwed down tightly against the upper spring plate and the load on the jack transferred to the rods by releasing at the pump. The same pump and jack were used as in the tensioning of the wires (Section 9(c)).

Much difficulty was experienced obtaining a true concentric load. The use of three springs makes this especially hard. A ball inserted between a 3/4-in. bearing plate at the top of the cylinder and the top frame bearing plate proved unsatisfactory. The method finally used was to control the loading with reference to the reading of the electric strain gages on the rods, and then read the concrete strains with the Whittemore gage. If they were not within 0.00005 in. of each other, the load on the cylinder was released, zero readings taken, and the cylinder again loaded with the total load so proportioned between the three rods that the difference in concrete strains was within the allowable. Then, the final concrete and spring strain readings were taken. The reading on the springs was taken primarily to check the total load on the cylinder as read by the rod strains, and also to measure the loss of force in the springs with time. Readings indicate that a total loss of approximately 4 percent can be expected.

Readings were taken regularly on both beams and loaded cylinders. On the average, this was every day for the first four days, every two days for the next four days, every week for the next two weeks and every three weeks thereafter.

Cylinders to measure shrinkage, two per beam, were placed in the control room at the same time as the beams (Table 4). Readings on these were neither taken so regularly nor so often as on the beams because of the relatively small strains involved.

VI. PRESENTATION OF TEST RESULTS

16. Cylinder Strains

Total strains and shrinkage strains measured from cylinders for each beam are shown on Fig. 17. The upper curves are total strains and the lower curves are shrinkage strains. Each point on the total strain curves represents the average of three readings from one loaded cylinder per beam, and each point on the shrinkage curves represents the average of six readings from two unloaded cylinders per beam. Curves of total strains measured from cylinders loaded for a week in the Olsen testing machine are not shown. Their results checked those of the cylinders loaded in the frames. Cylinders were loaded to a unit stress of 2000 psi. The origin of total strain readings refers to the time immediately after loading. Instantaneous strains are not included. The cylinders were loaded about 20 hours after release of prestress (see Table 4). The origin of the shrinkage strain curves indicates the initial reading taken in the controlled atmosphere room on the day of prestressing. The time of this reading is given in Table 4.

17. Beam Deflections

Plots of measured midspan deflections versus time for the unloaded and loaded beams up to 2000 hours are shown on Figs. 18 and 19. In all beams, the origin corresponds to the reading before prestress, that is, under dead load only. Upon release of the wires, prestress was transferred to the beam causing an instantaneous upward deflection. Approximately fifteen minutes were required to release the prestress completely. The magnitude of this deflection is indicated by the ordinate at zero time marked "After Prestress".

Three hours were required to remove the prestressing frame, convey the beam to the controlled atmosphere room, and install it in the storage frame. The upward deflection

caused by creep during this time was not recorded. All time deflections for unloaded beams are referred to the reading taken immediately after positioning the beam. This is the ordinate at zero time marked "In Storage Frame" on Fig. 18. The points "After Prestress" and "In Storage Frame" are identical on Figs. 18 and 19. The downward instantaneous deflection caused by the loading of ML-1 and ML-2 is shown on Fig. 19 as the difference between the two ordinates at zero time marked "In Storage Frame" and "After Load". The time required for loading was about one hour. Time deflections for the loaded beams have as their origin the ordinate at zero time marked "After Load".

On Fig. 20 the observed time deflections for all beams are plotted against the logarithm of time. The origin is the point "In Storage Frame" on Fig. 18 for unloaded beams, and "After Load" on Fig. 19 for loaded beams.

18. Distribution of Strain over Depth of Beam

Beam strains were measured on four gage lines on each side of the beam. In addition, gage lines were added on the top and bottom of the beam just before prestressing to obtain accurate instantaneous strains. A description of all gage lines is given in Section 11(b), and their layout is shown in Fig. 1 and 2. Successive strain distributions for beams MU-1, MU-2, ML-1, and ML-2 are shown on Figs. 21, 22, 23, and 24. Each strain is the average of four readings, two on one side of the beam and two on the other. Strains "Before Prestress" are represented by a vertical zero strain line at the left side of the figure. Strains "After Prestress" were obtained from readings on the top and bottom gage lines. Although it was not possible to measure the creep deflections during the three hours between releasing of wires and placing in the storage frame, it was possible to measure the creep strains. These are the differences in strain between the line "After Prestress"

and "In Storage Frame". The datum line for the time strain readings for unloaded beams is the last-named line.

Strain distributions immediately before loading for the loaded beams are given by the line marked "In Storage Frame", and after loading by the lines marked "After Load". The latter line then becomes the datum line for time strains. Time in hours measured from the above datum lines is marked above each strain distribution line at the top of the figures.

VII. INTERPRETATION OF TEST RESULTS

19. Discussion of Measured Strains and Deflection

(a) Cylinder Strains

Total Strains. Measured total strains for the loaded control cylinders are shown on Fig. 17. Cylinders were loaded nominally to 2000 psi. The actual unit load obtained from spring readings was within 3 percent of this value. The measured strains were later adjusted linearly to correspond to a unit load of 2000 psi. The cylinders were loaded with steel springs as described in Section 15(b). The loss in applied load amounted to only 3 percent in 2000 hours and was neglected. The curves of Fig. 17 represent the average of mechanical strain measurements on three 10-in. gage lines (Fig. 3). Averaging was felt to be permissable in this case since deviation from mean readings did not exceed 7 percent in any one case.

Because of the slowness of loading cylinders in the frames, the "instantaneous" strains included a certain proportion of creep strain, depending on the time required for loading. Thus, "instantaneous" strains ranging from 600 to 900 x 10^{-6} were recorded. With the exception of ML-2, which had somewhat weaker concrete (Table 3), the concrete properties of the cylinders were quite similar, and they were loaded at about the same age (Table 4). For this reason, instantaneous strains have been omitted in the plots of total strains.

The creep strains for the loaded cylinders are presented on Fig. 25. They were obtained by assuming that the shrinkage strains in the loaded cylinders of a given batch were the same as for the corresponding unloaded cylinders, and then taking the difference

between the total strains for the loaded cylinders and the shrinkage strains. Creep strains have been linearly corrected to 2000 psi. Instantaneous strains, measured in a screw-type testing machine, column (1), Table 5, and as described in Section 13, are compared below with total strains at 2000 hours (instantaneous plus creep strains):

Beam	Instantaneous Strain $\times 10^6$	Total Strain at 2000 Hrs. $\times 10^6$	Total Strain / Instantaneous Strain
MU-1	650	2170	3.4
MU-2	630	1870	3.0
ML-1	650	1990	3.1
ML-2	740	2670	3.6

The magnitudes of "instantaneous" and total strains depend on the modulus of elasticity of the concrete at loading, creep characteristics of the concrete, the age of loading, and the unit load applied. Factors which affect the creep characteristics of the concrete are the water:cement ratio and the storage conditions.

In order to compare the derived creep strains qualitatively, dimensionless plots of creep strains obtained as described above for the loaded cylinders of all beams are presented on Fig. 26. The abcissas of these plots are values of t/T expressed as a percentage, where t is the time of an intermediate reading and T is total time or 2000 hours. The ordinates represent the creep strain at the time t as a percentage of the total creep strain at 2000 hours under a constant load of 2000 psi. It is apparent from these curves that the creep strain curves for the cylinders were the same qualitatively in spite of small differences in concrete properties.

The dimensionless plot of creep strains versus time, shown on Fig. 27, is a reproduction of Fig. 56 from the Fourth Progress Report (1). Curves for two different stress

levels, 1000 psi and 2000 psi, up to 2500 hours are presented to indicate the validity of the assumption that the variation of creep with applied stress within these limits is linear. Creep strains were obtained by subtracting shrinkage strains from total strains. The slight difference in the curves is no greater than might be expected between two specimens at the same stress level. It should be noted, however, that these cylinders were loaded about 90 days after casting. Also the ratio f_c/f'_{ci} was smaller than in the present tests.

Concrete strengths at time of loading of the cylinders (Table 4) are given in the table below. They were obtained by reading the ordinate on the concrete strength curve corresponding to the time of loading (Fig. 12). Also shown is the actual unit load on the cylinder as measured from the springs, and the ratio of unit load to concrete strength. The latter is also shown for the unit load corrected to 2000 psi.

Beam	f'_{ci}	f_c	f_c/f'_{ci}	$2000/f'_{ci}$
	psi	psi		
MU-1	3760	2050	0.55	0.53
MU-2	3930	2000	0.51	0.51
ML-1	3800	2030	0.53	0.53
ML-2	3550	1940	0.55	0.56

This is consistent with current practice in which ratios of f_c to f'_{ci} as high as 0.60 are used.

Attempting to find some relationship between creep strains at a given time and the ratio of applied load to concrete strength, the best comparison was on the basis of 5-day concrete strengths which is tabulated below. The only conclusion permissible from these data is that for the same concrete stress a reduction in concrete strength causes an increase in creep strain.

Beam	ϵ_c^{2000}	f'_{ci}	Ratio of Strains	Ratio of Concrete Strengths
	$\times 10^6$	psi		
	(1)	(2)	(3)	(4)
MU-1	1520	3760	1.13	1.01
MU-2	1240	3930	0.92	0.97
ML-1	1340	3800	1.00	1.00
ML-2	1930	3550	1.44	1.07

Column (1) Concrete creep strain at 2000 hours for 2000 psi
(2) 5-day concrete strength
(3) Based on ML-1 equal to unity
(4) Based on ML-1 equal to unity

Although it appears from the arithmetic plot (Fig. 25) that the creep has almost ended, the plot of creep strains versus the logarithm of time presented on Fig. 28 indicates that some creep can still be expected. However, the rate of creep of all cylinders has decreased considerably at 2000 hours. Indications are that about 80 to 85 percent of the total creep has already taken place. Other creep tests (6) have recorded only about 60 to 70 percent of the total creep at 2000 hours, but for lower stresses, greater age at loading, and normal cement. Storage conditions were the same.

Shrinkage strains versus time are also presented on Fig. 17. Each shrinkage strain curve represents the average of six mechanical strain readings on two cylinders. Deviation from the mean did not exceed 10 percent between the three gage lines of a cylinder, nor 2 percent between the two cylinders. Within these limits, averaging was considered permissible.

Although ML-2 had the largest water:cement ratio, 0.80, it shows the least shrinkage strain in Fig. 17. The explanation is that readings were not begun until seven days

after casting (Table 4), whereas the unloaded cylinders of the other beams were first read five days after casting. The 48-hour difference would increase the shrinkage strains of ML-2 and make them compatible with the water:cement ratios.

The magnitude of the average shrinkage strains at 2000 hours is 0.00056. The Bureau of Public Roads, in its "Criteria for Prestressed Concrete Bridges" (7) assumes a value of 0.0002 for total shrinkage. R. W. Carlson (8) gives 0.00065 as the shrinkage at 2000 hours of 3 by 6-in. cylinders at 50 percent relative humidity and using normal cement. Size of specimen, water:cement ratio, storage conditions, and type of cement are probably the most important factors in obtaining a certain shrinkage strain at a given time. The shrinkage seems to be leveling off, but at least 15 to 20 percent more is anticipated.

(b) Beam Deflections

Unloaded Beam. Deflections at mid-span for unloaded beams are compared in Figs. 18 and 20. The instantaneous upward deflection at prestressing was the same for both MU-1 and MU-2. At 2000 hours the time deflection of beam MU-1 is 22 percent higher than that of beam MU-2. This compares well with a 27 percent difference in creep strains measured from their cylinders at the same time (Fig. 25). The two deflection curves appear to be qualitatively similar.

The following table is a presentation of the measured and computed instantaneous deflections, the total measured deflection, and the ratio of the computed instantaneous and total deflection:

Beam	Measured Deflection		Computed Instantaneous Deflection	Ratio
	Instantaneous	Total at 2000 hours	in.	Total/Computed Instantaneous
	in.	in.		
MU-1	.0865	.185	0.068	2.7
MU-2	.0865	.167	0.066	2.5

The computed instantaneous deflections were based on values of the modulus of elasticity of concrete indicated by tests of cylinders described in Section 13, and given in column (3), Table 5. The discrepancy between the computed and measured deflections may be attributed to the increase in deflection due to creep during the release of the wires.

The ratios of total to instantaneous deflection were smaller than the ratios of total strain to instantaneous strain presented in Section 19(a). The principal reason for this is that the strains were measured on cylinders creeping under a constant load while the load in the beams was decreasing due to prestress loss.

Although the arithmetic plots of Fig. 18 show a leveling off at 2000 hours, this is not so apparent in the semi-logarithmic plots of Fig. 20. Here the deflection is seen to be still increasing, but at a diminishing rate. Indications are that about 80 percent of the total deflection has already taken place.

Loaded Beams. Deflections measured at midspan for the loaded beams are shown on Figs. 19 and 20. The significance of the descriptive terms marked on the deflection axis has been explained in Section 17. The desired stress distribution before and after loading is given in Fig. 5. For beam ML-1, it was intended that the stress distribution of the unloaded beams at midspan be reversed by loading. For beam ML-2, the stress distribution was to be rectangular immediately after loading at midspan. Consequently, if there were no prestress loss in beam ML-2 there would theoretically be no angle change in the flexure span. Angle change would occur only at the ends producing an upward deflection at midspan. In reality, there would be a prestress loss, but computations indicated that the beam would have a final time deflection of zero at midspan. This beam would tend to deflect upward initially as described above, and then as prestress was lost, angle changes at the center would return it to a final zero deflection at midspan. The loss of load in the springs was also considered.

Unfortunately, the lower concrete strength produced larger prestress losses than were anticipated, and the large creep strains with time combined with stress conditions different from those desired produced downward midspan deflection of 0.035 in. at 2000 hours.

The measured instantaneous deflection caused by prestressing, the instantaneous deflection caused by loading, and the computed values for both of these are shown in the table below. Also presented in the following table are total deflections at 2000 hours, and the ratio of total deflection to the computed deflection caused by loading:

Beam	Measured Deflections			*Computed Deflections		Ratio of Deflections
	At Prestress	At Load	†Total	At Prestress	At Load	Total/Computed at Load
ML-1	.0831	.138	.254	0.063	.116	2.2
ML-2	.0960	.0625	.099	.078	.0665	1.5

* Based on modulus of elasticity shown in column (3), Table 5.
† Measured from the time immediately before loading.

The measured deflections at prestress differ from those of the unloaded beams. For ML-1 this is explained by the fact that a reduced initial prestress force (Table 1) was used to compensate for the lower bottom tensile stress produced by loading and thus reach the desired stress distribution shown in Fig. 5. This prestress force, by mistake, was actually smaller than it was computed to be. In the case of beam ML-2, the lower modulus of elasticity and larger creep strains resulting from a weak concrete caused a larger deflection at prestressing than for the unloaded beams, though the initial prestress was the same.

It is noted in the table that the ratio of the deflections caused by loading for ML-1 and ML-2 is 2.2, but that the ratio of the loads applied is 2.0 (Table 1). The difference in the two ratios is caused mostly by creep. The concrete stress was higher at the

extreme fiber for ML-1 than for ML-2 and the loading time was greater. Both of these factors tend to increase the creep deflections.

The computed instantaneous deflections were based on values of the modulus of elasticity indicated by tests of cylinders described in Section 13 and shown in column (3), Table 5. The discrepancy between the computed and measured deflections caused by prestressing can be attributed mostly to the increase in deflection caused by creep during release of the wires. The agreement of the computed deflections caused by loading with the measured deflections is better than for the deflections caused by prestress. In fact, for ML-2, the computed deflection is slightly greater than the measured. This can perhaps be attributed to a "hardening" effect caused by prestressing resulting in lower deflections at loading. In addition, the concrete stress in beam ML-2 was decreased from that produced by prestressing, thus reducing the effect of creep, and approaching more closely the "elastic" deflection condition (free of creep) which the modulus of elasticity is supposed to represent. Although the ratio of total to instantaneous deflection for ML-1 is much less than for the unloaded beams, the total deflection is much larger. In Fig. 20, it is seen that the time deflections of ML-1 are about 44 percent greater than those for MU-2. This is reasonable since loss of prestress reduces the bottom fiber compressive stress and increase the angle change.

The deflections of the loaded beams would be even greater if the load applied were constant. As the beams deflect, the force in the springs decreases. The magnitude of the decrease is seen in Figs. 15 and 16; 14 percent for ML-1 at 2000 hours, and 6 percent for ML-2. These curves were derived by assuming that the curve for the loss in load would be proportional to the deflection curve for the beam. Several spring readings were taken over

a period of time to establish the correct proportion. Curves presented in Section 21 show that the increase in deflection for a constant load of 4000 lb on ML-1 is 28 percent. This would raise the ratio of total deflection to computed instantaneous deflection to about the same magnitude as those of the unloaded beams.

(c) Beam Strains

Unloaded Beams. The strain distributions through the depth of the unloaded beams MU-1 and MU-2 are shown in Figs. 21 and 22. A description of these figures has been given in Section 18. Strain lines between gage lines 1 and 4 have been extrapolated to the top and bottom of the beam, except for the line "After Prestress". In this case the readings were taken on the top and bottom of the beam. Each strain reading at a gage line is the average of four readings, two on each side of the beam. For readings on the same side of the beam an average 3 percent deviation from mean was noted, and the same deviation was noted for the opposite sides. The strain distribution is linear up to 2000 hours.

The small amount of tension indicated in the top fiber on the line "After Prestress" was probably the result of a slightly greater eccentricity of the wires than that required to place them at the lower kern point. For the strain change between "After Prestress" and "In Storage Frame" the strain line should rotate about the point of zero strain, since three hours was too short a time for shrinkage strains to cause any movement of the point of rotation. This is clearly the case for MU-1, but a slight deviation is apparent for MU-2.

The strains indicated on the top fiber of the beam are shrinkage strains reduced by a small amount of creep in tension. The table below compares the shrinkage strains indicated by the unloaded cylinders and the strains measured at the apparent level of zero stress in the beams:

Measured Shrinkage Strain

Beam	Time	Beam Strain	Cylinder Strain
	Hours	$\times 10^{-6}$	$\times 10^{-6}$
MU-1	2081	520	530
MU-2	1914	560	580

The comparison is quite good, indicating that the difference in size between the beam and the cylinder produced little or no difference in shrinkage strains.

Loaded Beams. The strain distributions through the depth of the loaded beams ML-1 and ML-2 are shown on Figs. 23 and 24. A description of these figures has been given in Section 18. In Fig. 5 is shown the desired stress distributions for the loaded beams. The prestress losses at the level of the steel can be obtained from the strain measurements shown on Figs. 23 and 24. The approximate stress distribution can then be determined from the effective prestress. This is done in Section 20(b). Strain lines between gage lines 1 and 4 have been extrapolated to the top and bottom of the beam except at "After Prestress" where readings were taken on the top and bottom gage lines. Each strain reading at the gage line is the average of four readings, two on each side of the beam. These beams exhibited more variance among the four readings than did MU-1 and MU-2. The beam ML-1 seemed to have some torsion in it. Comparing readings on the same gage line, an average 5 percent deviation from mean was noted for both beams, while a maximum 14 percent variation existed between gage lines on opposite sides of ML-1. The torsion does not seem to have affected the linearity of strain distribution except for gage line 2 of ML-1 where a slight deviation was noted.

Both beams show about the same tensile strain in the top fiber after prestressing— 60×10^{-6}. This would correspond to about 140 psi. This might have been caused by the

wire reinforcement being located outside the kern point of the concrete cross-section.

It is noted on Fig. 23 that the strains at the bottom of the beam are much less than the strains at the top of the unloaded beams (Figs. 21 and 22). According to the desired stress distributions shown on Fig. 5, these should be planes of zero stress. The explanation, however, is that with prestress loss an initial stress condition of zero stress in the bottom fiber at midspan of a loaded beam would change to one of tensile stress. These tensile stresses would result in tensile strains reducing the compressive strains caused by shrinkage. This seems to be the case for beam ML-1. The computations of Section 20(b) have attempted to establish the actual initial stress distribution in the beams.

20. Description of Analysis for Deflections

(a) Assumptions and Scope of the Analysis

Preceding these tests, a theoretical analysis was undertaken by G. McLean (3) to predict prestress loss in a beam creeping under a constantly changing stress. Losses due to shrinkage and steel relaxation were also considered. It is now desired to follow this method through using the data obtained in these tests, but substituting a numerical analysis for the algebraic one proposed by McLean. Deflections for both loaded and unloaded beams are computed on the basis of several simplifying assumptions. This represents the "exact" analysis. Following this, some "approximate" methods are attempted. These methods are not entirely valid because they neglect certain variables, but it is interesting to see the error involved when these short-cut methods are used.

The following general assumptions were made:

(a) Creep strains are linearly proportional to the sustained stresses.

(b) Shrinkage strains are independent of stress and uniform over the depth of the beam.

In addition to these assumptions, the following factors used in the exact analysis were treated as described:

(a) Wire relaxation data were obtained from Fig. 7. The curve of relaxation loss for wire No. 12 was used after release of prestress.

(b) Creep strains were corrected for the "elastic" change in strain caused by the loss in prestress. For this computation the modulus of elasticity was assumed to vary with time according to the curve on Fig. 13.

(c) The load on the beams ML-1 and ML-2 was assumed to vary with time. The reduction in load was made according to the curves of loss of spring load versus time shown on Figs 15 and 16.

(d) Full transfer of prestress between supports was assumed in all calculations.

(e) Deflection calculations were started at stage "In Storage Frame" for the unloaded beams and at stage "After Load" for the loaded beams. The stress distribution determined at these stages in Section 20(b) and shown on Fig. 29 was used as the initial condition in the deflection computations.

(f) Since cylinder time readings did not begin until about 15 hours after beam readings (Table 4), a linear change in creep strains was made for the increase in concrete strength. This amounted to a 3 percent increase in creep strains for all beams, representing the average change in concrete strength. Although no direct relationship could be found between the creep strains for different concrete strengths, such a change within narrow limits was considered valid for concrete of the same mix.

(g) As shown in Section 19(a), it was not possible to establish a direct relationship between a creep coefficient and the f_c/f'_{ci} ratios of the four beams. A correlation

could be devised applicable only to these tests, but that would not constitute a "general creep function". Instead, creep strains corrected linearly to a 2000 psi load, increased 3 percent for time of loading as explained in (f), and adjusted to be qualitatively the same as ML-1, which represented a median, were used in the computations. The adjustment involved in eliminating qualitative irregularities was very small; it did not exceed 2 percent. The dimensionless plot resulting for all beams is shown on Fig. 30. The individual creep curves used in the computations are shown on Fig. 31.

Also shown on Fig. 31 is the average shrinkage curve used in the calculations. The difference between the actual curves was judged small enough to warrant the use of an average curve.

The increase in deflection due to time-dependent variables was considered in small intervals of time. These intervals were short, about 50 hours, at the early stages of the test when creep strain rate was high, and long, about 500 hours, at the later stages of the test when the creep strain rate was low. The computation of total deflection at the end of each interval involved the following steps:

(1) Determine the conditions of stress at the beginning of the interval.

(2) Determine the creep strain during the interval corresponding to the stress distribution established in step (1).

(3) Compute the loss in prestress corresponding to the total change in strain at the level of the steel and the relaxation loss during that interval.

(4) Correct the change in strain distribution obtained in step (2) for the "elastic" change in strains caused by the loss in prestress.

(5) Obtain the angle change at the end of the interval considered from the resulting strain distribution in step (4).

(6) Compute the deflection by considering the distribution of angle change along the length of the beam.

(b) Assumed Stress Distribution in the Beams at Beginning of Computed Deflections

The desired stress distributions in the concrete for the loaded and unloaded beams after prestressing and loading are shown on Fig. 5. Due to losses in the initial prestress caused by creep of concrete, elastic shortening of the concrete, and relaxation of the steel, the actual stress distributions differed from those desired. Since strain measurements through the depth of the beam had been taken before and after prestressing and loading, it was possible to obtain the prestress loss from the change in strain at the level of the steel. Strain distributions for the unloaded beams are shown on Figs. 21 and 22, and for the loaded beams on Figs. 23 and 24. The figures have been discussed in Section 19(c). Having obtained the prestress loss, the effective prestress and the resulting stress distribution were determined. These values, at the stages "After Prestress", "In Storage Frame", and "After Load" are shown in Table 6. The difference of three hours in the first two stages is reflected in the strain measurements at the level of the steel for each. This difference is about 75×10^{-6} except for beam ML-2 which shows a greater difference. This difference is caused by creep of the concrete during the three hours.

For the computations it was assumed that the center of gravity of the wires was located at the kern point of the concrete cross-section, and therefore there was no tension in the top fiber. This is not the actual condition, however, as the strain distributions shown on Figs. 21, 22, 23, and 24 indicate. In these figures, tensile strains at the stage "After Prestress" are clearly shown on the top of the beam. The effect of this behavior

on instantaneous deflections caused by prestressing would be to increase them due to a greater prestress moment. Time deflections for unloaded beams would be increased slightly while time deflections for loaded beams would be slightly decreased. This is assuming that the rate of creep is the same in both tension and compression. Since the magnitude of these tensile stresses could be determined only approximately, and since their effects would be small, they were neglected in computing deflections. A graphical representation of the stress distributions assumed for computations taken from the values given in Table 6 is shown on Fig. 29.

It was also possible to determine the modulus of elasticity of concrete in the beam from measured strains extrapolated to the bottom fibers for the values of the stresses given in column (5), Table 6. These values of modulus of elasticity are shown in column (6), Table 5. They are lower than the values given in column (3), Table 5, which were determined from cylinders. The difference is caused chiefly by the creep strain produced in the 15 or 20 minutes required to release the wires.

21. Comparison of Measured and Computed Deflections

(a) Unloaded Beams

Plots of measured and computed deflections based on an "exact" analysis up to 2000 hours for beams MU-1 and MU-2 are shown on Figs. 32 and 33. The assumed stress distribution in the beams at the beginning of deflection measurements are shown on Fig. 29. Also shown on the same figures are deflection curves computed for a stress 5 percent greater and 5 percent less than the assumed compressive stress in the bottom fiber. Referring to Figs. 32 and 33 it is seen that the computed deflection curves describe the behavior of the beam quite well qualitatively up to 2000 hours. The computed deflections are slightly less

than the measured before 300 hours and by 2000 hours have become about 14 percent greater. This behavior is the same for both MU-1 and MU-2. A comparison of the three computed deflection curves indicates that inaccuracies in assuming the initial stress conditions are directly reflected in the computed deflections.

From a comparison of measured and computed deflections it is noted that the measured deflections seem to be the result of a higher stress than computed in the early stages and a lower stress than computed in the later stages. Computing the deflections under a higher initial stress during the early stages of the test and under a lower initial stress during the later stages would result in a curve having good correlation with the measured deflections as indicated by the curves shown.

Partial prestress at the supports due to insufficient transfer length would tend to reduce the measured deflections. However, it is also possible that quantitive differences between the measured and computed deflection curves might be caused by a fundamental difference in the creep behavior of an axially-loaded cylinder, from which the creep strains were taken, and a prestressed beam.

The deflection curves for MU-1 and MU-2 which were computed by approximate analyses are shown on Figs. 34 and 35. Computations performed in Method A assumed no prestress loss, and therefore no change in the initial stress conditions, which were the same as in the "exact" analysis. This incorrect assumption gives deflections for both MU-1 and MU-2 which are about 55 percent greater than the measured deflections at 2000 hours. The deflections indicated by Method B were computed in the following manner: The prestress loss at any time was computed for the total strain at that time at the level of the steel assuming a constant initial stress distribution (Fig. 29). From the effective prestress remaining, the corresponding bottom fiber stress was determined. The total angle change was

obtained assuming that creep took place under this stress up to the time considered. "Elastic" change in strain caused by a loss in prestress was neglected. Steel relaxation was also neglected. This method has the advantage that a deflection can be obtained at any time by a simple computation without knowing the intermediate changes in concrete stress. The agreement between the measured and computed deflections is quite good, indicating only that the approximations were taken in the right direction. At 2000 hours the computed deflection is 4 percent greater than the measured deflection.

(b) Loaded Beams

Plots of measured and computed deflections based on an "exact" analysis for beams ML-1 and ML-2 appear on Figs. 36 and 37. The assumed stress distribution at the beginning of the deflection measurements is shown in Fig. 29. Also shown on Figs. 26 and 37 are deflection curves computed for a stress 5 percent greater and 5 percent less than the bottom fiber stress assumed before loading. Referring to the curves of Fig. 36, it is seen that the qualitative and quantitative agreement of the computed curves with the measured curves is quite good. At 2000 hours the computed deflection for the assumed initial stress distribution before loading is only 8 percent greater than the measured. The similarity between these curves and the computed curves for the unloaded beams (Figs. 32 and 33) is quite evident.

The loaded beams have the added variable of the stress distribution at the ends of the span. This has been assumed to be the same as at the midspan before loading. However, there were no strain measurements taken here and therefore there was no way of checking this assumption. A partial prestress condition at the supports of a loaded beam, however, would tend to increase the measured midspan deflections. This behavior is the reverse of that for an unloaded beam with partial prestress at the support. The computed deflection

curves shown on Fig. 36, which are based on full prestress throughout the length of the beam do not indicate such a condition. On the other hand, tension in the top fiber, which was neglected in the computations, would tend to decrease the measured deflections in loaded beams.

It was noted that the deflections computed for a 5 percent increase in initial stress before loading were about 4 percent less than those computed for the assumed initial stress, while the deflections for a 5 percent decrease in initial stress were 4 percent greater than those deflections computed for the initial stress. This is just the reverse of the unloaded beams, where an increase in assumed initial stress resulted in an increase in computed deflections.

The computed deflection curves for beam ML-2 are shown on Fig. 37. The curves become qualitatively similar as 2000 hours is approached. It should be noted that the total measured deflections are quite small - less than one-third of the measured deflections of ML-1. It is also to be noted in Fig. 37 that a decrease of 5 percent in the assumed initial bottom fiber stress before loading results in a 29 percent increase in deflections at 2000 hours, and good agreement with the measured deflections. An increase of 5 percent in the initial assumed bottom fiber stress before loading results in a 30 percent decrease in deflections at 2000 hours. It is quite evident from these curves that a beam having a nearly rectangular stress distribution at midspan after loading is very sensitive to small changes in prestress or load. The cause of the slight "hump" appearing in all computed deflection curves up to 500 hours is not fully understood. It should be noted, however, that it tends to disappear as the assumed initial stress before loading is decreased.

It should also be mentioned here that the magnitude of the creep strains of ML-2 had a large influence on the deflections. Referring to Fig. 31, which shows the cylinder

creep strains for all beams as used in computations, it is seen that the strains of ML-2 are about 40 percent greater than those of ML-1. Using the creep strains of ML-1 in computing the deflections of ML-2 resulted in a deflection less than half as large at 2000 hours than was computed using ML-2's own creep strains.

The deflection curves computed by the approximate analyses for the loaded beams are shown on Figs. 38 and 39. The procedure used for Method A and Method B was identical to that described for the unloaded beams except that strain distributions at support and at midspan were considered independently. In addition, deflections were computed by Method B assuming a constant load. The deflections indicated by Method A for beam ML-1, Fig. 38, are about 37 percent less than the measured deflections. The use of a varying load with Method B gives very good agreement with the measured deflections. Assuming a constant load in the computations results in deflections which are 28 percent greater at 2000 hours than those for a varying load, while the decrease in load was about 14 percent. This difference appears to be correct not only because Method B has given good correlation between measured and computed deflections of loaded and unloaded beams, but also because any change in strain distribution caused by flexural stresses produces twice the angle change of a variation in bottom compressive stress of a beam with prestress only as is done for the 5 percent deflection curves.

Approximately computed deflections are compared with the measured deflections for beam ML-2 on Fig. 39. It is apparent that the use of Method A gives deflections which are very much in error, and do not define the actual behavior of the beam at all. This demonstrates the importance of considering prestress losses in a loaded beam with a nearly rectangular stress distribution at midspan. The deflections computed according to Method B

exhibit fairly good agreement with the measured deflections except in the early stages. However, Method B also fails to describe the actual deflection behavior of the beam.

22. Beam Deflections on the Basis of Beam Strains

The measured deflections of beams MU-1 and MU-2 are compared in Fig. 40 with deflections obtained from the angle changes in the measured strain distributions for beams. The method of obtaining the strain distribution through the depth of the beam by means of measured strains has been described in Sections 18 and 19(c). Measured strain distributions at various times for the unloaded beams are shown on Figs. 21 and 22.

The total angle change at any time was determined as the difference in strains on gage lines 1 and 4 divided by the distance between gage lines, 5 inches. The strains were measured from the reference line "In Storage Frame" to the strain distribution line at a given time. Deflections computed in this manner constitute an "internal check" and the agreement with measured deflections should be quite good. As is seen on Fig. 40, these deflections are less than those actually measured. For MU-1 the computed deflections are 11 percent less than the measured deflections, and for MU-2 they are 8 percent less. A partial prestress condition at the supports is not the reason for this difference as this would result in computed deflections greater than the measured.

Curves similar to those of Fig. 40 are not shown for the loaded beams. No strain measurements were taken at the ends of the span and therefore the strain distribution there had to be assumed. Although it would have been possible to substitute the strain distributions at midspan of the unloaded beams for the end strain distributions of the loaded beams, it is doubtful if the interpretation would have had any value because of the small errors usually involved.

23. Prestress Losses

The instantaneous and time prestress losses at midspan in percent of initial stress versus time are shown on Fig. 41. The instantaneous losses were derived from strain measurements on the beam in the manner described in Section 20(b) are shown in column (8), Table 6. The time losses were determined from the computations for deflections by the procedure outlined in Section 20(a).

The variables used to compute the time loss were the creep strains, shrinkage strains, and relaxation loss for each beam. For all practical purposes, the latter might have been omitted. At the beginning of time readings, the stress level of the wire reinforcement in all beams was about 48 percent of the ultimate stress. After 2000 hours this had dropped to 35 percent. As has been shown in previous tests (1), the relaxation losses between these levels is negligible. The losses of wire No. 12 were used in the calculations. These amounted to 1000 psi at 2000 hours or about 2 percent of the total losses of the beams.

In the following table are given the instantaneous prestress loss and computed time prestress loss at 2000 hours from the curves shown on Fig. 41. The initial stresses are shown on the curves:

Beam	MU-1	MU-2	ML-1	ML-2
	ksi	ksi	ksi	ksi
Instantaneous Prestress Loss	21.7	20.8	19.8	25.2
Time Loss	38.4	34.7	24.8	36.2
Total Loss	60.1	55.5	44.6	61.4

As is seen in the table, the instantaneous loss occurring in the first 3 hours amounted to 35 to 45 percent of the total loss. The main factors influencing the instantaneous prestress

losses are the stress intensity, modulus of elasticity of the concrete, its creep characteristics and age of concrete at release. Relaxation loss, the greater portion of which takes place before release, also contributes to the magnitude of the instantaneous prestress loss. The main factors influencing the prestress losses with time are the initial stress distribution, the intensity of stress, and the creep and shrinkage characteristics of the concrete, which in turn are affected by the storage conditions.

Also shown on Fig. 41 are total prestress losses based entirely on strain measurements at the level of the steel. Their magnitude is shown by a short horizontal line at 2000 hours. The measured losses are about 10 percent less than those shown in the table. Some of the difference can be accounted for by the fact that relaxation losses are included only in the measured instantaneous loss.

VIII. SUMMARY

The object of the tests described in this report was to study the combined effects of time-dependent variables on the behavior of prestressed concrete beams.

Four pretensioned beams were tested. They were nominally 4 by 6-in. in cross-section and 7 ft. 6 in. long. Six 0.196-in. high strength steel wires were used for reinforcement. The center of gravity of the wires was at the lower kern point of the cross section. The initial prestress was 150 ksi in three beams and 137 ksi in the other. Two beams remained unloaded after prestressing while two beams were loaded by springs at their third points. All beams were supported on a 6-ft span in a specially constructed storage frame located in a controlled temperature and humidity room.

Strains through the depth of the beam were measured mechanically over 10-in. gage lines. Deflections were measured at midspan of all beams.

Each beam had four 4 by 16-in. control cylinders. One of these was loaded by means of springs to 2000 psi compressive stress in a special frame, and the other was loaded to the same stress in a screw-type testing machine. Strain measurements taken with a Whittemore strain gage on three 10-in. gage lines provided creep strain data. The other two companion cylinders remained unloaded to provide data on shrinkage strains.

Three beams were prestressed at 5 days, and one beam at 7 days. The effect of creep on deflections at prestressing and loading was found to be rather large. Slight differences in concrete properties were reflected in the comparative magnitudes of the time deflections of the unloaded beams. The deflection versus time curves were qualitatively similar, however. Comparison of measured deflections due to time effects for a loaded and unloaded beam with about the same compressive stress intensity at midspan showed that the

deflections were greater for the loaded beam.

Creep strain curves obtained from the control cylinders differed in magnitude for each beam, but were qualitatively the same. This was also true for the shrinkage strains.

Computed deflection curves based on several simplifying assumptions regarding the creep and shrinkage behavior of concrete, and using the measured cylinder strains, were slightly greater than the measured deflections for the unloaded beams and varied for the loaded beams. It was noted that any reasonable method of predicting the time deflections based on representative curves of creep and shrinkage strains in the concrete gave good results if the reduced concrete stress resulting from a loss of prestress was considered. Computed prestress losses were found to be about 10 percent greater than those obtained from actual strain measurements at the level of the steel.

IX. BIBLIOGRAPHY

1. Fourth Progress Report of the Investigation of Prestressed Concrete for Highway Bridges, Engineering Experiment Station, University of Illinois, 1955.

2. Fifth Progress Report of the Investigation of Prestressed Concrete for Highway Bridges, Engineering Experiment Station, University of Illinois, 1956.

3. McLean, G., "A Study of the Time-Dependent Variables in Prestressed Concrete", M.S. Thesis, University of Illinois, June 1954. Issued as part of the Third Progress Report of the Investigation of Prestressed Concrete for Highway Bridges.

4. Janney, J. R., "Nature of Bond in Pretensioned Prestressed Concrete", Journal ACI, Vol. 25, May 1954.

5. Jensen, V. P., "Ultimate Strength of Reinforced Concrete Beams as Related to the Plasticity Ratio of Concrete", University of Illinois Experiment Station Bulletin 345, June 1945.

6. Davis, R. E., H. E. Davis, and J. S. Hamilton, "Plastic Flow of Concrete Under Sustained Stress", Proc. ASTM, Vol. 34, pt. II, 1934.

7. "Criteria for Prestressed Concrete Bridges", Department of Commerce, Bureau of Public Roads, 1954.

8. Carlson, R. W., "Drying Shrinkage of Concrete as Affected by Many Factors", Proc. ASTM, Vol. 38, pt. II, 1932.

TABLE 1. PROPERTIES OF BEAMS

Beam	b	h	No. of Wires and Area A_s	Wire Type	f'_{ci}	F_i	f_{si}	Total Load - applied at third points
	in.	in.	sq. in.		psi	lb	ksi	lb
MU-1	3.96	5.94	6-0.181	X	3760	27030	149.4	0
MU-2	3.96	5.94	6-0.181	X	3930	27030	149.4	0
ML-1	3.96	5.94	6-0.181	X	3800	24860	137.4	4000
ML-2	3.96	5.94	6 0.181	X	3550	27030	149.4	2000

TABLE 2. TYPICAL SIEVE ANALYSIS OF AGGREGATES

	Gravel Sieve	Percentage Retained
Pea Gravel	3/8"	7.2
	4	84.8
	8	96.4
	16	97.7
	30	98.5
	50	99.0
	100	99.4
	Sand Sieve	
Sand	4	2.7
	8	20.1
	16	42.6
	30	71.0
	50	95.5
	100	98.6
	Fineness Modulus	3.30

TABLE 3. PROPERTIES OF CONCRETE MIXES

Beam	Cement:Sand:Gravel by weight	Water:Cement by weight	Slump inches	7-Day Compressive Stress psi	Age at Test days	Cement Type
MU-1	1:2.98:3.35	0.76	3"	4070	5	III
MU-2	1:2.99:3.32	0.74	3"	4300	5	III
ML-1	1:2.97:3.36	0.745	2 1/2"	4170	5	III
ML-2	1:2.96:3.33	0.80	5"	3550	7	III

TABLE 4. TEST CHRONOLOGY

Beam	Date of Tensioning of Wires	Date of Casting Beams and Cylinders	Date of Release of Prestress in Beam	*Beam Installed on Storage Frame	*Beam Loaded at Third Points	4 by 16-in. Cylinder *Loaded in Olsen Testing Machine	* Initial Reading on Shrinkage Cylinder	* 4 by 16-in. Cylinder Loaded in Frame
MU-1	4-11-57	4-12-57	4-17-57	+3.0		+44.5	- 4.0	+19.0
MU-2	4-18-57	4-19-57	4-24-57	+3.5		- 3.5	+ 6.5	+28.5
ML-1	5-1-57	5-2-57	5-7-57	+3.0	+4.5	- 4.5	+ 7.0	+22.0
ML-2	5-9-57	5-10-57	5-17-57	+5.5	+6.0	- 1.5	+15.0	+14.0

* Hours after Release of Prestress (+)
Hours before Release of Prestress (-)

TABLE 5. MODULI OF ELASTICITY

Beam	Modulus of Elasticity From Cylinders			Modulus of Elasticity From Beams		
	ϵ_c (1) in./in. x 10^6	f_c (2) psi	E_c (3) x 10^6 psi	ϵ_c (4) in./in. x 10^6	f_c (5) psi	E_c (6) x 10^6 psi
MU-1	650	2000	3.08	800	1963	2.46
MU-2	630	2000	3.18	790	1970	2.50
ML-1	650	2000	3.08	755	1800	2.38
ML-2	740	2000	2.70	900	1938	2.15

Column (1) and (4) Compressive strain.
(2) and (5) Stress causing compressive strain.

TABLE 6. COMPUTED STRESS DISTRIBUTION IN BEAMS

Beam	Stage "After Prestress"					Stage "In Storage Frame"					Stage "After Load"			
											Flexural Stresses		Final Stresses	
	ϵ_{ce}	f_{sr}	ΔF	F_{se}	f_F^b	ϵ_c^s	f_{sr}	ΔF	F_{se}	f_F^b	f_{ct}	f_{cb}	f_{ct}	f_{cb}
	(1)	(2)	(3)	(4)	(5)	(6)	(7)	(8)	(9)	(10)	(11)	(12)	(13)	(14)
	in/in x 10^6	psi	lb	lb	psi	in/in x 10^6	psi	lb	lb	psi	psi	psi	psi	psi
MU-1	525	3400	3460	23570	-1963	610	3400	3925	23110	-1926				
MU-2	517	3400	3420	23610	-1970	575	3400	3740	23290	-1938				
ML-1	470	3400	3170	21590	-1800	545	3400	3580	21280	-1770	-2000	+1922	-2000	+152
ML-2	580	3500	3780	23250	-1938	725	3500	4 570	22460	-1875	-1000	+ 954	-1000	-921

Column (1), (6) Total strain at level of steel measured from before prestressing

(2), (7) Relaxation loss.
(3), (8) Prestress Loss
(4), (9) Effective Prestress
(5), (10) Bottom Fiber compressive stress in concrete computed on basis of gross section
(11), (12) Stresses induced by loading computed on basis of transformed section.
(13) Column (11)
(14) Algebraic sum of column (10) and (12)

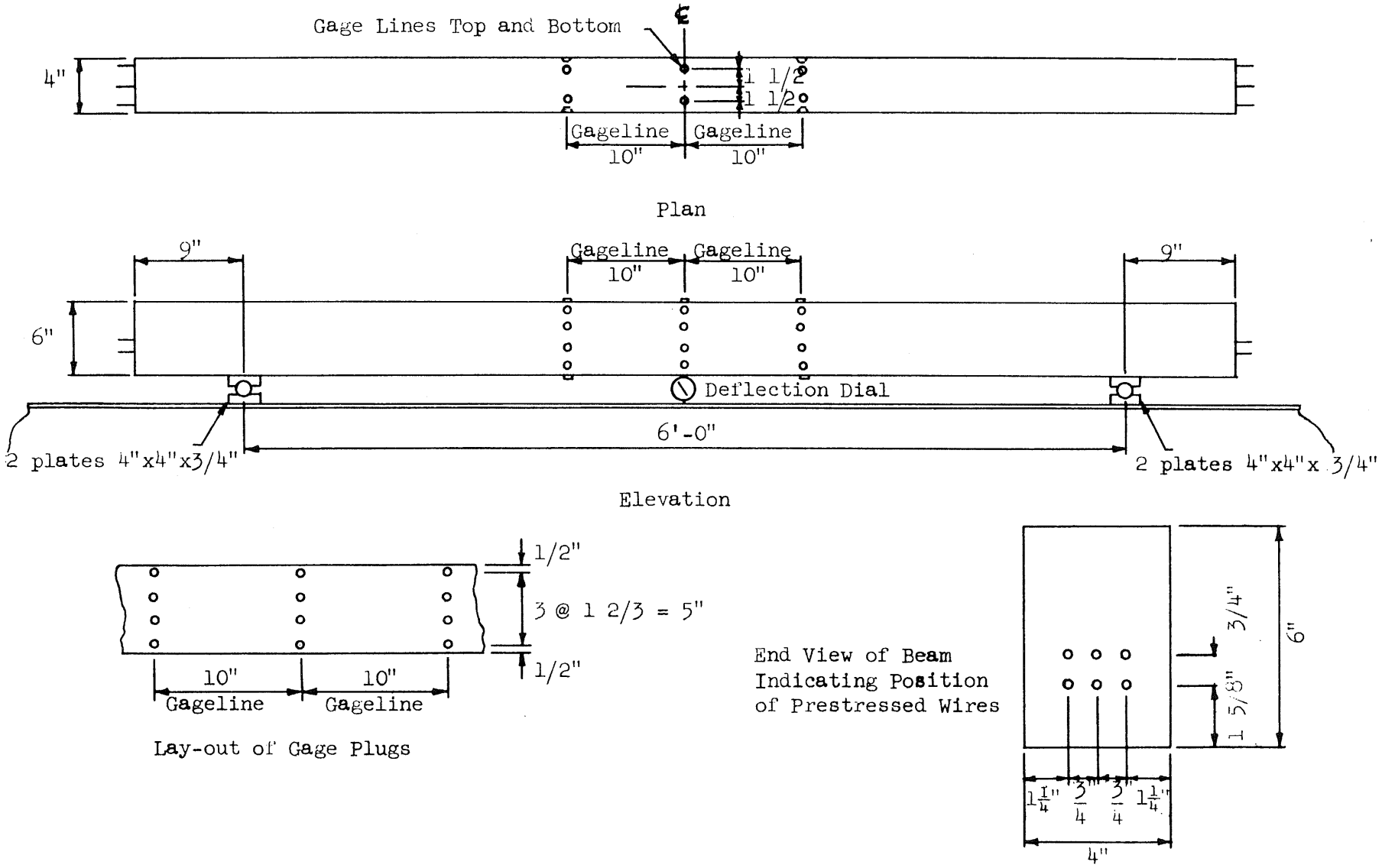

Fig. 1. Dimensions for Beams MU-1 and MU-2

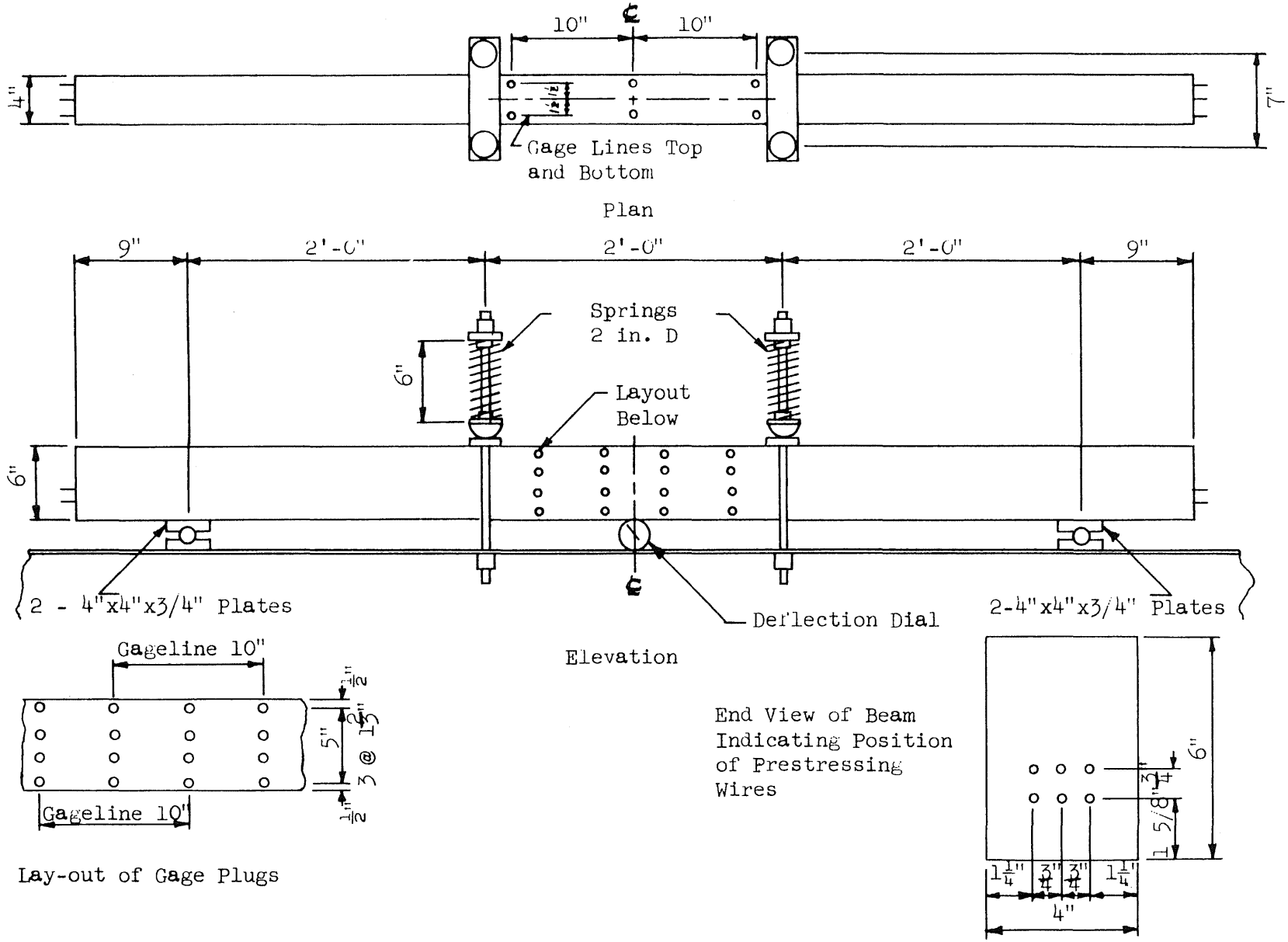

Fig. 2. Dimensions and Loading Arrangement for Beams ML-1 and ML-2

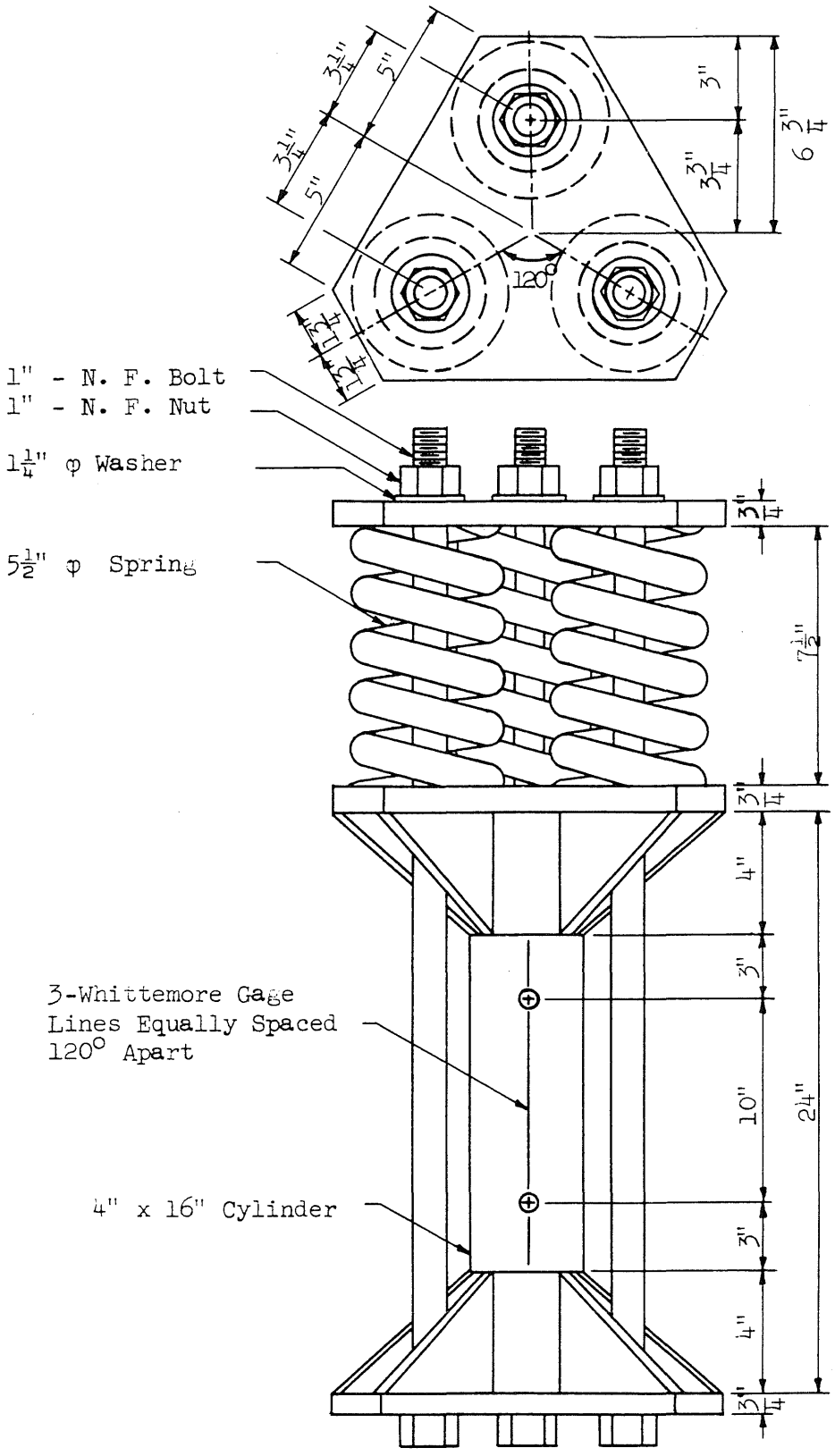

Fig. 3. Dimensions and Loading Arrangement for the 4" x 16" Cylinders

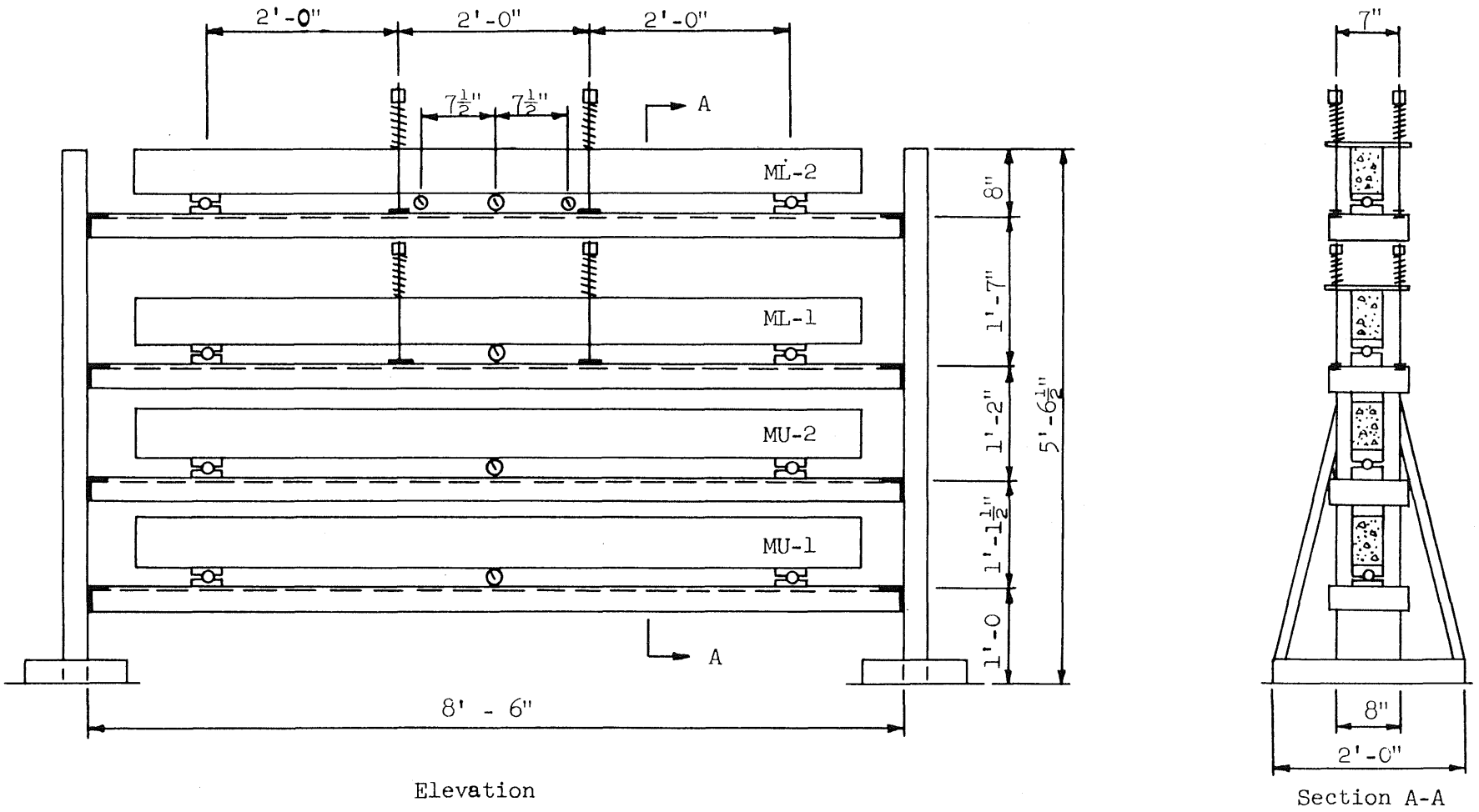

Fig. 4. Beams in Place on Storage Frame

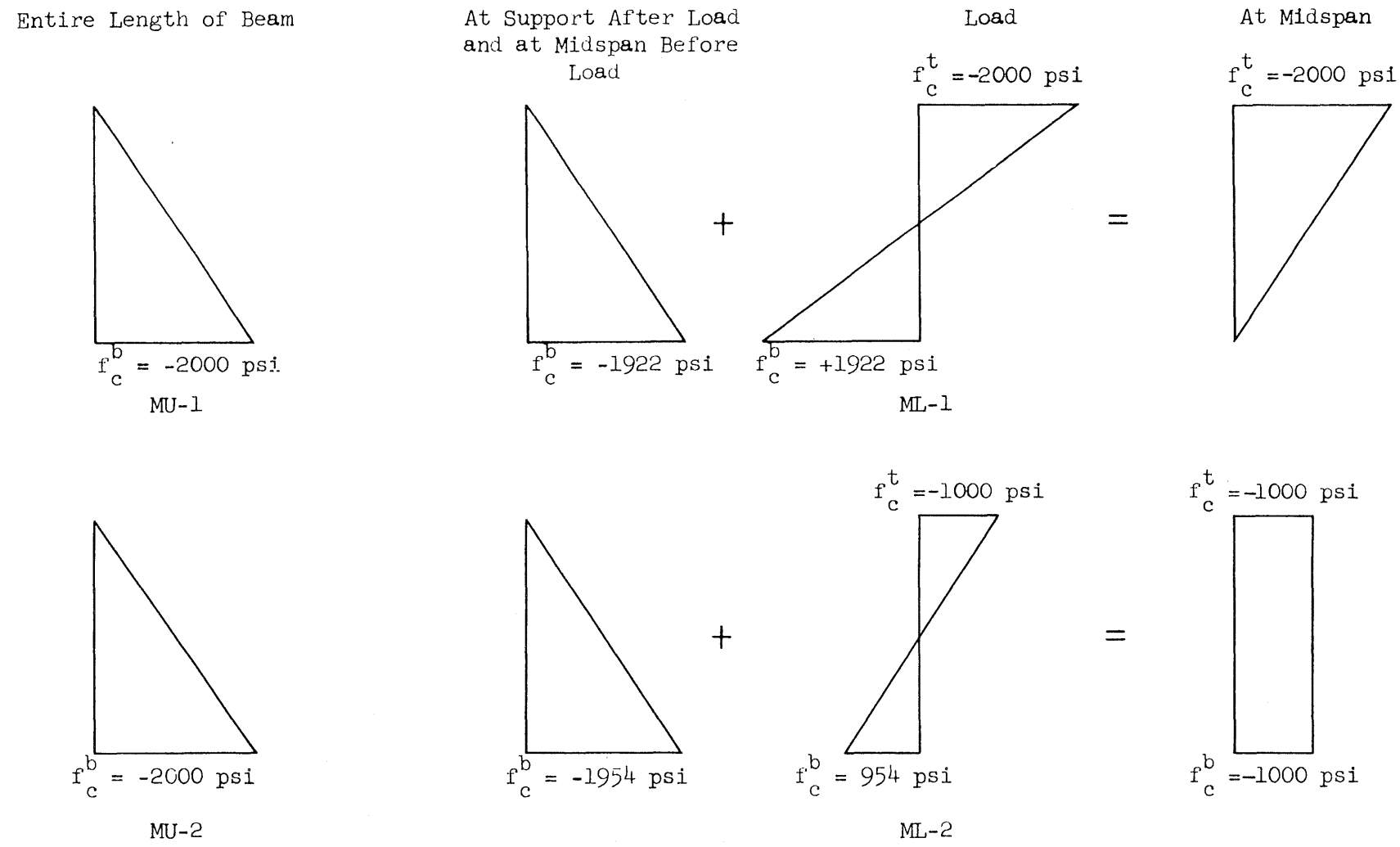

Fig. 5. Nominal Stress Distribution in Beams

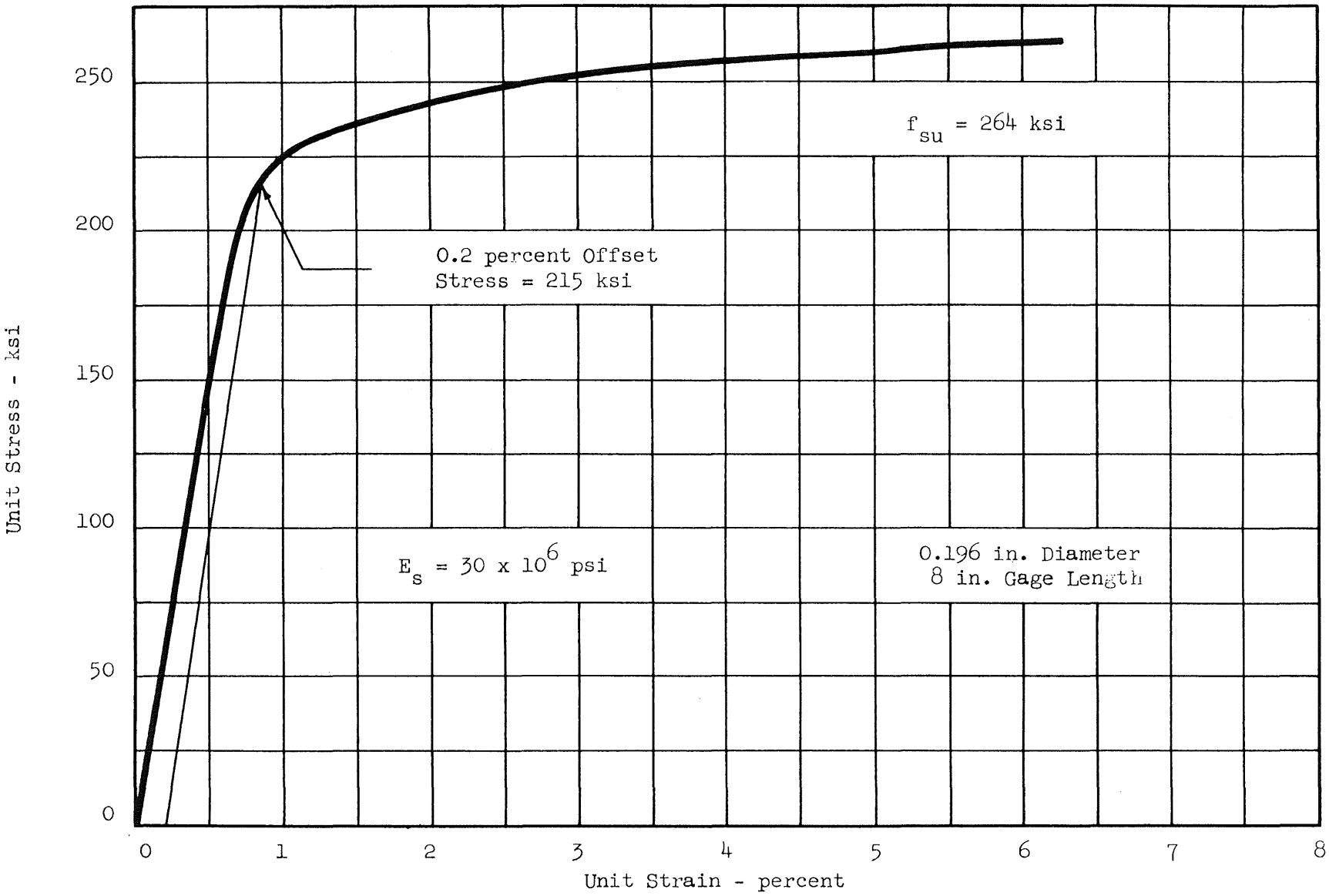

Fig. 6. Stress - Strain Relationship for Type X Wire

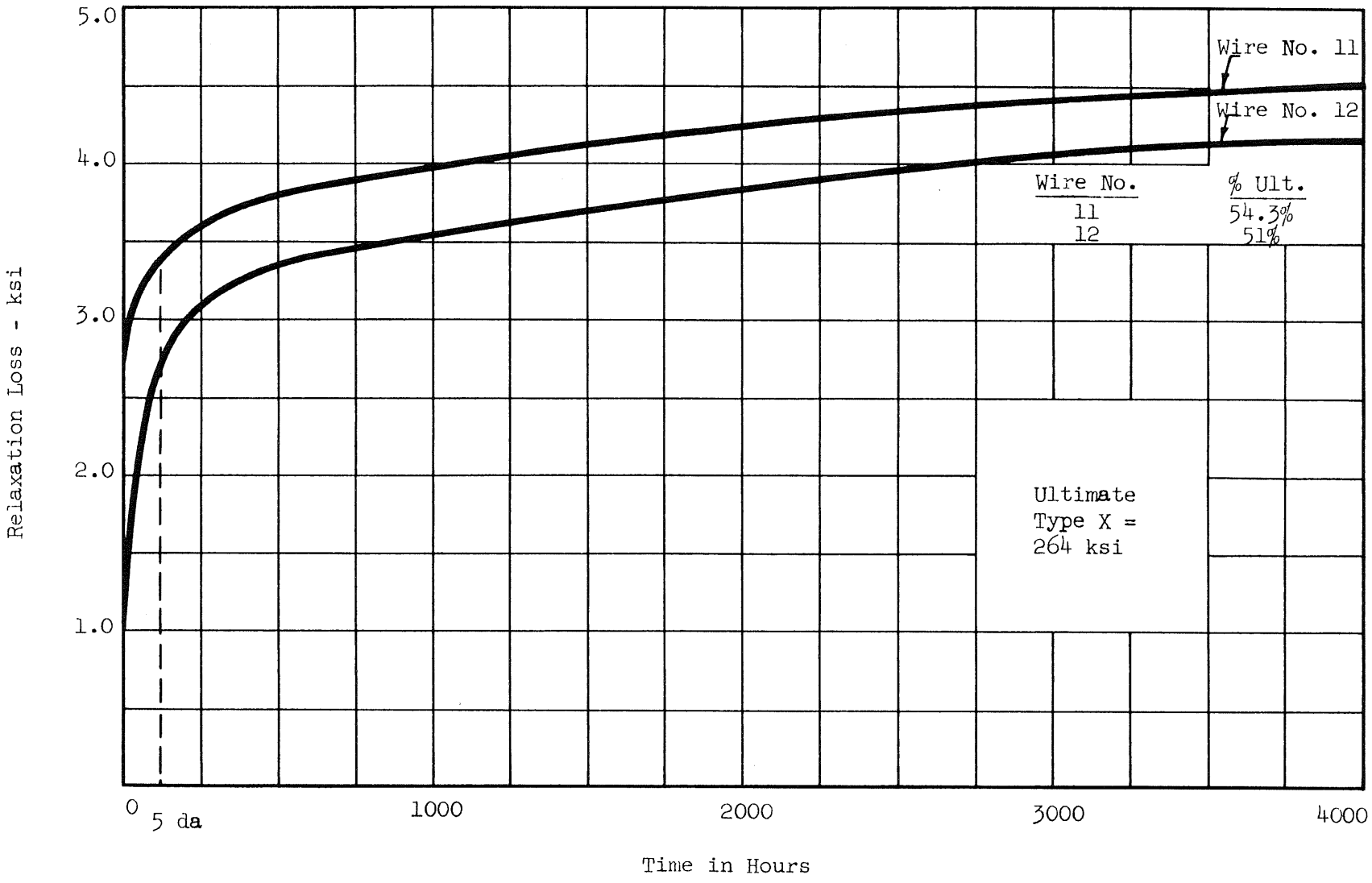

Fig. 7. Plot of Relaxation Loss Versus Time for Type X Wires

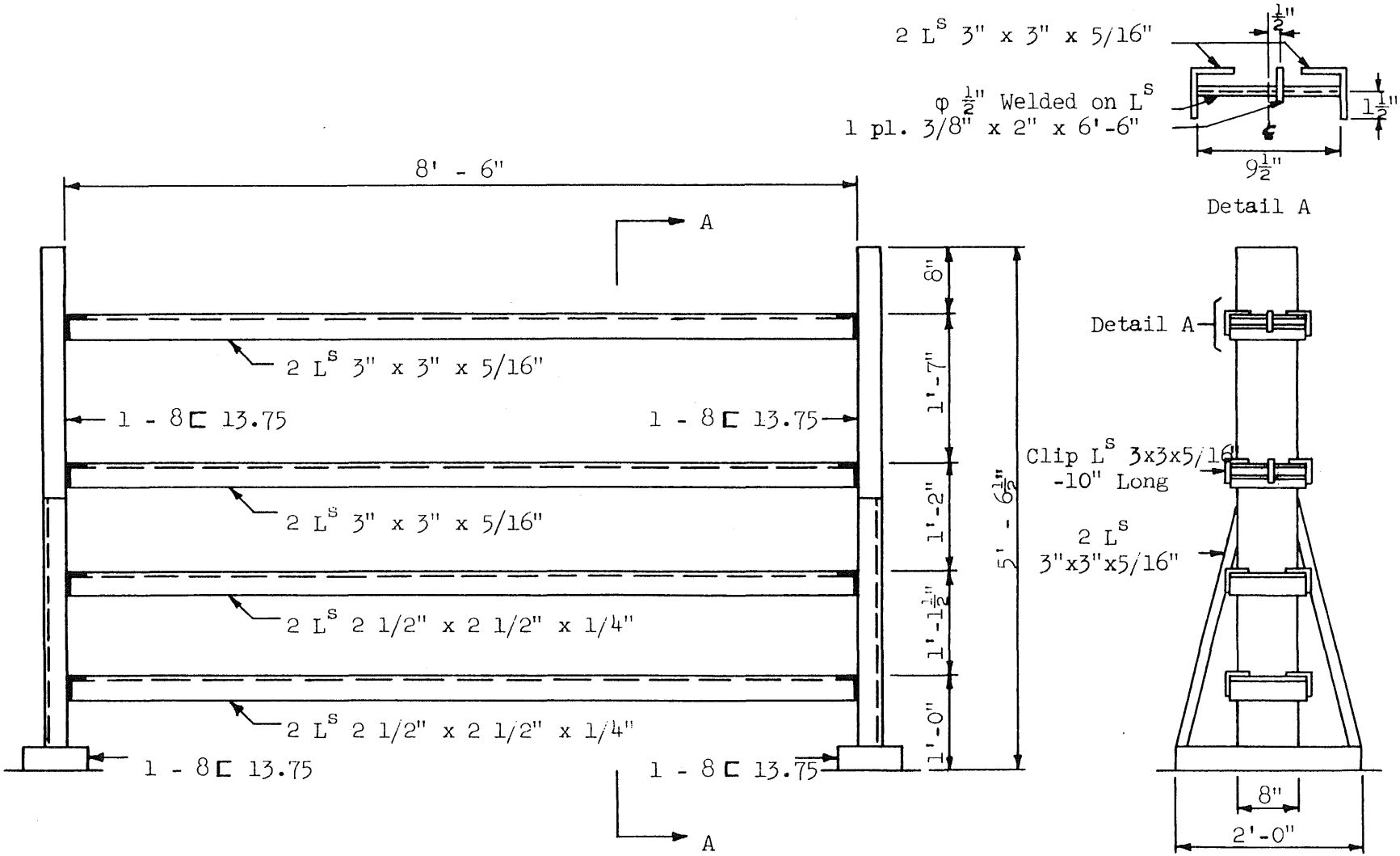

Note: All connections are welded.

Fig. 8. Dimensions of Storage Frame for Beams

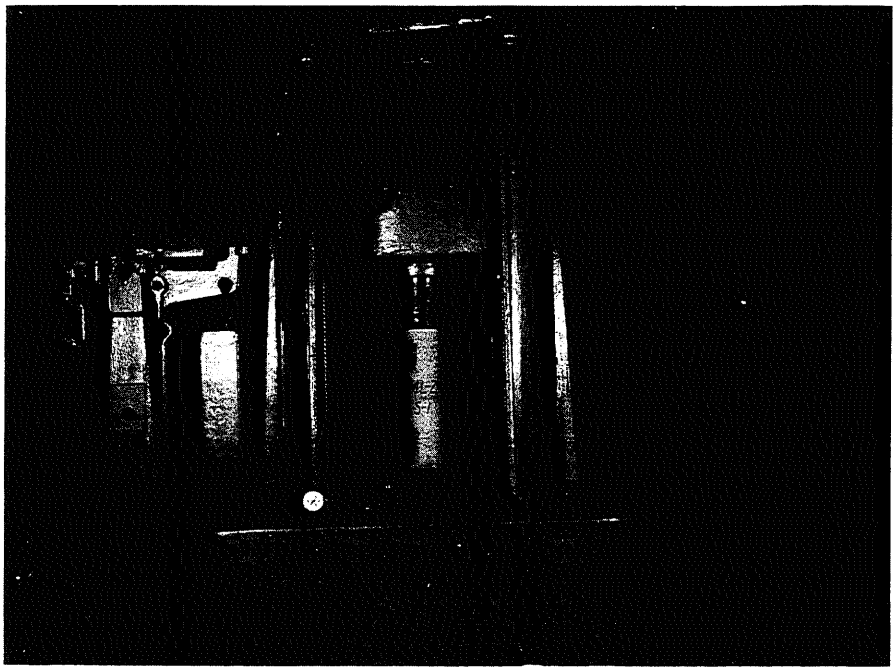

Fig. 9. Loading of 4 by 16-in. Cylinder in Olsen Testing Machine

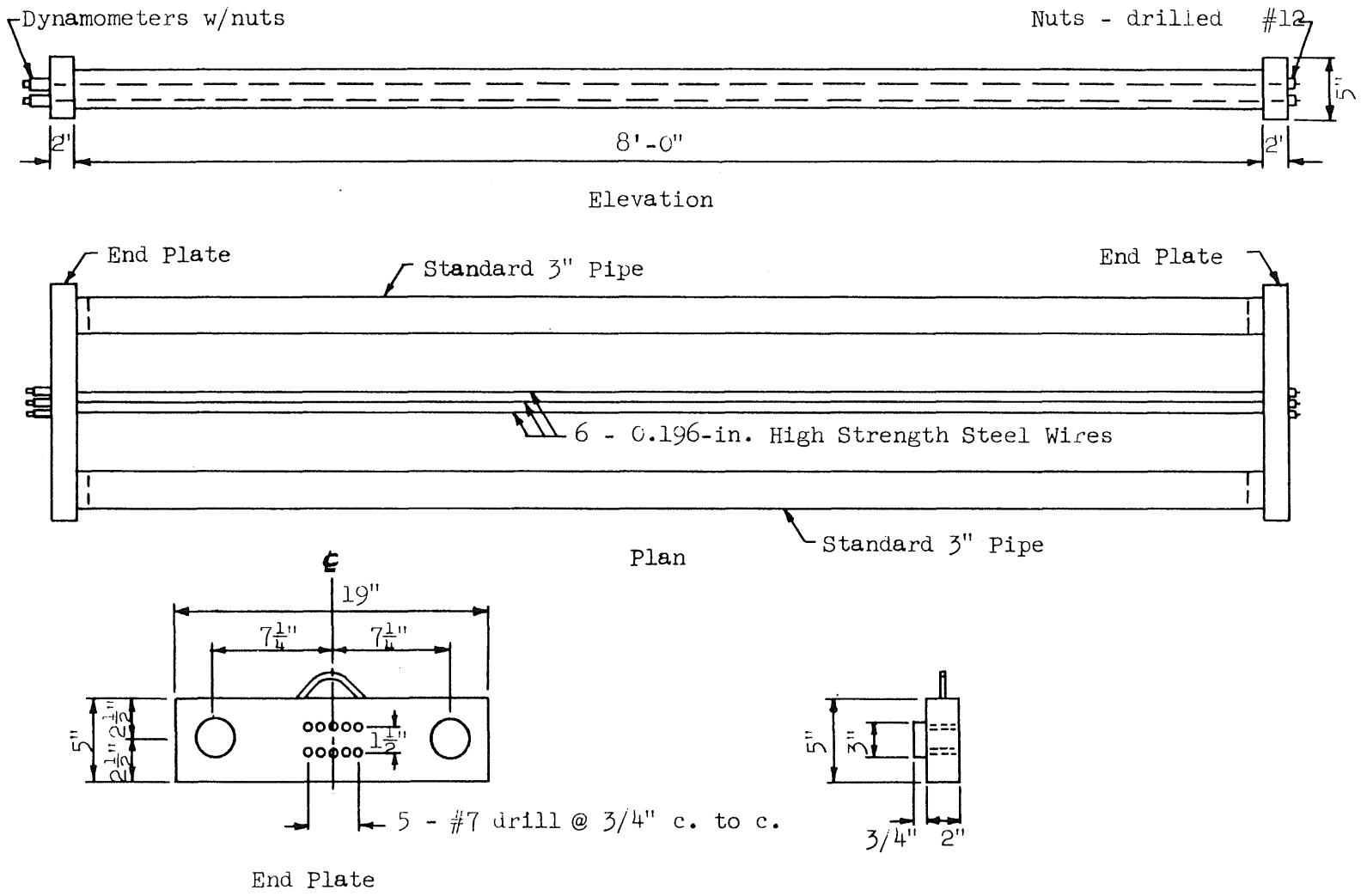

Fig. 10. Dimensions of Prestressing Frame

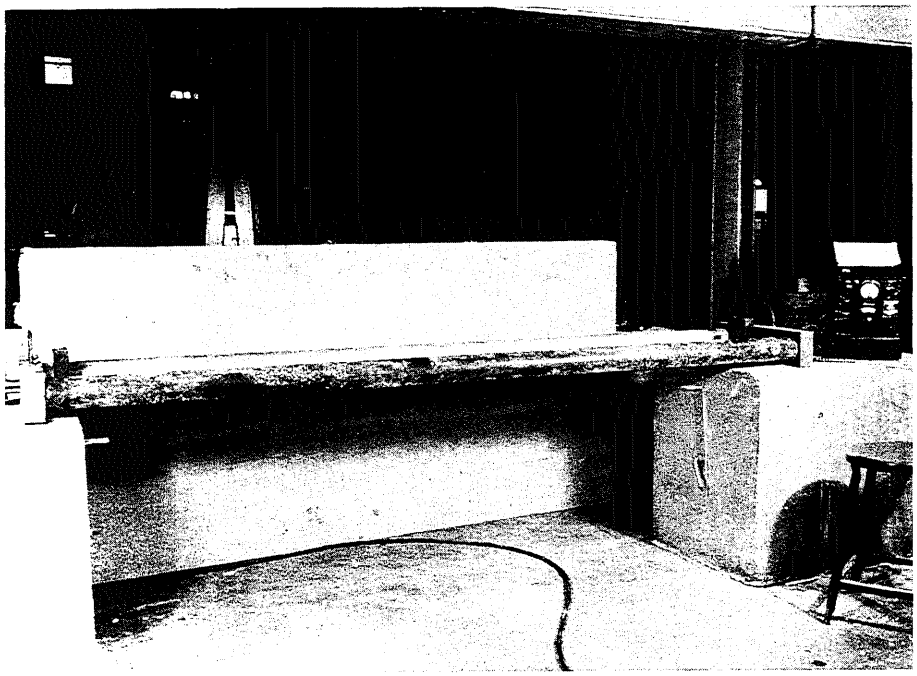

Fig. 11. View of Prestressing Frame
During Tensioning of Wires

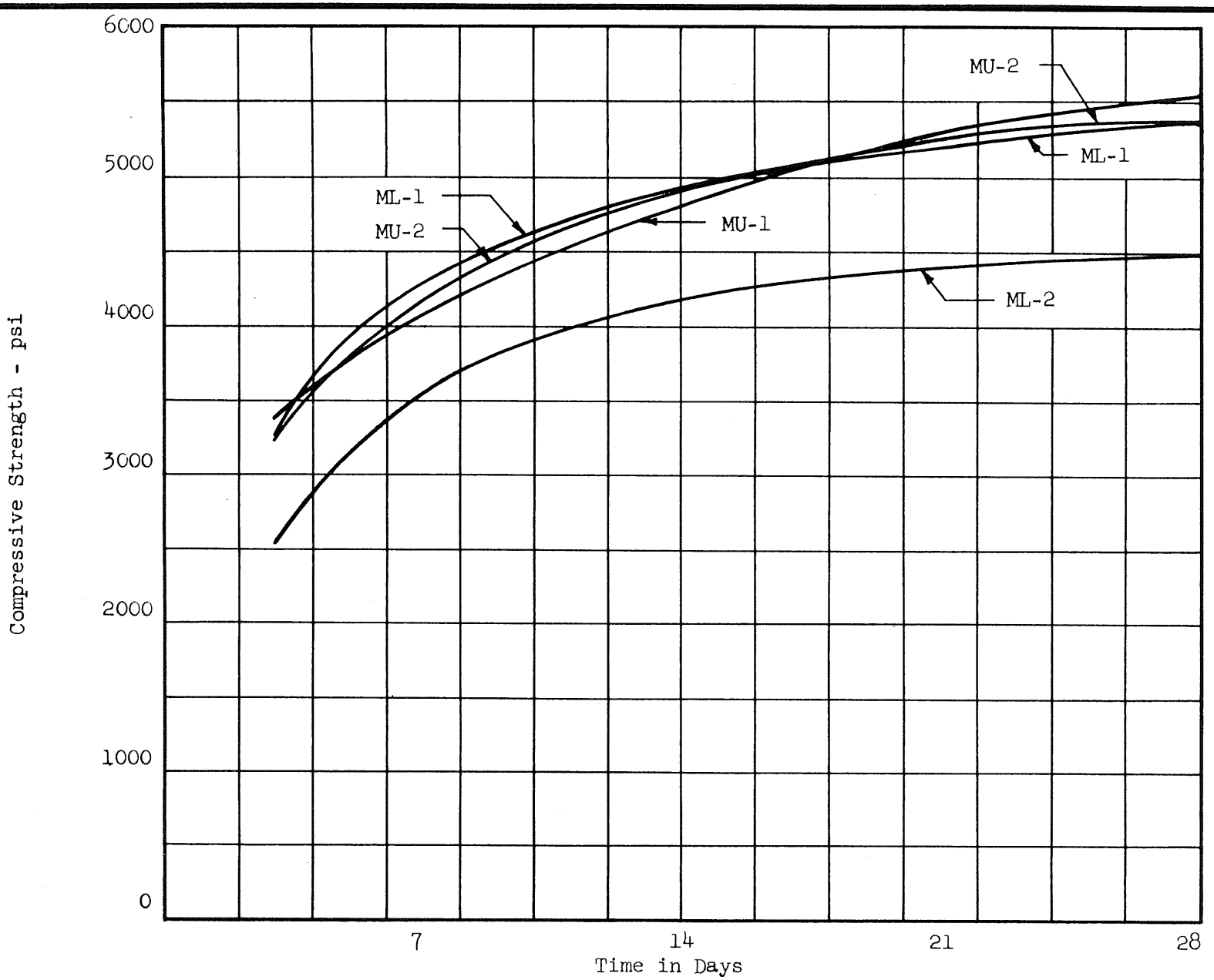

Fig. 12. Plot of Concrete Strength Versus Time Based on 6 by 12-in. Cylinders

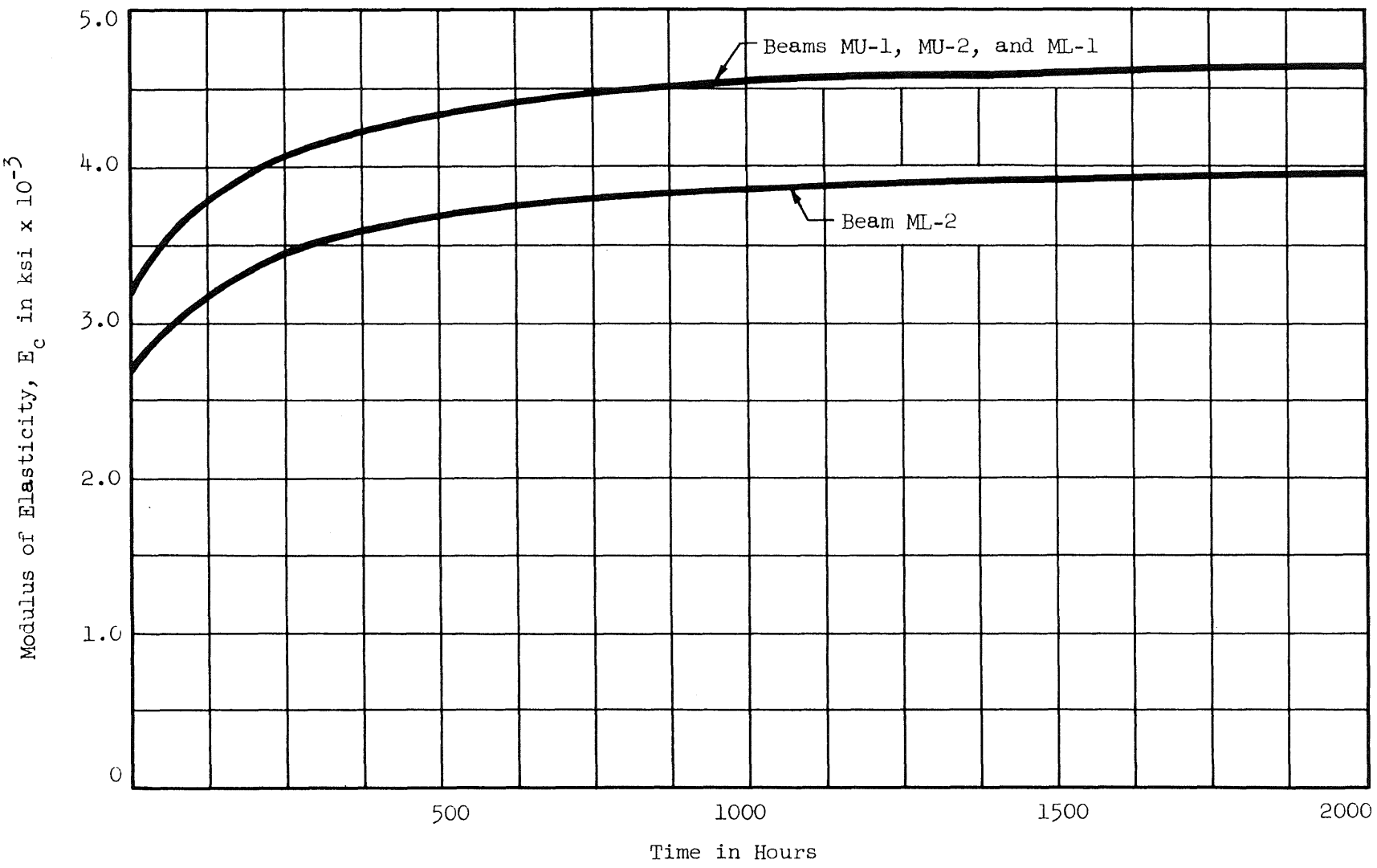

Fig. 13. Plot of Modulus of Elasticity Versus Time

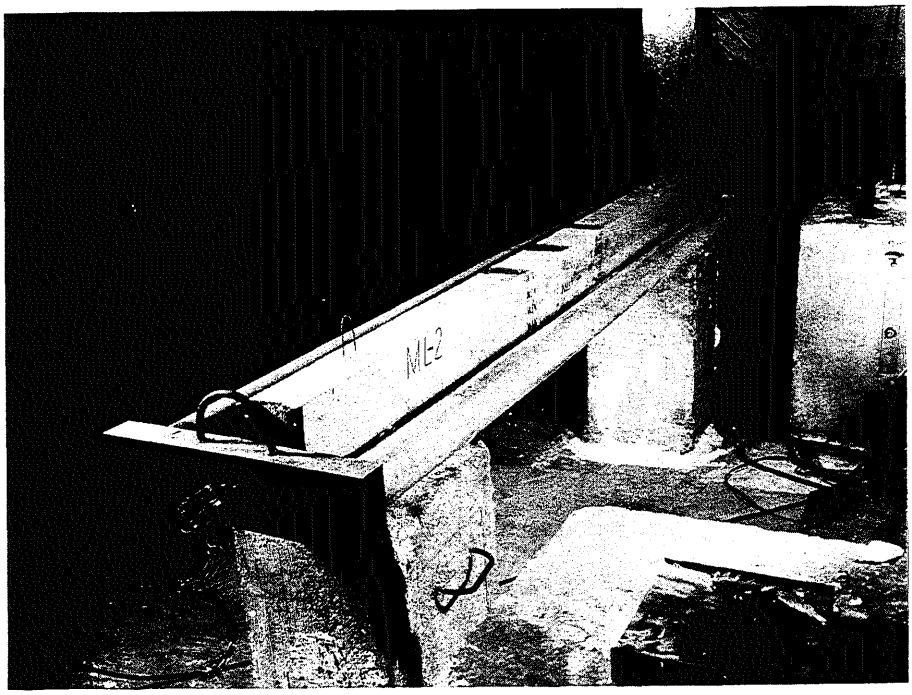

Fig. 14. View of Beam Before Release

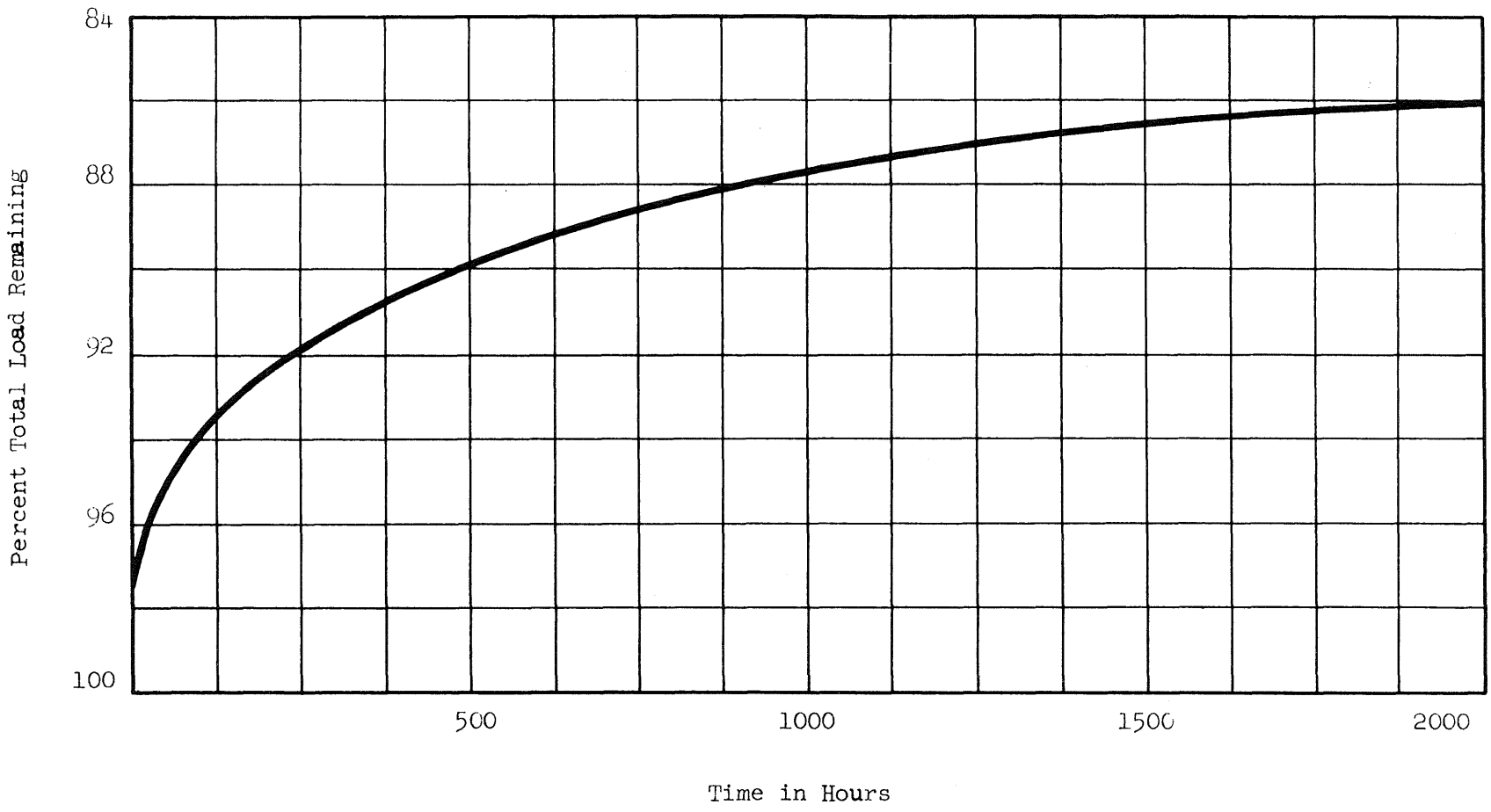

Fig. 15. Plot of Loss in Spring Load Versus Time for Beam ML-1

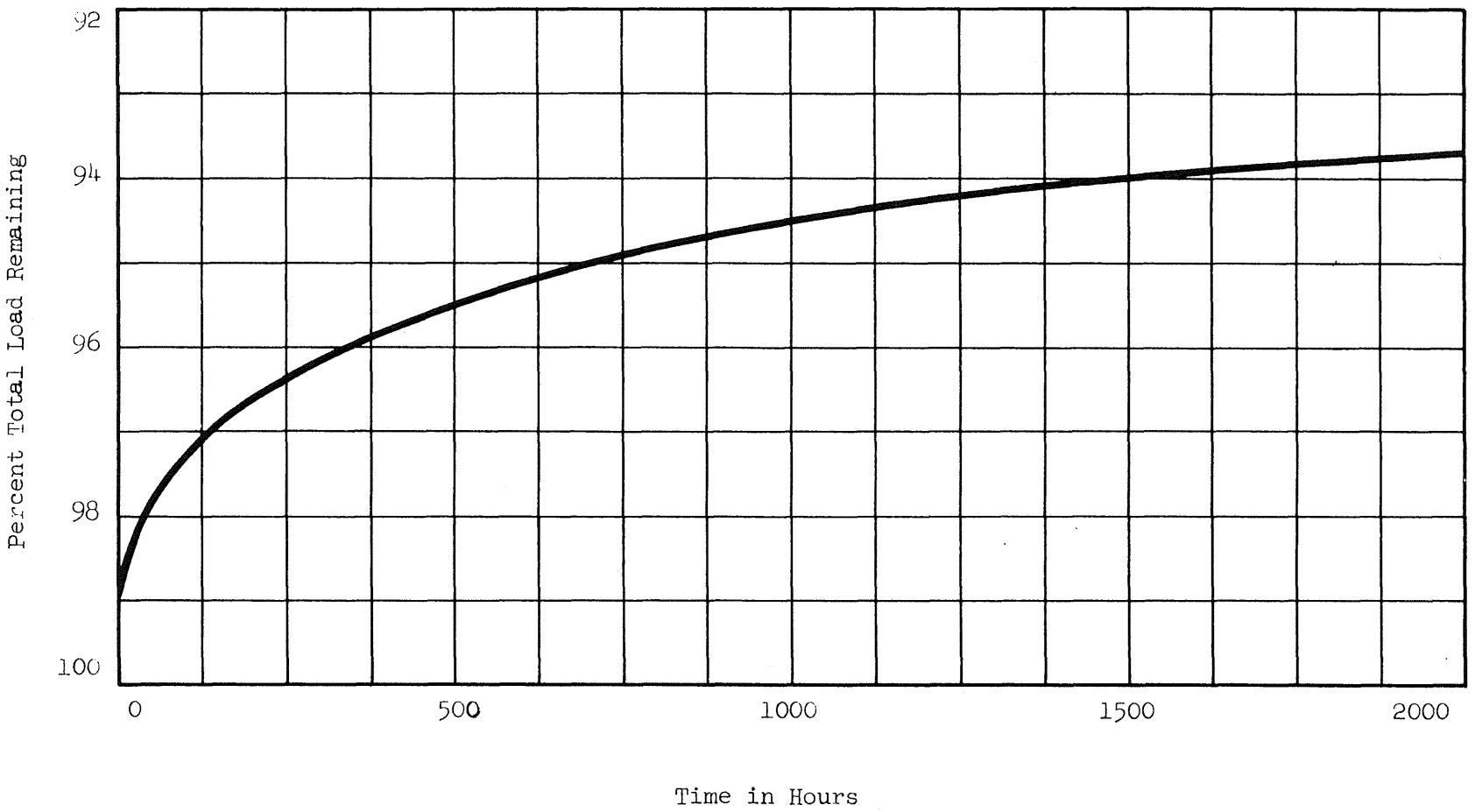

Fig. 16. Plot of Loss in Spring Load Versus Time for Beam ML-2

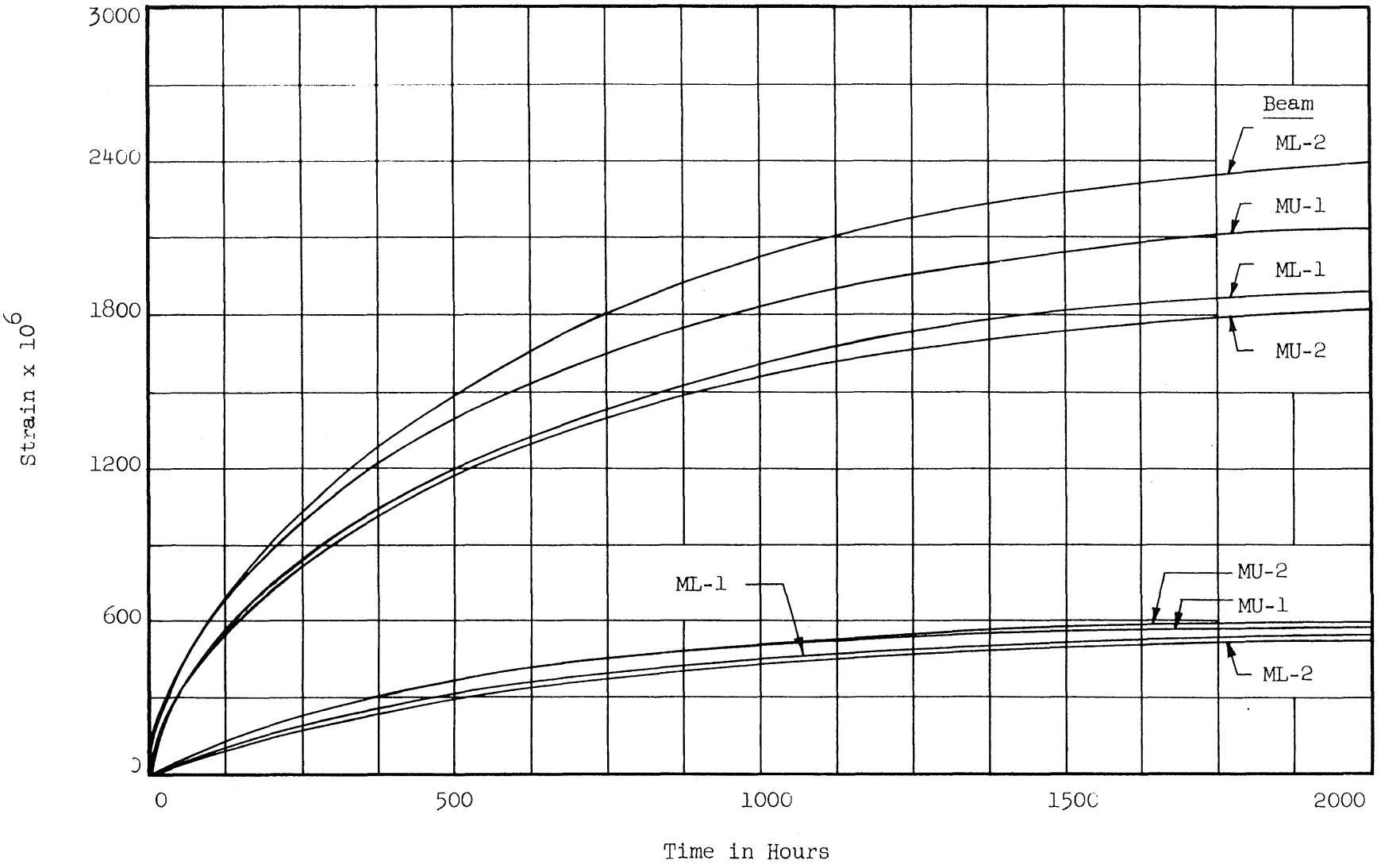

Fig. 17. Measured Total Strains for 4 by 16-in. Cylinders

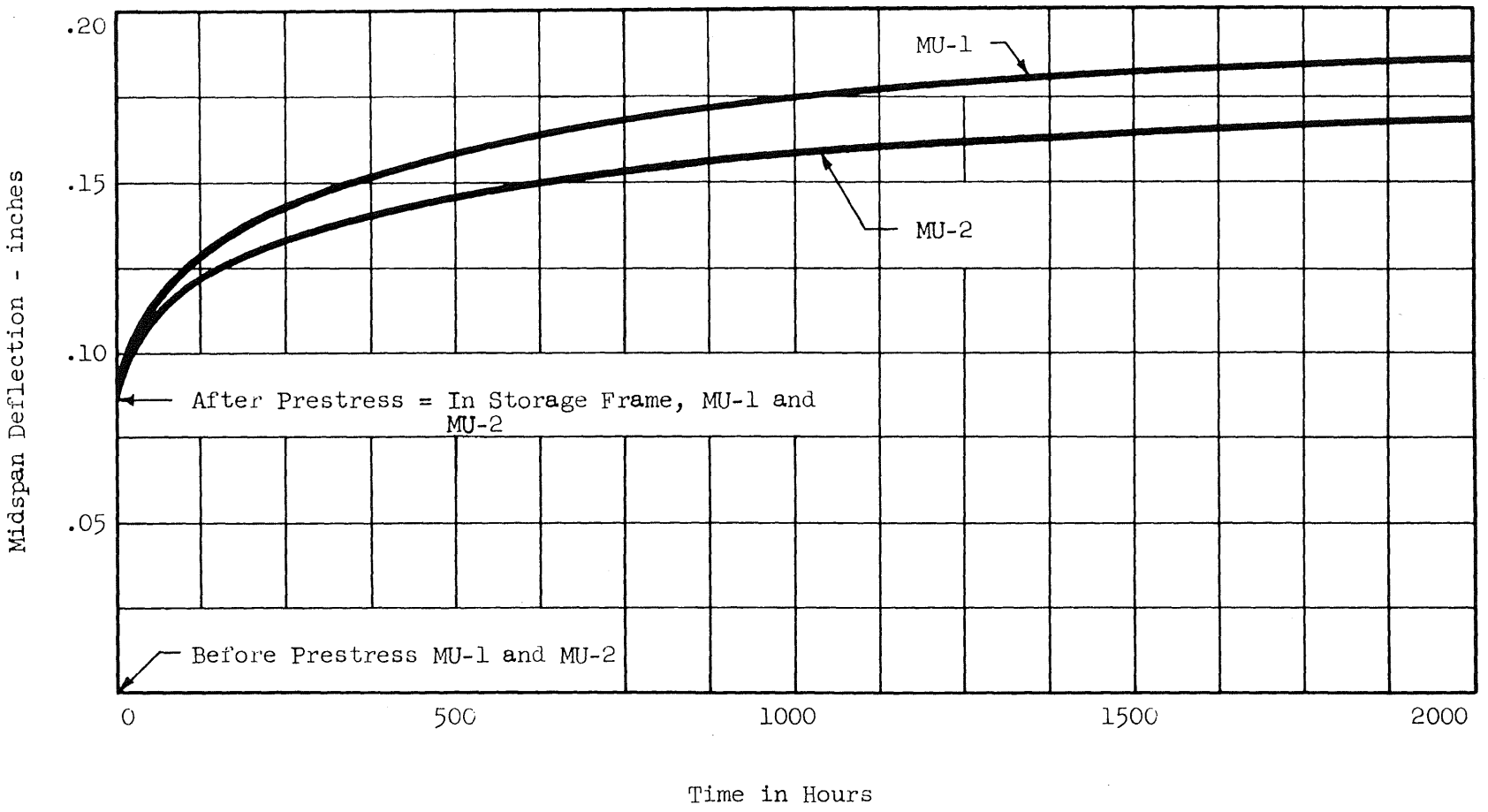

Fig. 18. Midspan Deflection Versus Time for Unloaded Beams

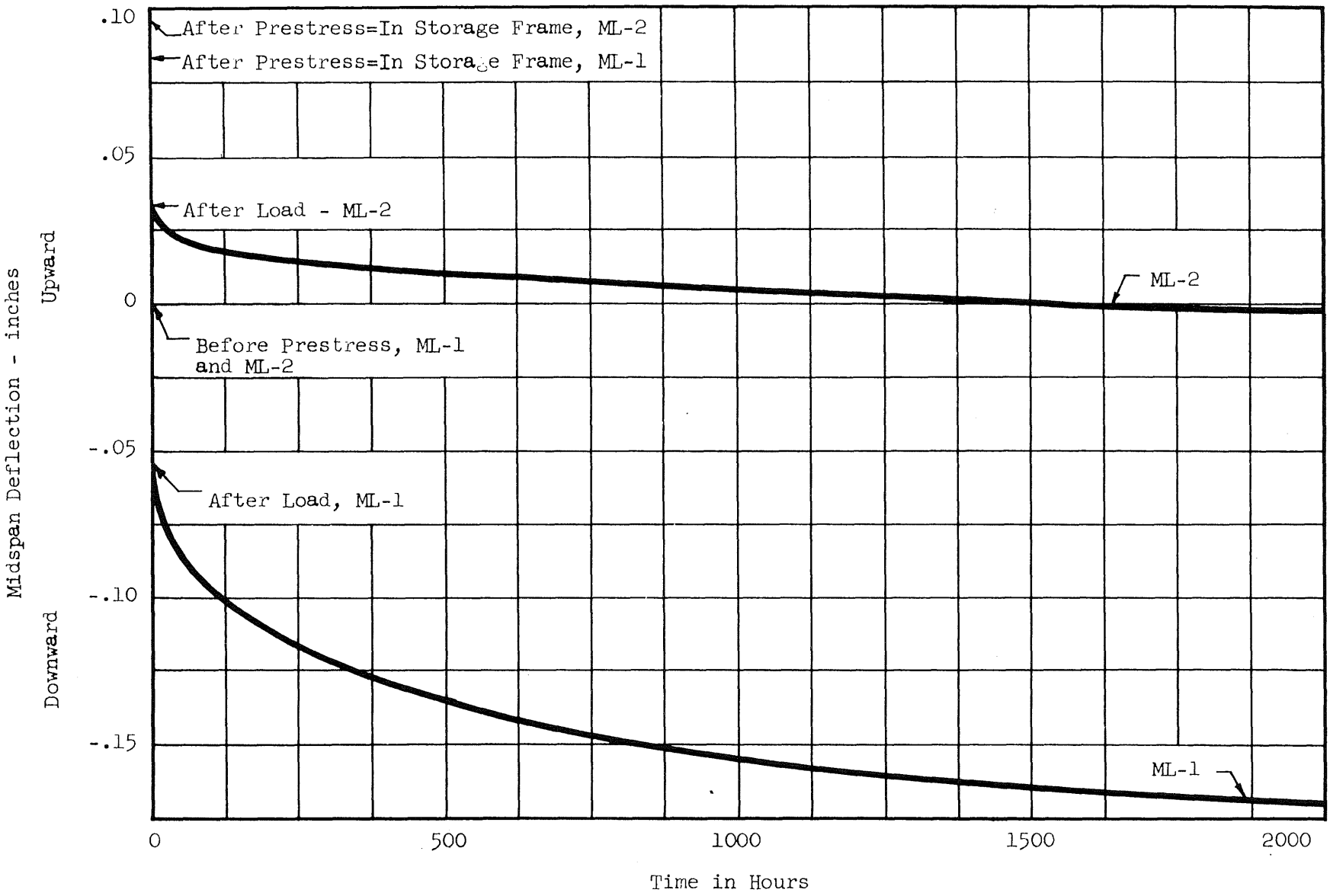

Fig. 19. Midspan Deflection Versus Time For Loaded Beams

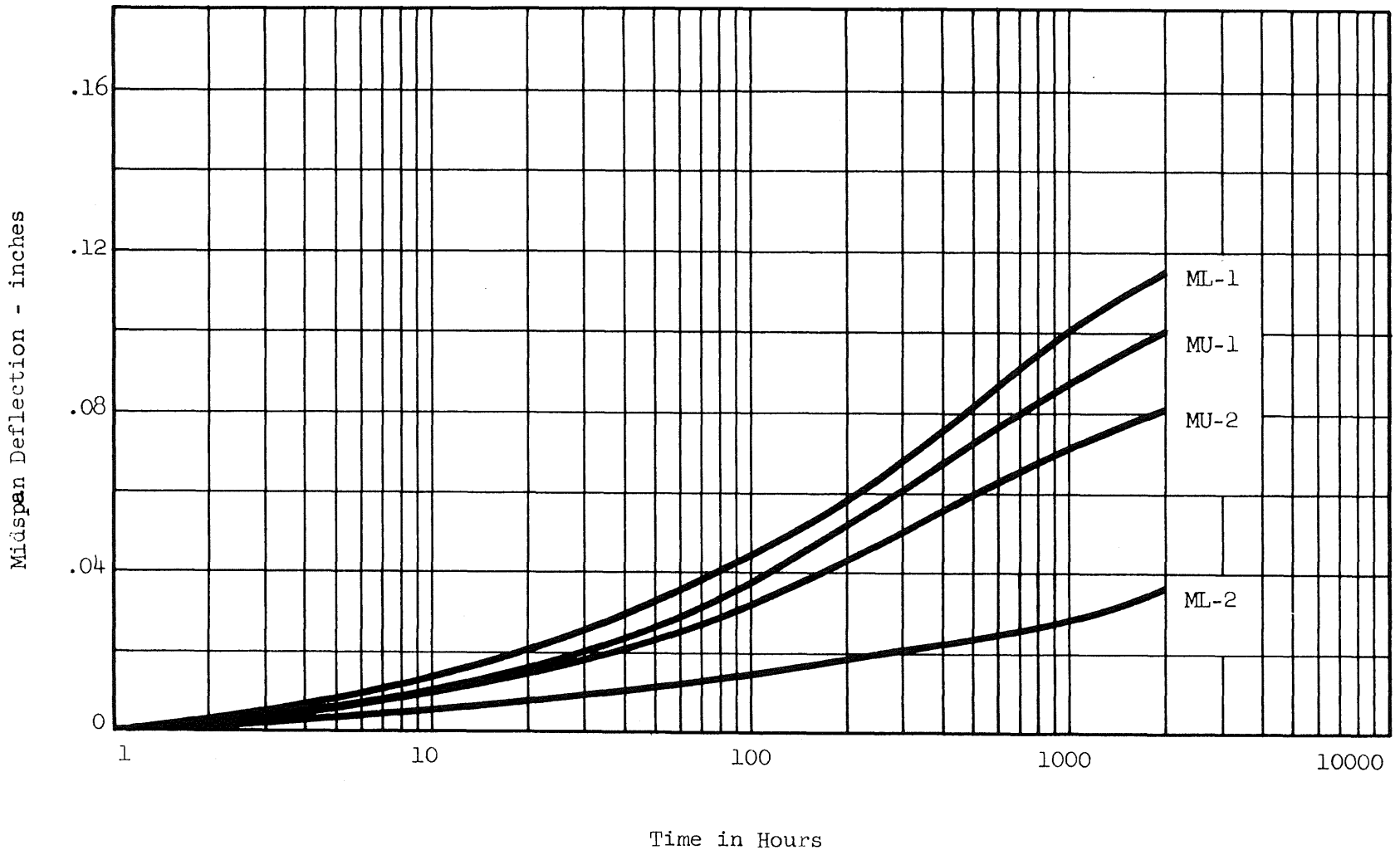

Fig. 20. Comparison of Midspan Deflections for Beams Versus Time

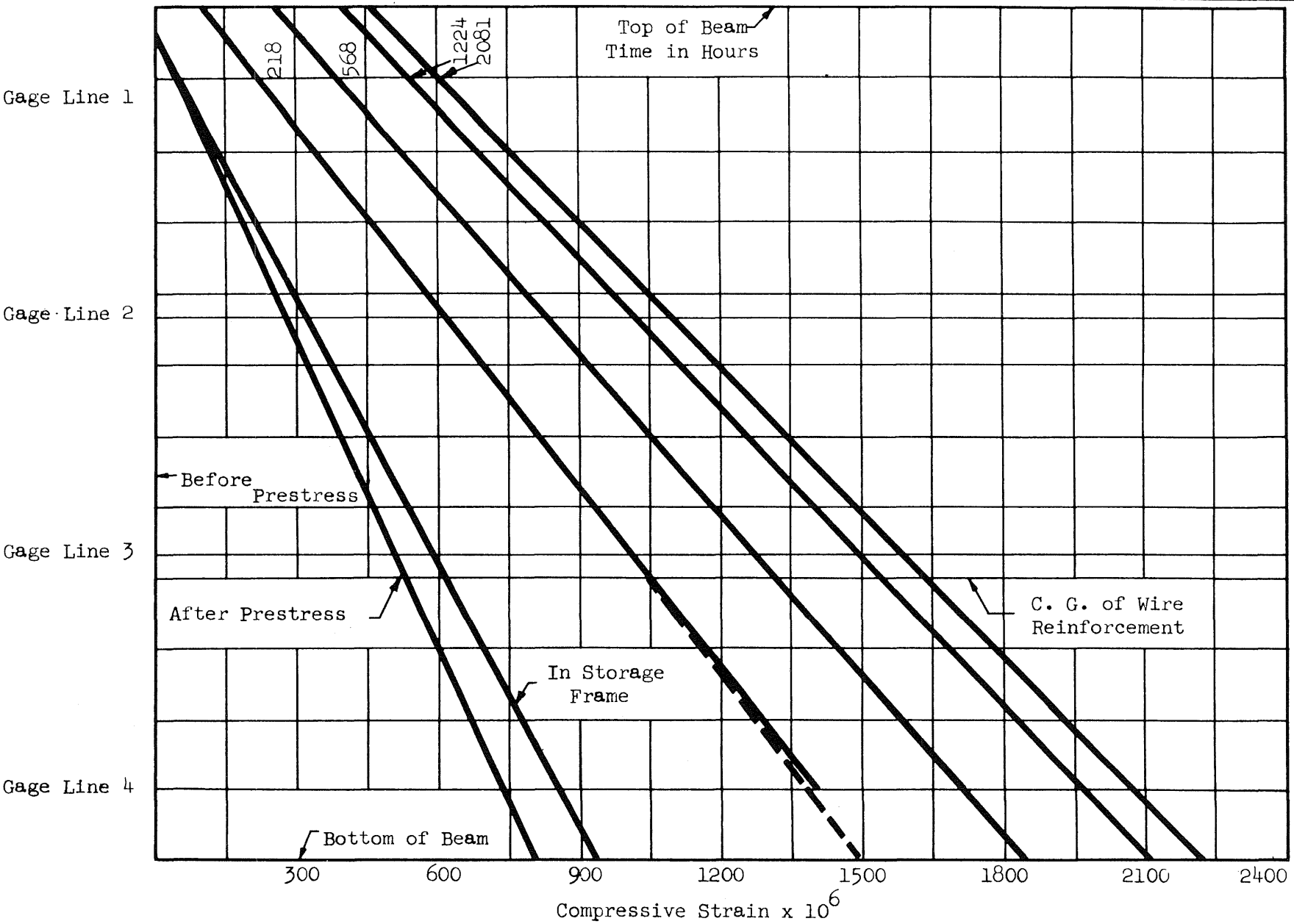

Fig. 21. Successive Strain Distributions in Beam MU-1

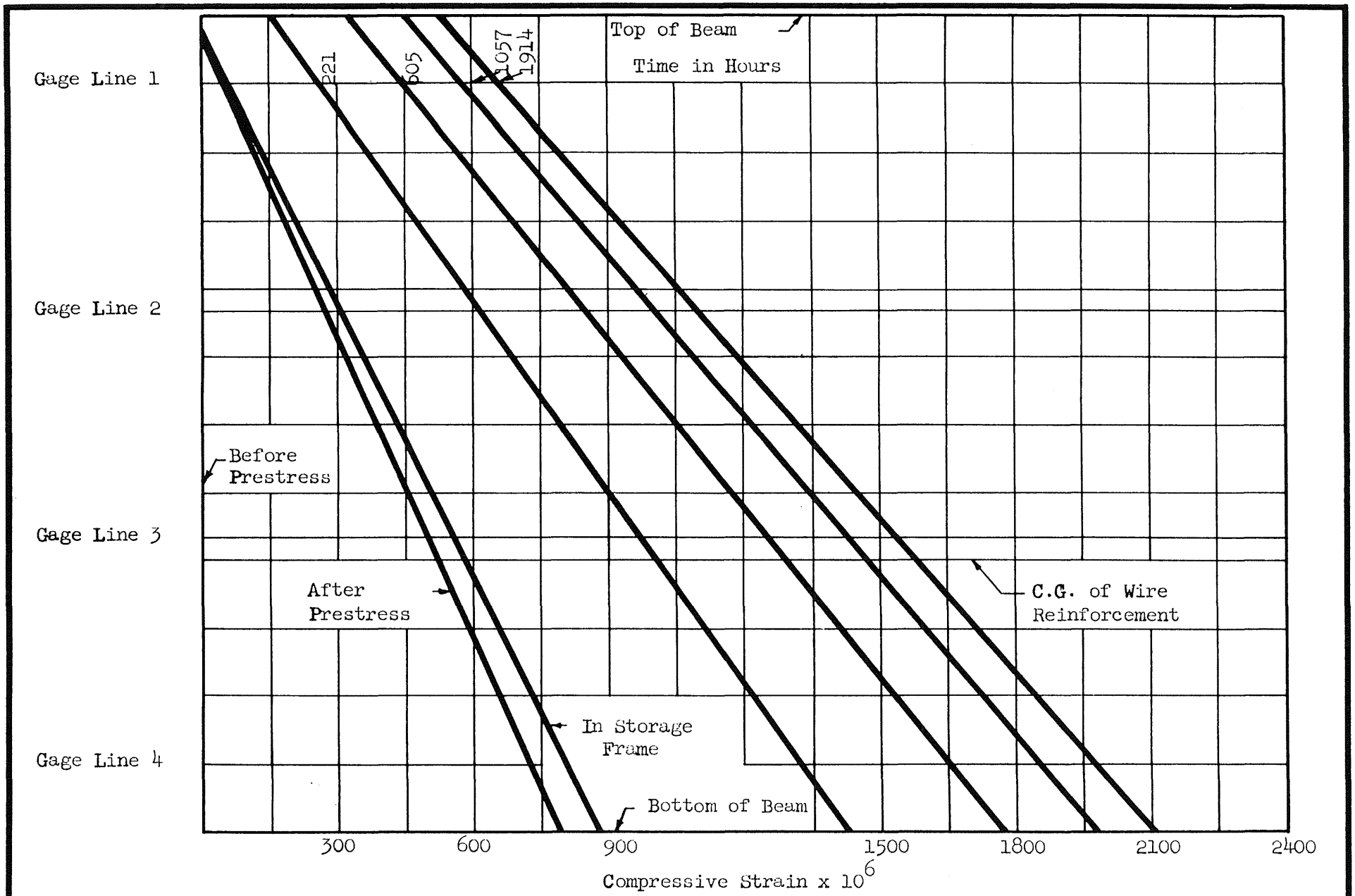

Fig. 22. Successive Strain Distributions in Beam MU-2

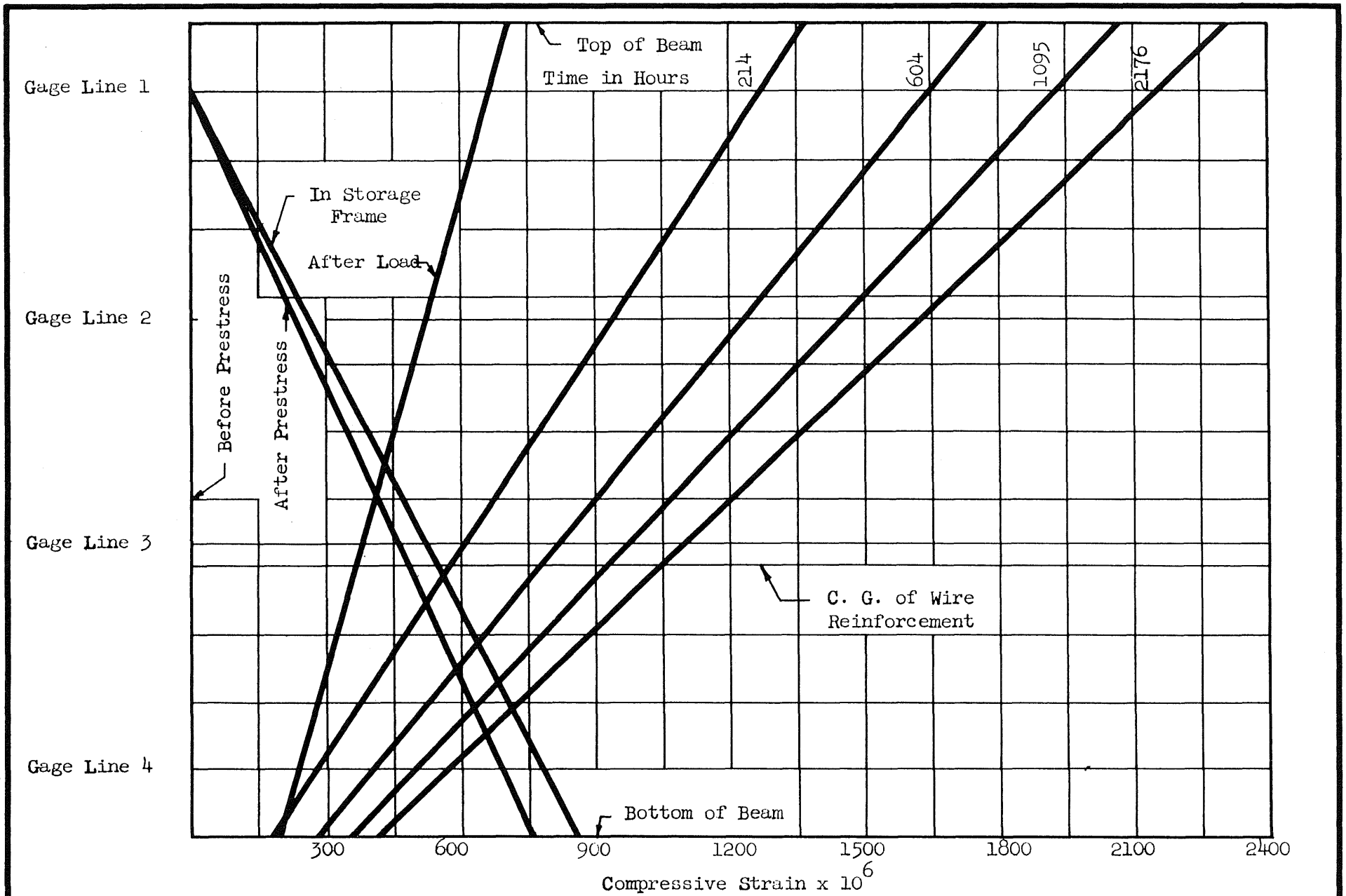

Fig. 23. Successive Strain Distributions in Beam ML-1

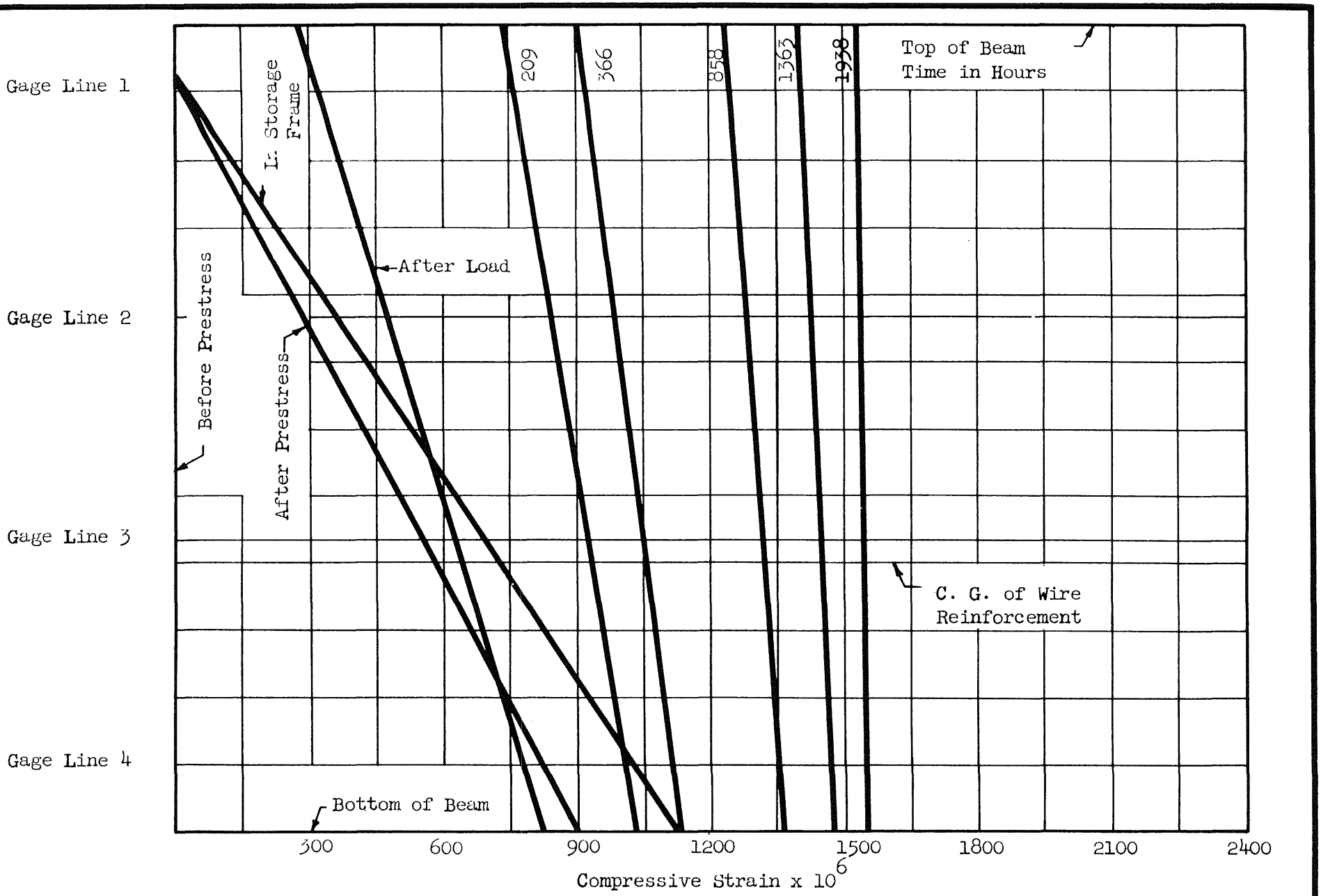

Fig. 24. Successive Strain Distributions in Beam ML-2

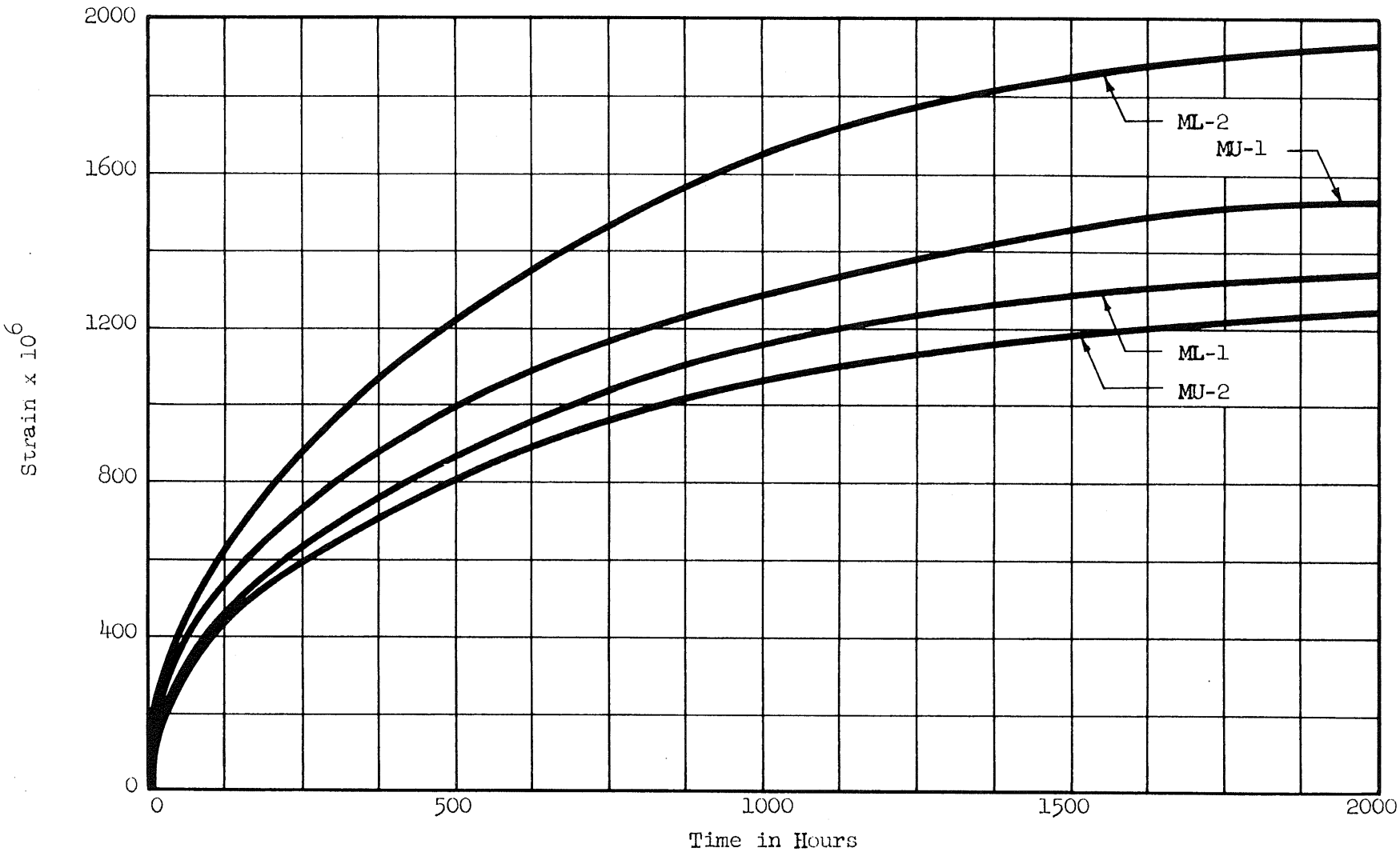

Fig. 25. Creep Strains Versus Time for Loaded Cylinders

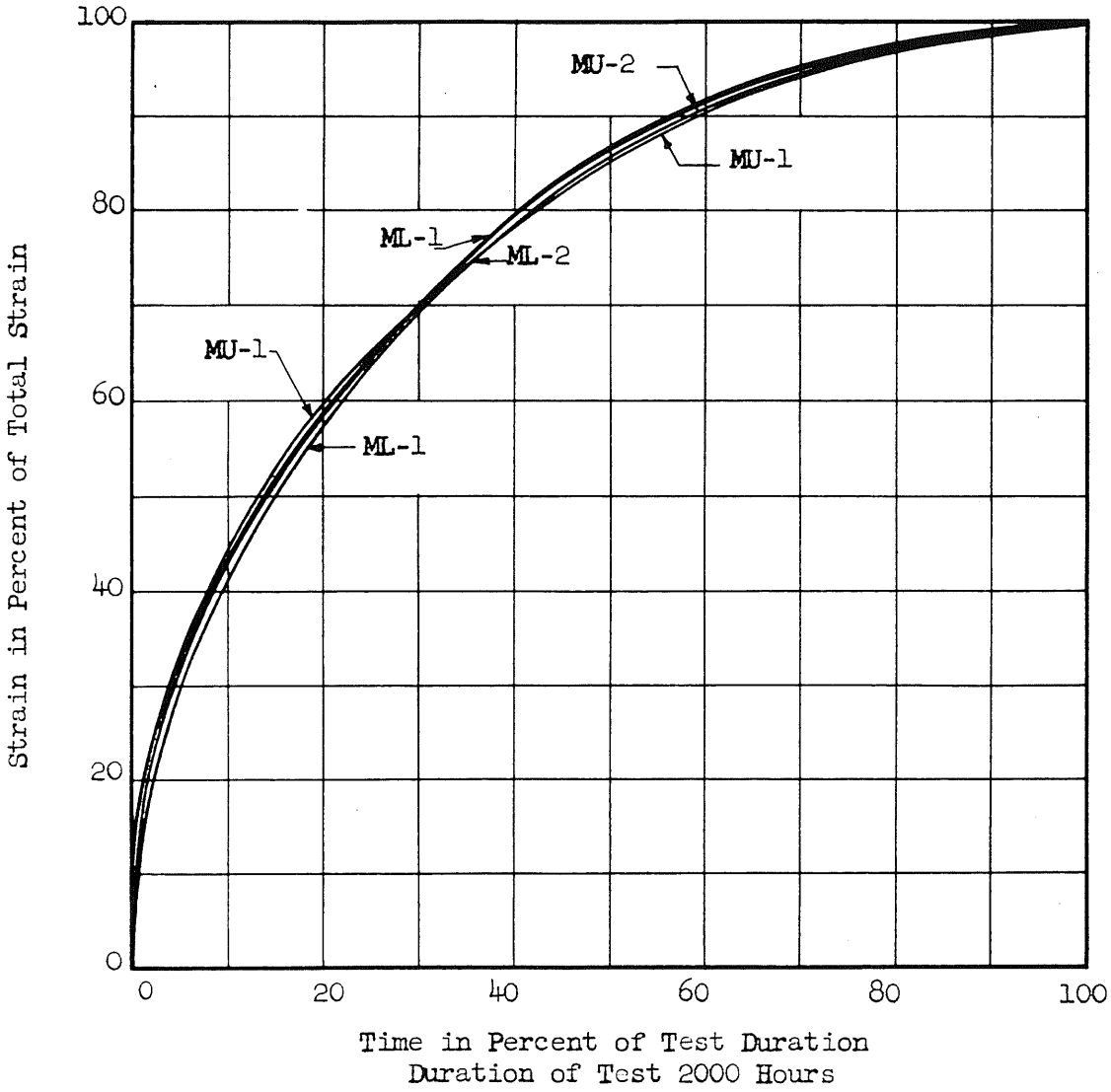

Fig. 26. Dimensionless Plot of Creep Strains Versus Time for Loaded Cylinders

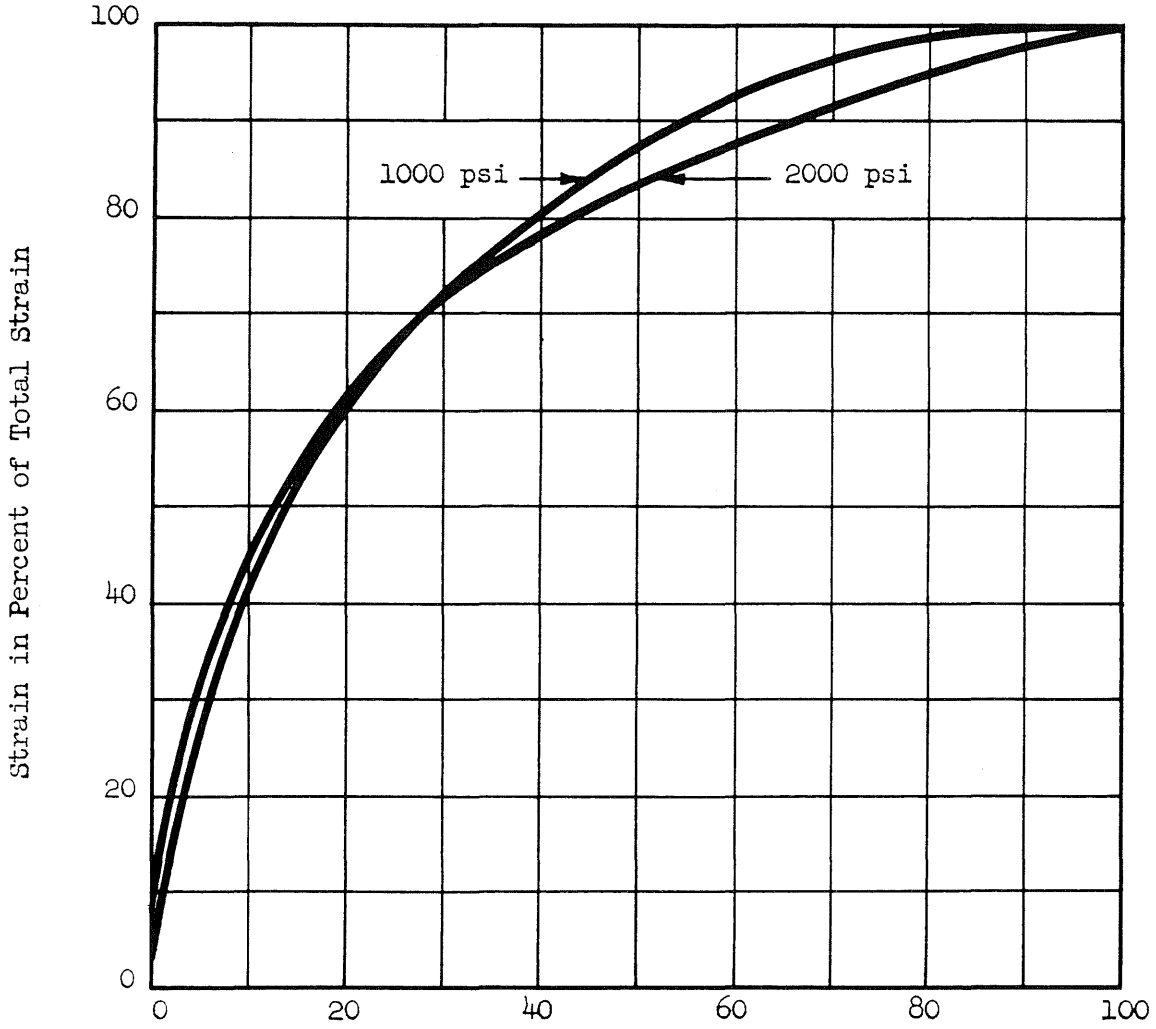

Fig. 27. Dimensionless Plot of Creep Strains Versus Time at Different Levels of Stress

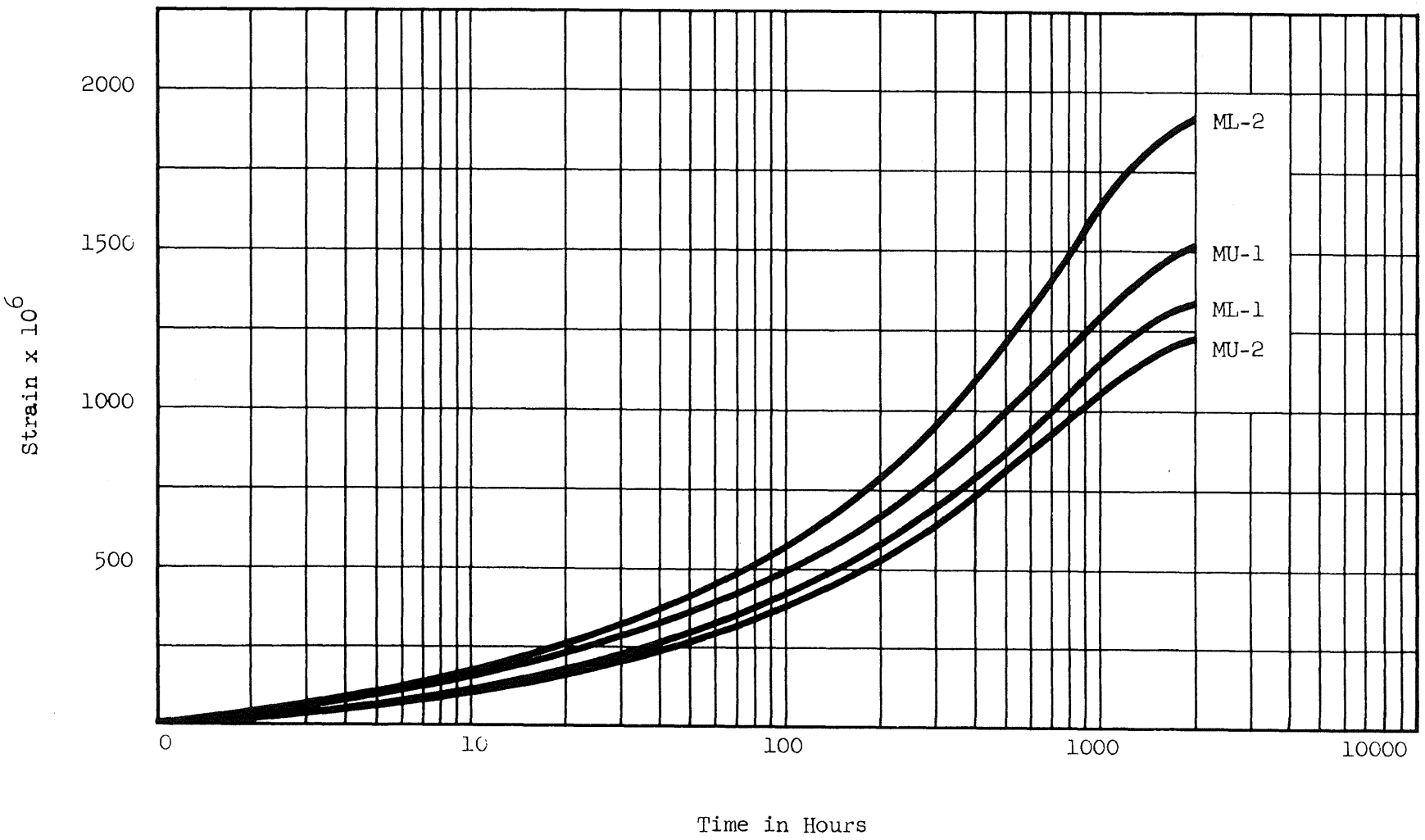

Fig. 28. Comparison of Creep Strains for Loaded Cylinders Versus Time

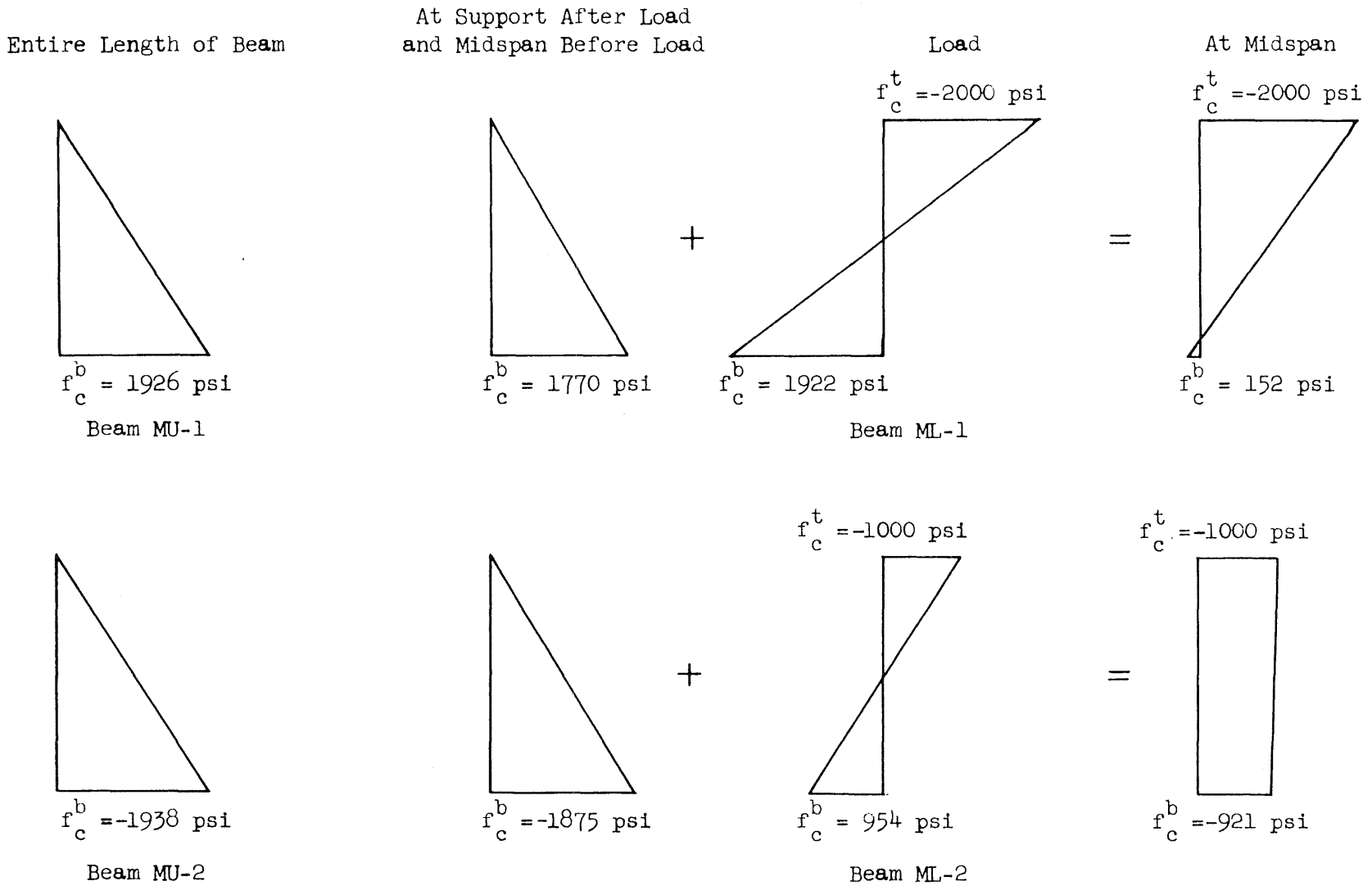

Fig. 29. Computed Stress Distribution in Beams

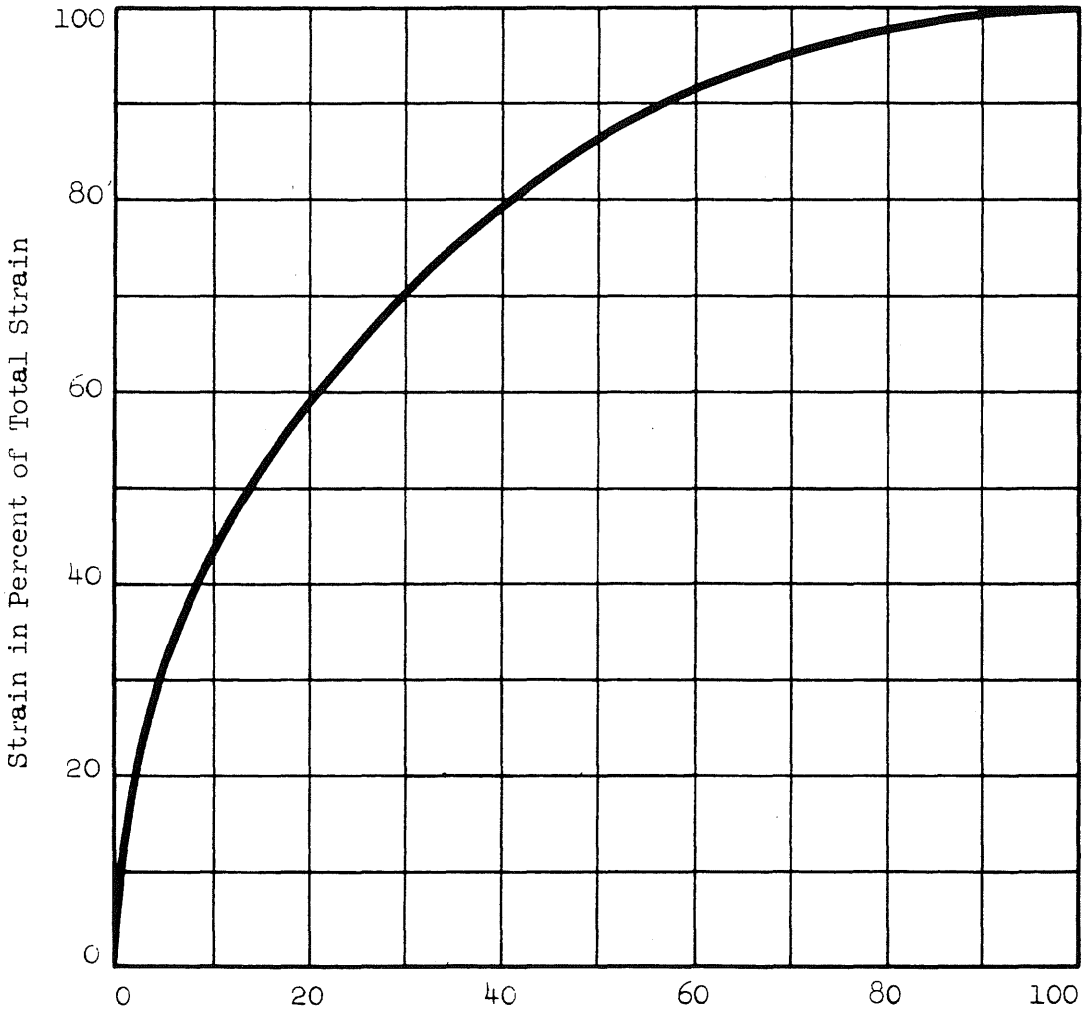

Fig. 30. Dimensionless Plot of Creep Strains for Computations Versus Time

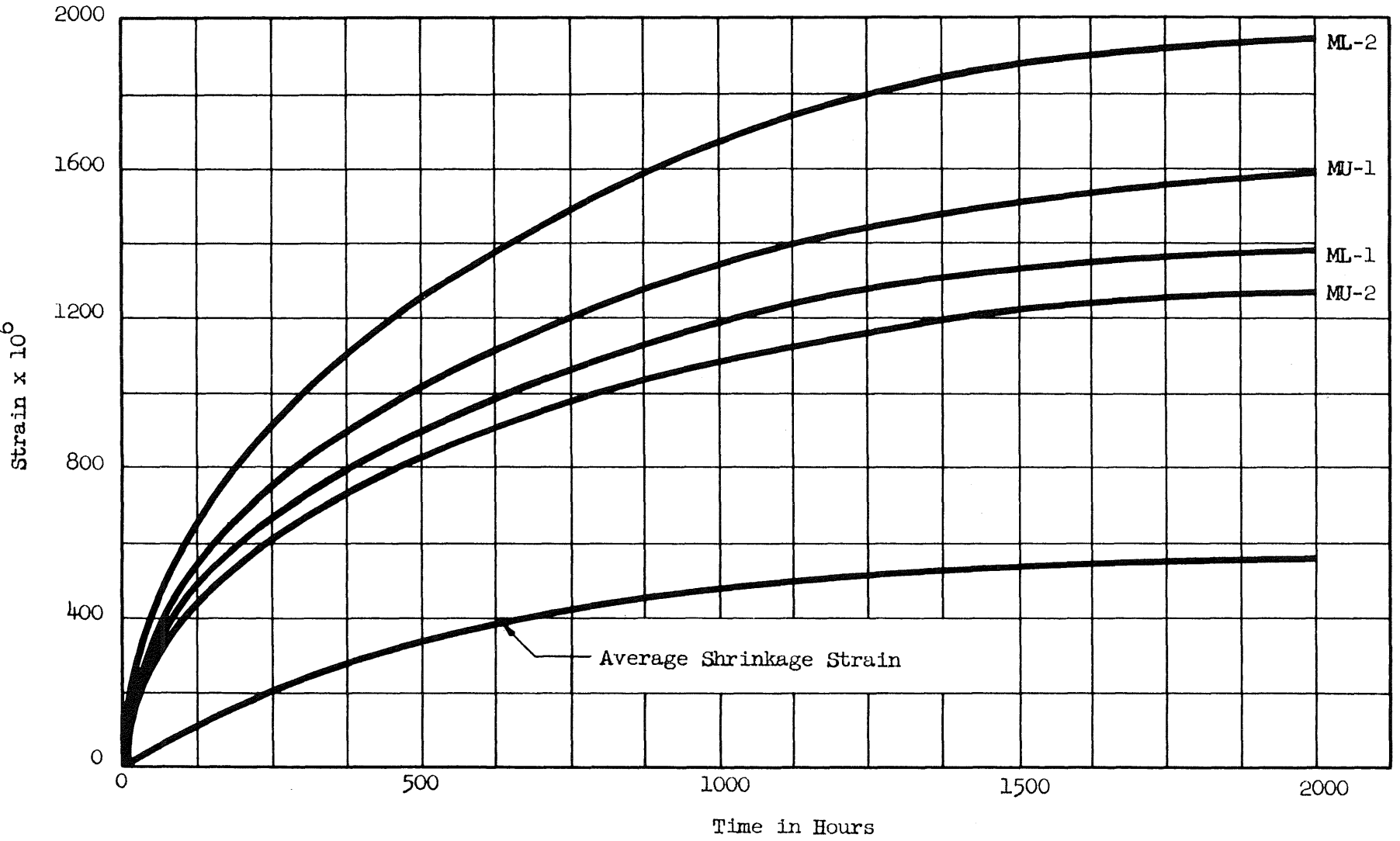

Fig. 31. Creep Strains for Deflection Computations Versus Time, And Average Shrinkage Strains Versus Time

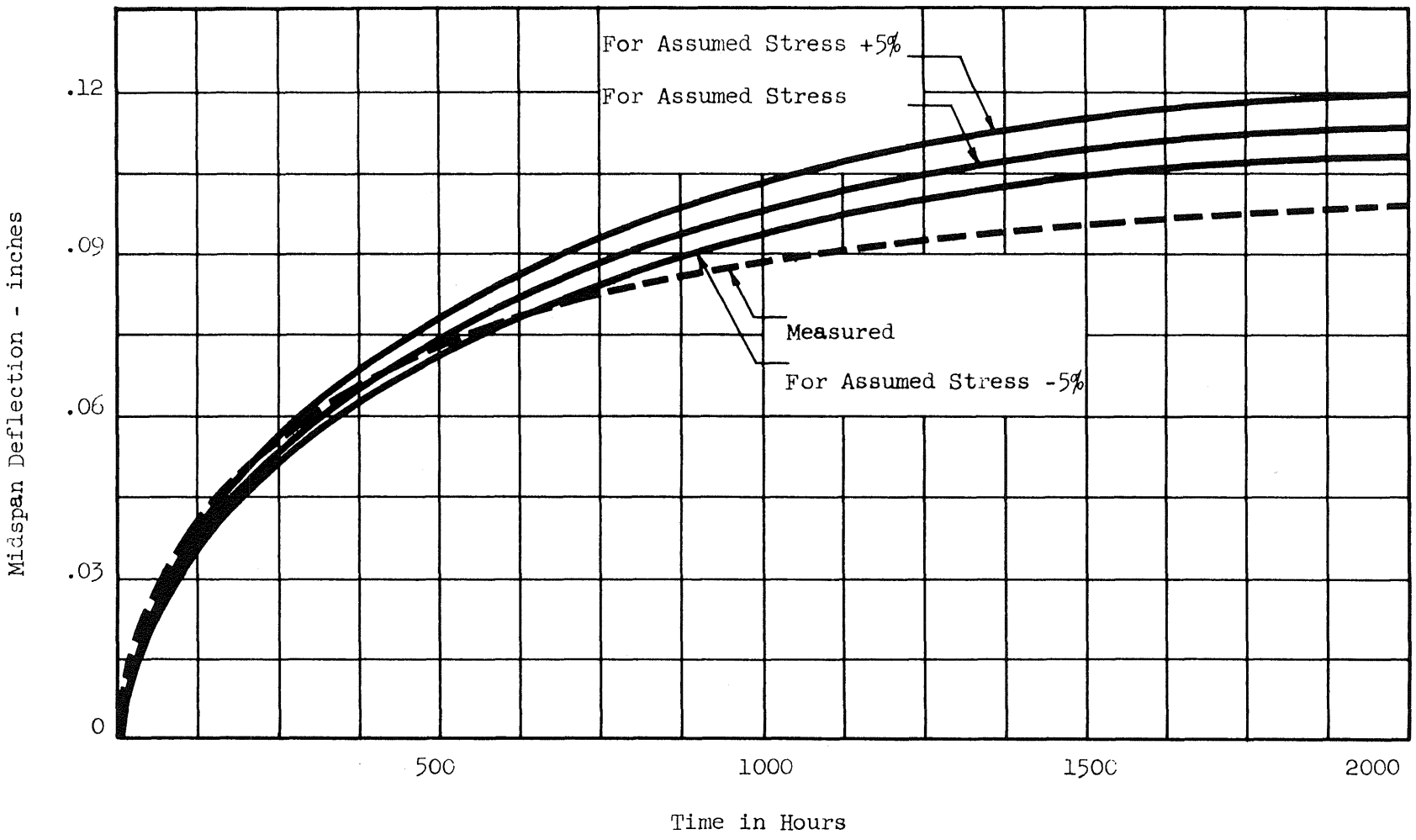

Fig. 32. Measured Deflections and Computed "Exact" Deflections for Beam MU-1

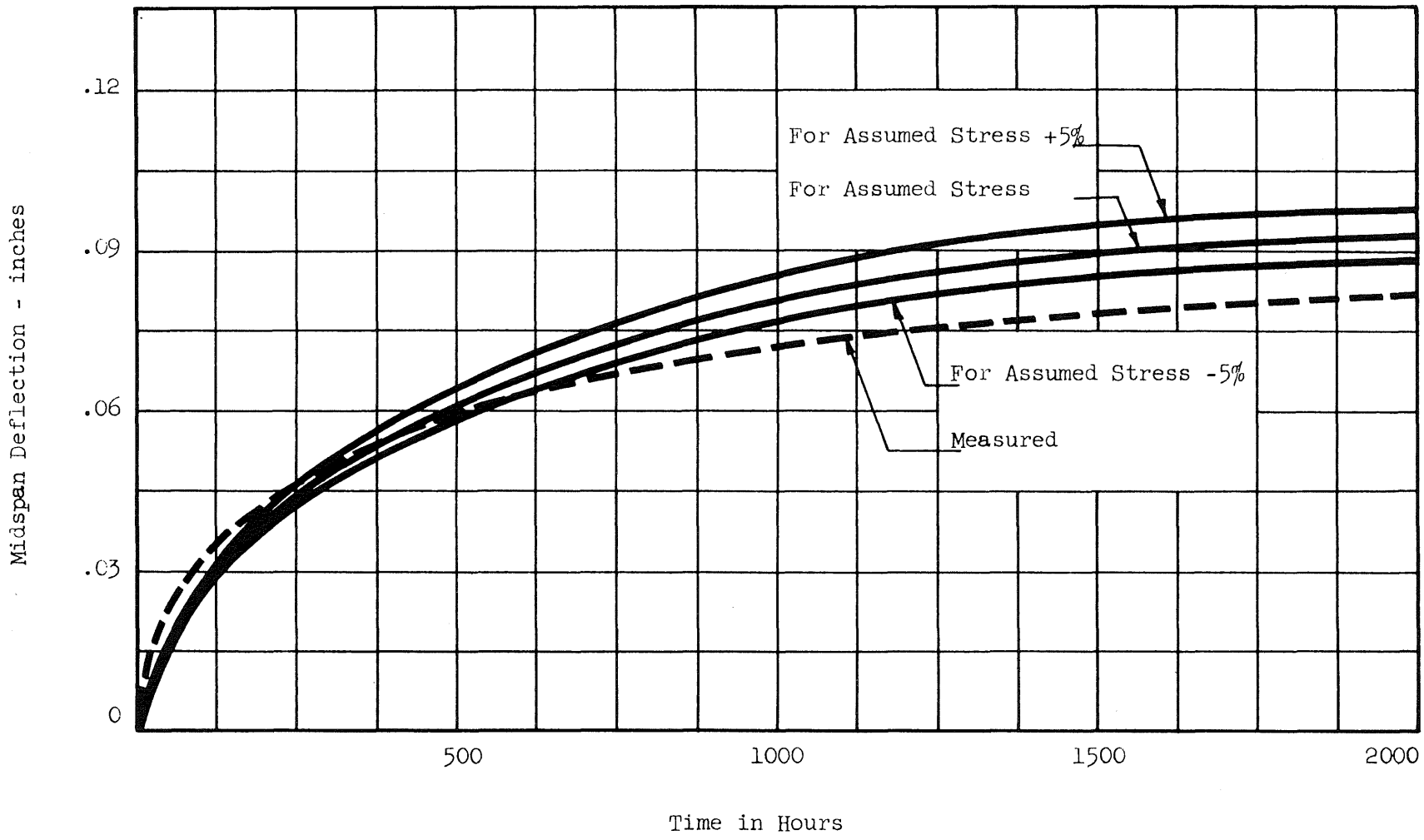

Fig. 33. Measured Deflections and Computed "Exact" Deflections for Beam MU-2

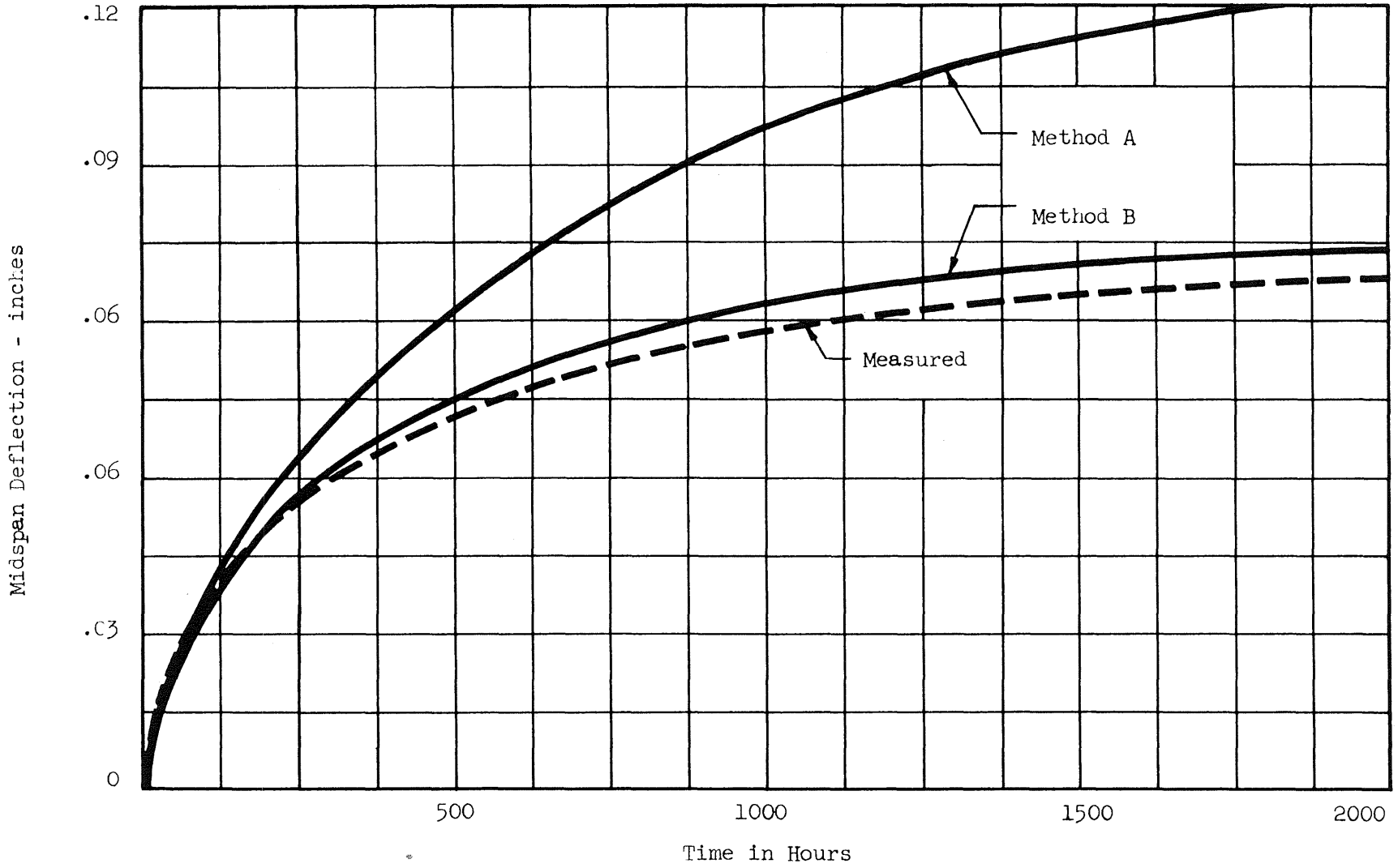

Fig. 34. Measured Deflections and Computed "Approximate" Deflections for Beam MU-1

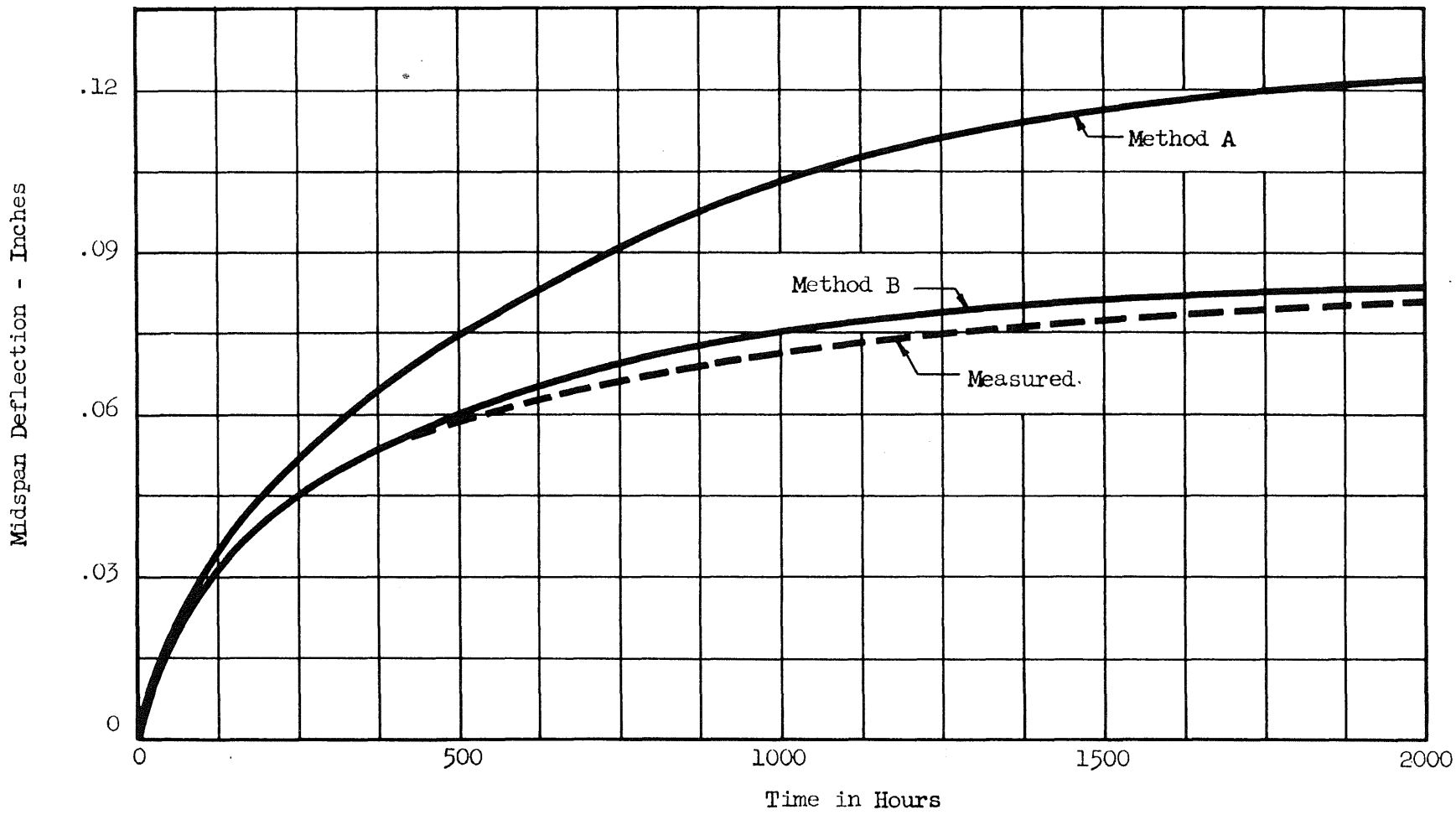

Fig. 35. Measured Deflections and Computed "Approximate" Deflections for Beam MU-2

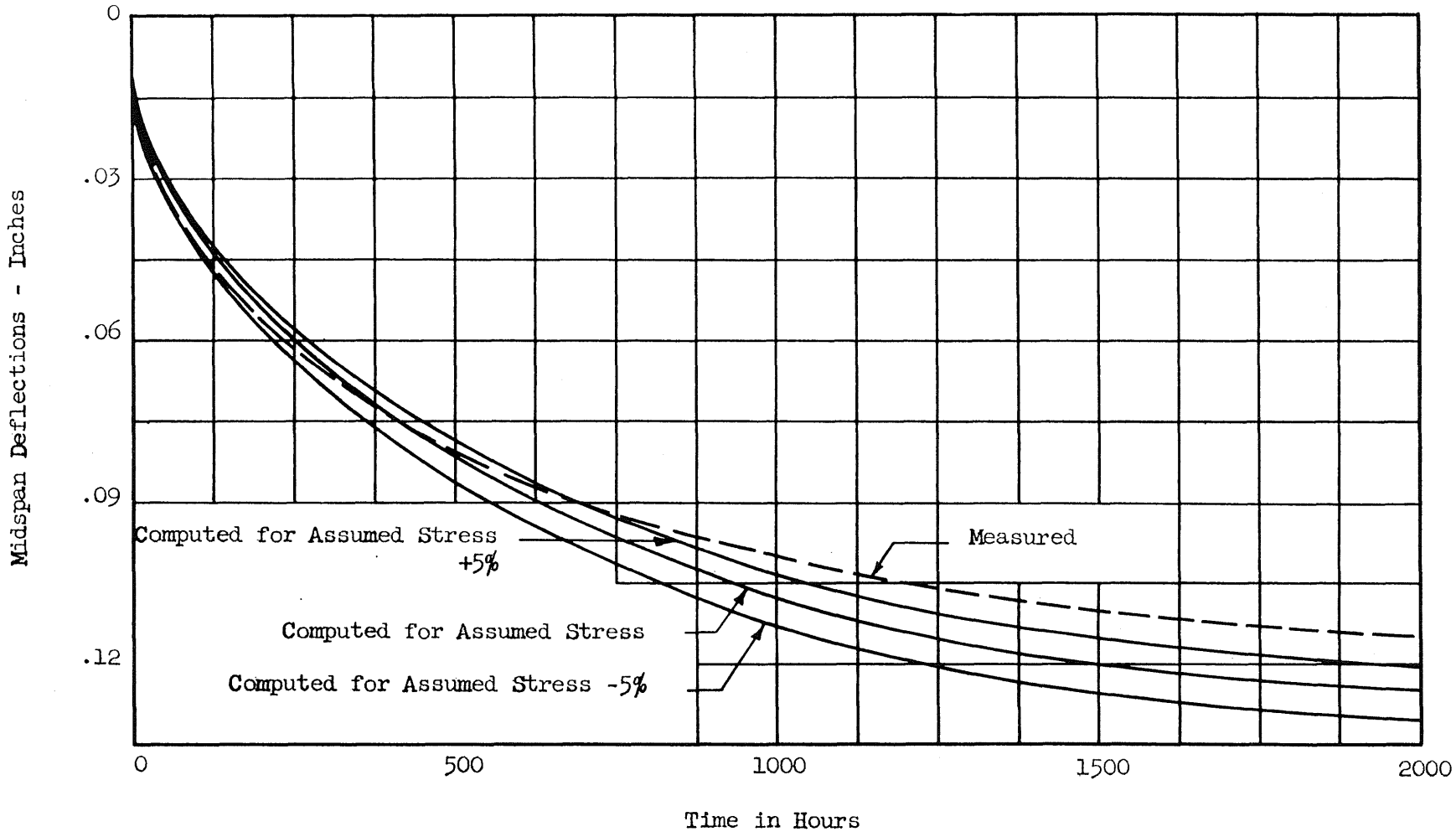

Fig. 36. Measured Deflections and Computed "Exact" Deflections for Beam ML-1

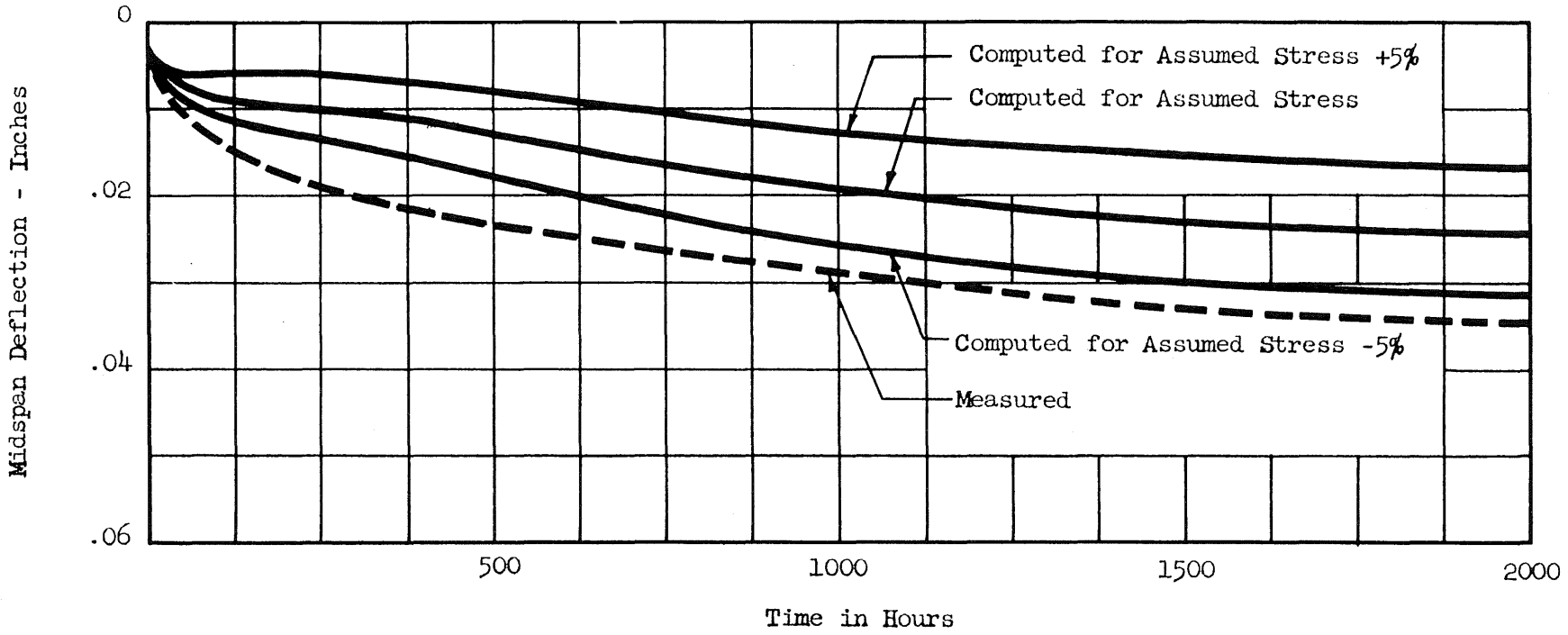

Fig. 37. Measured Deflections and Computed "Exact" Deflections for Beam ML-2

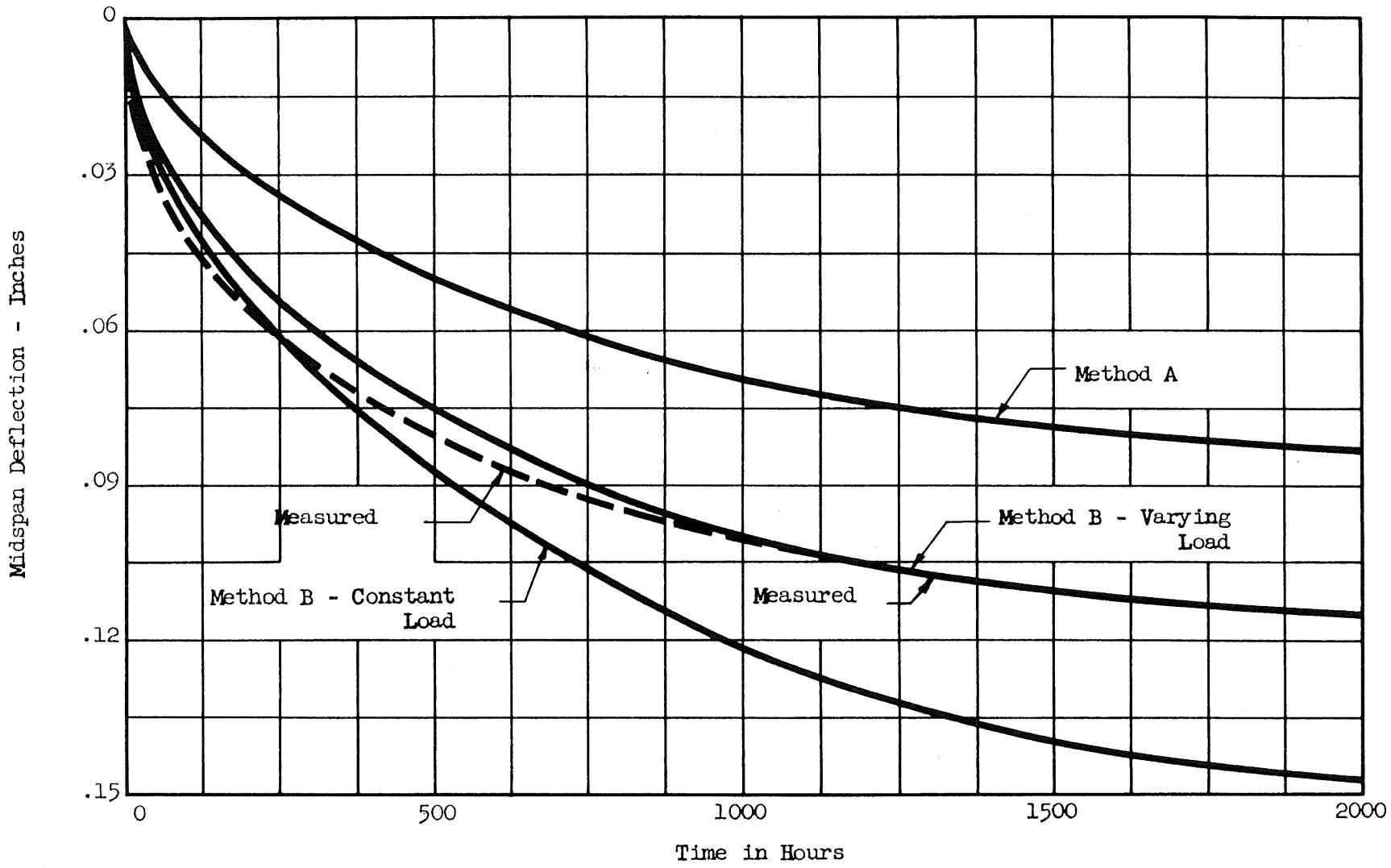

Fig. 38. Measured Deflections and Computed "Approximate" Deflections for Beam ML-1

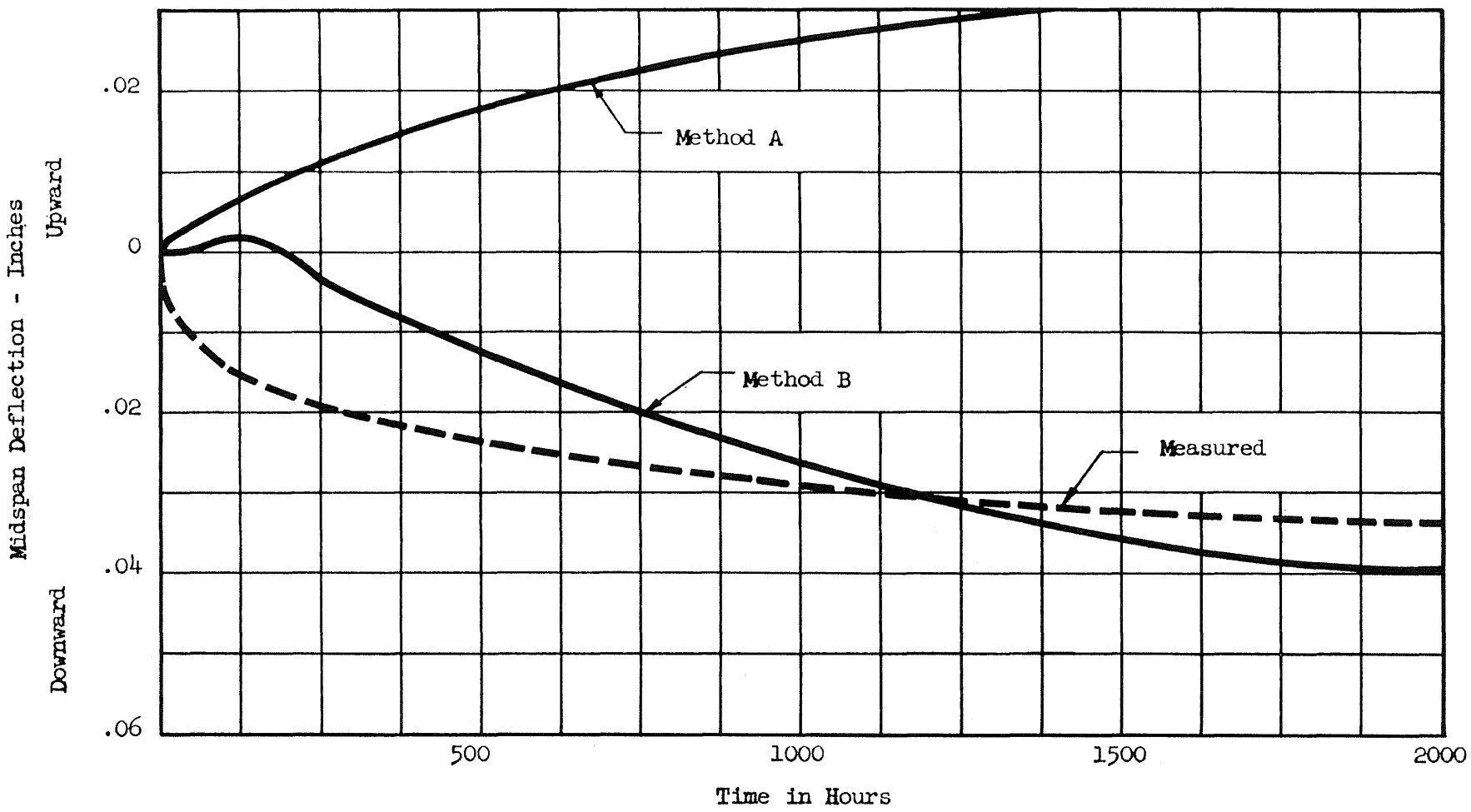

Fig. 39. Measured Versus Computed "Approximate" Midspan Deflections for Beam ML-2

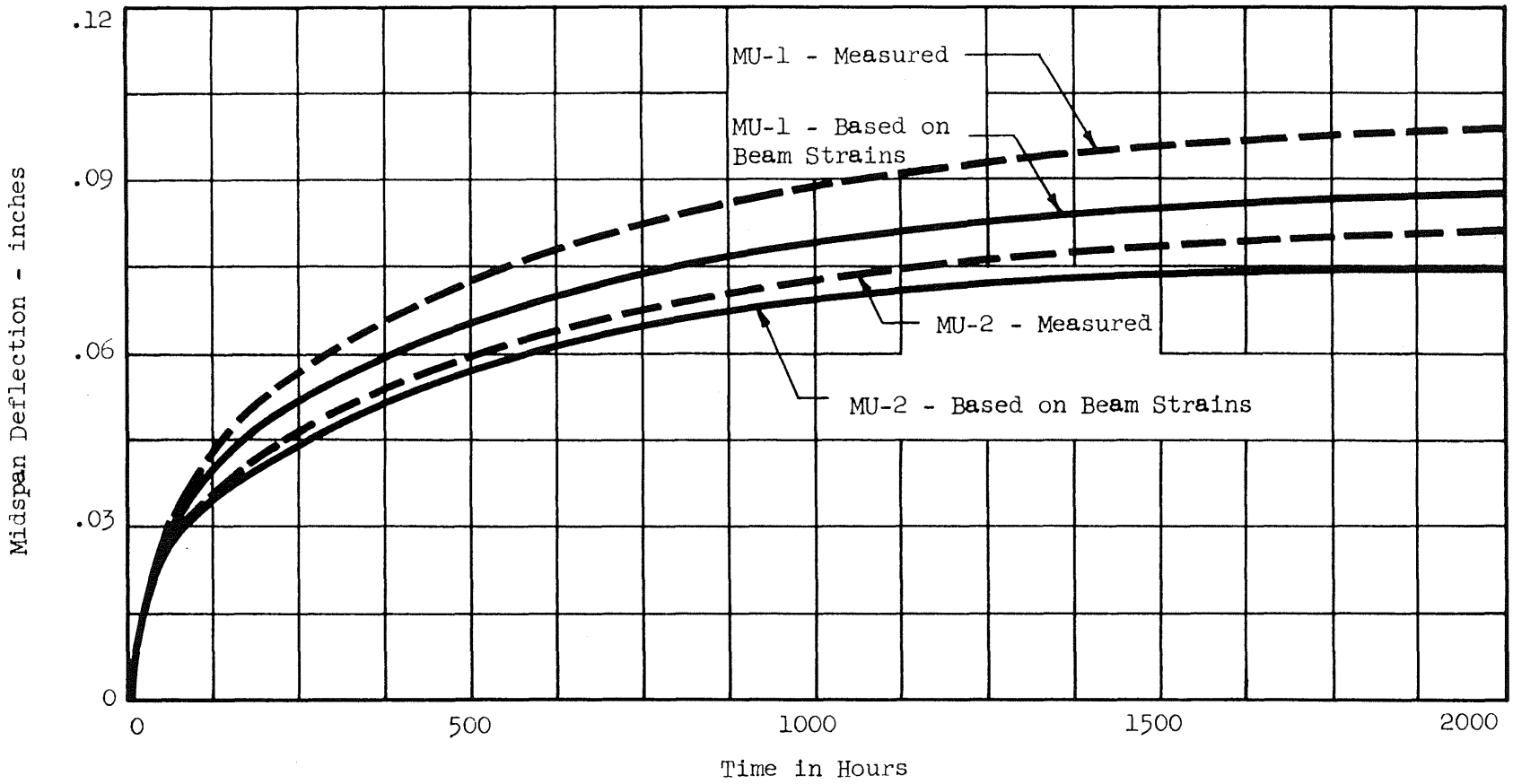

Fig. 40. Measured Deflections and Deflections Based on Beam Strains for Unloaded Beams MU-1 and MU-2

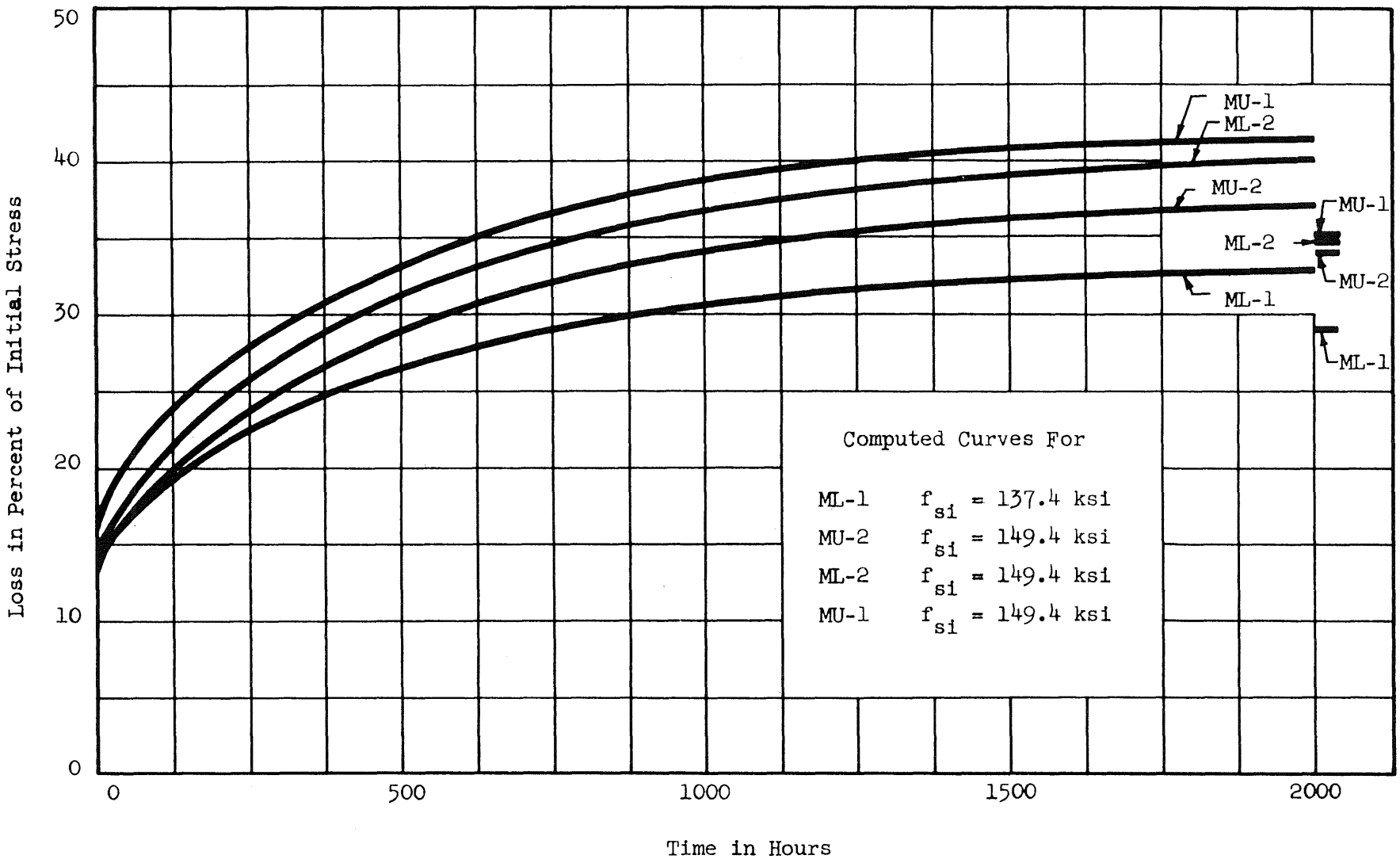

Fig. 41. Plot of Prestress Losses for all Beams